Pipeline for the Zebrafish Model as a Predictor of Specific Teratogenic Effects

---

By

Rachna Mirchandani

A dissertation submitted to the Department of Biology and Biochemistry,

College of Natural Sciences and Mathematics

in partial fulfillment of the requirements for the degree of

Doctor of Philosophy in Biochemistry

Chair of Committee: Dr. Jan-Ake Gustafsson

Committee Member: Dr. Maria Bondesson

Committee Member: Dr. Robert Schwartz

Committee Member: Dr. Tasneem Bawa-Khalfe

Committee Member: Dr. George T. Eisenhoffer

University of Houston
May 2020

ACKNOWLEDGEMENTS

First, I would like to thank Dr. Maria Bondesson for her unwavering support and trust in me even during times of my self-doubt. She has been there for advice, as an ear to listen, a shoulder to cry on and a voice of reason whenever I felt stuck. She has allowed me to think, grow, and experiment while at the same time always been there like a safety net. She has pushed me when I am uncertain and gently corrected me when she sees something wrong. She has been one of my biggest cheerleaders through this whole grueling process. She has truly been an excellent mentor, friend and teacher. Even today there is so much I would still like to learn from her, most of all her level headedness and patience.

I would also like to thank my committee members. Dr. Jan-Ake Gustafsson and Dr. Robert Schwartz who are senior professors and achieved so much themselves, have always been supportive, encouraging, and enthusiastic about my work. Giving sound advice and asking pertinent questions as I talk about my work. I am especially grateful to Dr. Gustafsson for allowing me to join the CNRCS team and providing financial support. Dr. Tasneem Bawa-Khalfe and Dr. George T. Eisenhoffer always ask thought-provoking, practical questions that helped me look at my project through new perspectives. They would encourage me to look at the new aspects of my work without fear due to their enthusiasm to share their knowledge with me.

Dr. Steven Bark and Dr. Wilna Moree have also been a great source of inspiration and encouragement especially during my first few months of uncertainty when I first started my degree. They made it safe for me to say that I am uncertain about my path, reassured me it is normal, and

then gently encouraged me to explore what I enjoy. I will never forget their faith in my ability to achieve whatever I wished to do.

I am grateful to have had a chance to work with Dr. Chad Wayne. I truly feel like my time at UH would have been incomplete if I hadn't had the pleasure to work with him. He advised me on so many things, usually more related to real life than to work. From, how to be a more effective teacher? To, how to deal with difficult people in life? Conversations with him were always fun and eye-opening.

I would also like to express my gratitude towards Dr. Sharanya Kalasekar for sharing her knowledge of everything zebrafish, from husbandry to experiment planning. I would also like to thank Nestor Narvaez, Juan Narvaez and Muzamil Haq, without whom our fishes wouldn't be the happy little creatures they were. They also saved me from a lot of heavy lifting in the lab. The two undergraduates, Divya Chilukuri and Sara Flores have also been such an important part of achieving the work I have during my PhD. I absolutely enjoyed their company and working alongside them all. It made coming into the lab so much fun.

I would like to thank Dr. Igor Bado, Dr. Fahmi Mesmar and Dr. Jeff Spencer for being such a great source of knowledge and encouragement in the lab. They were always around to bounce ideas off of or to give advice or to calm my nerves as I waited for the results of all the major exams.

Our team at IU consisting of Dr. Sherry Clendenon, Dr. Jason Coral, Beas Bhattacharya, Maram Muhsen, and Silvia Karim made me feel welcome and shared with me not just their lab space but also their friendship. They made me feel at home and were part of the reason for me falling in love

with Bloomington. Their support played a big role in me being as productive as I was during my time there.

I would like to take this opportunity to also thank Dr. Savini Thrikawala, my closest friend, a wonderful colleague, and one of the most encouraging influences in my life. She would continue believing in me even when I wouldn't, and she always brought out the best in me. My talks and discussions with her always left me feeling positive and uplifted. She was the only person who could make sense of all the garbled stuff I would say when stressed and I will be forever thankful for her friendship. I am also very grateful for Dr. Priyanka Srivastava's friendship through all the years of my doctoral degree. She was always there to be the level-headed, practical and responsible person. With a maternal streak, she was one of the people responsible for me being on track with everything work related. Always positive while being an eternal worrier, she made me feel safe and cared for.

I am grateful also for the friendship of Rochelle Savage, Dr. Jason Atkins, TaQuida Boclair, Mitch Lombard, and Jocelyn Lombard. They were my mid-night calls, my cheerleaders and my support system that helped me keep it all together. They have been there for all my ups and downs and stood by me through it all.

Finally, and most importantly I would like to thank my parents, brother and sister-in-law. Without them I wouldn't be where I am today. They are my safety net, my advisors and the people who have enabled me to go after my dreams with everything I have got. Most of all I am grateful for my son, Kiaan who is the sunshine of my life, the force that drives me and the person who makes it feel like everything will be just fine.

ABSTRACT

Over 80,000 synthetic chemicals are currently in commercial use without a full assessment of their adverse effects, especially on developmental stages of life. Exposure to some of these chemicals has been linked to birth defects, chronic disease, and cancer. Synthetic chemicals are also present in everyday items, such as food, household cleaners, and lawn care products. Zebrafish (*Danio rerio*) are an effective alternative *in vivo* model to standard mammalian models for teratogenic studies owing to their rapid development, low cost, and genetic homology to humans. The availability of transgenic fish that express fluorescence in specific tissues or organs allows for detection of tissue-specific structural malformations in live fish. We have used the zebrafish model to understand the adverse effects that potential teratogens have on living systems, and to establish a rapid and reliable screening method *in vivo*. Transgenic fish were used to screen for chemicals that perturb angiogenesis and posterior lateral line (PLL) development, and the screening results subjected to computational toxicology to elucidate the molecular pathways by which teratogens cause these specific phenotypic effects. We screened 175 ToxCast Phase I chemicals in zebrafish for vascular teratogenicity (vascular disrupting chemicals; VDCs) and identified ten chemicals that interfered with intersegmental vessel (ISV) development. For PLL teratogenicity (PLL disruptors, PLLDs), we tested all 292 chemicals from the ToxCast Phase I library and identified 22 chemicals that reduced the number of deposited neuromasts. The chemical hit lists for each of the developmental perturbations observed were then compared to the ToxCast *in vitro* assays to produce a phenotype-specific assay profile of genes or molecular pathways through which these chemicals may be acting. The assay profiles were used to predict other chemicals from the ToxCast Phase II library that could be potential VDCs or PLLDs. In summary, we have established a rapid

screening method for phenotypic outcomes in zebrafish and combined it with computational analysis of ToxCast *in vitro* data to obtain phenotype-specific assay profiles that can further be used to rank toxicants tested in the Tox21 project to speed up prioritization of chemicals for further testing *in vivo*, and in the long run result in an improved risk assessment for human and environmental health.

TABLE OF CONTENTS

LIST OF TABLES

LIST OF FIGURES

CHAPTER 1: INTRODUCTION

1.1 ENVIRONMENTAL TOXICANTS

Environmental toxicants are synthetic or naturally occurring chemicals that can impair or damage biological systems and can cause serious health effects. Problems can develop from acute, chronic, or excessive exposure. With the production of new compounds in global manufacturing and the reduction in environmental regulatory agencies in some countries, the inherent risk to public health has increased. Exposure to environmental toxicants directly contributes to 3% of birth defects observed (Center for Disease Control and Prevention, 2020). United States Department of Health and Human Services has reported the commercial use of over 80,000 chemicals in the United States, but only about 2% of those have been assessed for their safety (National Toxicology Program, 2020). In 2018, over 3.8 billion pounds of chemicals were released into the environment (Environmental Protection Agency, 2018).

1.1.1 Chemical Regulation

Due to the growing concern about the exposure and potential impact of environmental toxicants, the U.S. Environmental Protection Agency (EPA) was formed in 1970 (National Research Council, 2007). The EPA has established an environmental toxicants registration process to identify harmful chemicals to comply with state and federal laws. However, prior to 1976, existing industrial chemicals were not regulated and did not require toxicity testing (Kraska, 2001). By 2007, there were more than 10,000 compounds that required assessment (Dix *et al.,* 2007). The EPA requires the safety assessment of existing chemicals under the Toxic Substances Control Act (TSCA) (Environmental Protection Agency, 2018). The first step in assessing the safety of existing chemicals is structural-activity relationship analysis, which compares the structural relationship of chemicals with unknown biological activity to those with known activity (Environmental

Protection Agency, 2018). To expedite the testing of environmental chemicals for environmental safety, the EPA initiated a research program entitled "ToxCast" (Toxicity Forecaster) (Dix *et al.*, 2007; Richard *et al.*, 2016).

1.1.2 Toxic Substance Control Act

The Toxic Substance Control Act (TSCA) is a federal law that regulates industrial chemicals that have the potential to be harmful to humans or to the environment (Environmental Protection Agency, 2018). This law restricts the commercial production or import and export of industrial chemicals prior to EPA approval (Environmental Protection Agency, 2018).

1.1.3 ToxCast Program

In order to remedy the current limitations of toxicant screening, the EPA has initiated the ToxCast program (Dix *et al.*, 2007; Judson *et al.*, 2010). The ToxCast Program is an acumination of several integrated technologies that are used to determine the potential toxicity of chemicals in the TSCA data bank. Through its Computational Toxicology Research (CompTox) Program, EPA is attempting to identify and evaluate the safety of these chemicals by compiling structurally-similar and biologically active chemicals with those of known toxicants into an algorithm that will prioritize chemicals for testing based on their potential toxicity in humans (Environmental Protection Agency, 2018). This system can evaluate thousands of chemicals for potential toxicity and prioritize them for further testing. ToxCast is a multi-year, multi-phase, automated high-throughput screening program used to determine the potential toxic activity of chemicals identified in the CompTox analysis (Environmental Protection Agency, 2018). ToxCast was established to not only speed up the identification of environmental toxicants but also to limit the number of required laboratory animals used in classical toxicity screening. The initial phase (Phase I) of the

ToxCast program screened 292 chemicals in over 700 high-throughput screening assays (Environmental Protection Agency, 2018). The majority of these chemicals were also evaluated in animal models which allowed the direct comparison of the ToxCast screening to the standard animal models. ToxCast Phase II and III resulted in the screening of over 4500 chemicals, and the results, which are publicly available, have changed the way chemicals are identified and evaluated for human and environmental safety (Environmental Protection Agency, 2018).

1.1.4 ToxPi GUI

The Toxicity Prioritization Index (ToxPi) graphical user interface (GUI) is an analytical framework developed by EPA that allows toxicity data from various sources or assays to be transformed into integrated, visual profiles that offers the most effective means of communicating complex data. In addition to this, ToxPi GUI has the ability to assess chemical safety by prioritizing the order of chemicals, as well as visualizing the contribution of each data source towards a chemical's activity or risk profile (Marvel *et al.*, 2018).

1.1.5 Limitations of Current Toxicant Screening Methods

Traditional toxicology testing relies on specific toxicological endpoints that are determined through *in vivo* and *in vitro* testing. The current safety evaluation of environmental toxicants involves multiple rounds of *in vitro* biochemical and cell-based assays that focus on high-throughput screens using models that target specific candidate pathways. Although these *in vitro* models are relatively fast, cost-effective, and have identified several potential biological drug targets, many of the effects found in the *in vitro* studies are not replicated when tested *in vivo*, suggesting inefficacies in the cell-based assays. In some cases, these studies have identified several potential biological-targeting drugs, but these initial findings often fail to produce

satisfactory results in *in vivo* testing since they lack relevant whole-organism metabolism and physiology, and are therefore not indicative of whole-organism pharmacokinetics or dynamics. On the other hand, *in vivo* studies in mammalian animal models, such as rodents, typically takes over five years before a full quantifiable safety assessment can be completed, not to mention the extensive cost of these animal models (Dix *et al.*, 2007; Kleinstreuer *et al.*, 2011). These factors limit the number of chemicals that can effectively be evaluated using traditional mammalian models. Although these cell-based and animal models have provided useful information pertaining to the toxicity of said chemicals, they are often not indicative of human metabolism and physiology, or they are expensive and low-throughput. Given the sheer number of untested chemicals in the TSCA data bank currently, methodology and testing will take years to be established and new methodologies need to replace traditional animal toxicology testing.

1.2 ZEBRAFISH (*Danio rerio*)

The zebrafish, *Danio rerio* (Hamilton, 1822), is a freshwater fish that has emerged as a model organism for both genetic analyses and developmental biology of vertebrates because of its rapid development, small size, external fertilization, and transparency during early development (Teraoka, Dong and Hiraga, 2003). Zebrafish has a very rapid embryonic development, in which all major organs are formed 24 hours post-fertilization (hpf) (Dahm and Geisler, 2006). Zebrafish reach sexual maturity in approximately three months and a healthy female can produce one hundred eggs a day (Hill *et al.*, 2005). Since the embryos are completely transparent, they enable detailed live observations of developmental processes, especially since a vast number of transgenic lines expressing fluorescence in specific tissue or cell types are now available (Carvan *et al.*, 2006; Gorelick and Halpern, 2011; Lee, Green and Tyler, 2015). The availability of transgenic lines has

also enabled the observation and characterization of specific perturbations caused by environmental toxicants (Carvan *et al.*, 2006; Lee, Green and Tyler, 2015). In addition to this, zebrafish can also be used to model human diseases since they not only share over 70% homology of the human protein-coding genes but also share over 80% of the human disease-associated genes (Teraoka, Dong and Hiraga, 2003; Bugel, Tanguay and Planchart, 2014). Zebrafish also share with humans the same basic developmental processes and organ systems, such as the hematopoietic system, heart, liver, kidney, and blood-brain barrier (Driever *et al.*, 1994; Lieschke and Trede, 2009; Sipes *et al.*, 2011; MacRae and Peterson, 2015). Despite some major differences observed as a result of their adaptation to the aquatic environment, the cardiac electrophysiology of zebrafish, and not rodents, is more closely related to that of humans (MacRae and Peterson, 2015). The zebrafish is also a reliable model to study drug and cellular metabolism owing to the expression of the full range of cytochrome P450 (Cyp) genes as well as the processes of adsorption, distribution, metabolism, and elimination being fairly well developed in this species (Goldstone *et al.*, 2010). All of these features make it possible to model the health effects of environmental toxicants and their underlying mechanisms of action in zebrafish that could very well translate into mammalian systems (Hill *et al.*, 2005). Such new model systems need to be implemented to more accurately assess the risk of emerging compounds.

1.2.1 Zebrafish as a High Throughput Screen Model

The zebrafish is highly amenable to high throughput screening due to its high fecundity, small size, rapid development, and suitability for live imaging. Due to these attributes, the zebrafish is being used as a first-pass screen to shortlist chemicals with the highest likelihood of posing risk to humans and which would require further mammalian testing (Dix *et al.*, 2007). Even researchers

at the EPA have used the zebrafish developmental assay to screen 1060 compounds from the ToxCast Phase I and II libraries for 18 different endpoints in five days post fertilization (dpf) zebrafish to add information to the toxicity assay database of the ToxCast library (Reif *et al.*, 2010; Padilla *et al.*, 2012). Furthermore, in 2009, an international group of pharmaceutical companies formed a consortium to establish a zebrafish development assay to test whether ten teratogenic compounds and ten non-teratogens could be correctly distinguished and the results in zebrafish showed 60-70% concordance to mammalian data for the same compounds. A further 38 proprietary pharmaceutical compounds were tested in zebrafish by two independent laboratories and demonstrated a high concordance (79%) in their classifications (Gustafson *et al.*, 2012; Ball *et al.*, 2014). Thus, efforts to build databases and develop assays to predict human toxicity have capitalized on the use of zebrafish as a quick, medium to high-throughput *in vivo* system to accurately predict human toxicity.

1.2.2 Zebrafish Lateral Line

The zebrafish lateral line is made up of mechanosensory organs called neuromasts which function to keep the fish oriented in response to water currents. The mature neuromast contains a group of hair-cells in the center which are surrounded by support cells which are then surrounded by mantle cells (Whitfield, 2002). The neuromasts are deposited in a reproducible pattern on the surface of the body making them easily accessible for chemical exposure (Chiu *et al.*, 2008). In addition, there are several transgenic lines, such as the GW57A that express GFP in the support cells of the neuromasts, or the *Tg (cldnb:GFP)* which expresses GFP in the migrating primordium as well as in the mature neuromasts, allowing for live imaging (Haas and Gilmour, 2006; Pinto-Teixeira *et*

al., 2015). Therefore, the hair cells in the zebrafish lateral line can be rapidly screened for toxic effects from targeted chemical(s).

The zebrafish lateral line is an excellent system to study mammalian inner ear hair cell toxicity because the hair cell structure, function, and development is well conserved between the two including the cilia being organized with specific cell polarity and mechanotransduction (Brignull, Raible and Stone, 2009). Even the functional mechanisms are conserved at the cellular level since several orthologs of human deafness genes identified in zebrafish also disrupted lateral line hair cell function (Nicolson, 2005; Brignull, Raible and Stone, 2009). It has also been demonstrated that several ototoxic drugs identified in mammals and patients, such as aminoglycoside antibiotics like neomycin, and metal-based drugs like platinum drugs used for cancer, cause dose-dependent neuromast hair cell death (Brignull, Raible and Stone, 2009; Namdaran *et al.*, 2012). The PLL and its development is further described in Chapter 2.

1.2.3 Zebrafish Vascular System

Zebrafish are a great model system to study vascular development and perturbations *in vivo* owing to its ability for other organs and tissues to continue developing normally for several days in the embryos even when the cardiovascular system is disrupted by chemical exposure, whereas such disruptions are fatal to mammalian embryos (Gore *et al.*, 2012; Hogan and Schulte-Merker, 2017). It is believed that the early fish embryo survives without a vasculature because its small size allows for oxygen diffusion to all cells. This trait allows for the identification of specific disruptors of the vascular system. Furthermore, zebrafish and mammals express a common set of early hematopoietic and endothelial cell genes, such as stem cell leukemia (scl) and vascular endothelial growth factor receptor 2 (vegfr2) (Gore *et al.*, 2012; Wilkinson and Van Eeden, 2014). The rapid

development of the vascular system, where circulation has already begun by two dpf and the availability of several transgenic lines expressing fluorescence in the vasculature, also make it a promising model system for chemical screens or study of vascular development (Isogai, Horiguchi and Weinstein, 2001; Gore *et al.*, 2012; Wilkinson and Van Eeden, 2014). The zebrafish has been a very important contributing factor to understanding mammalian vascular development (Hogan and Schulte-Merker, 2017). The zebrafish and mammalian vasculature don't just have common early genes, but also share anatomy of the vascular system such as having a closed circulatory system, and share the molecular mechanisms involved in vessel formation (Gore *et al.*, 2012; Hogan and Schulte-Merker, 2017).

1.2.4 Limitation of the Zebrafish Model System

Although the zebrafish model system is genetically and physiologically similar to humans, there are several limitations to this system. The zebrafish do not have lungs or placenta and therefore toxicological assessments pertaining to these systems are difficult. However, although not all disease-related phenotypes can be identified in zebrafish, many of the developmental and signaling pathways leading to these diseases are conserved between zebrafish and humans (Padilla *et al.*, 2012).

Another limitation is that the zebrafish life cycle is limited to water. This results in the zebrafish getting exposed to chemical metabolites due to excretion in their growth media, which is not the case in mammalian systems. This can easily be overcome by frequent media replacement or having systems with continuous water exchange (Ali *et al.*, 2011). Furthermore, the early developmental exposures in zebrafish are dermal since they do not swallow water to breathe, which is different from human exposure which is mostly through ingestion. Therefore, some exposures to toxic

chemicals may not be equivalent to those experienced in human. This may lead to differences in ADME (absorption, distribution, metabolism, and excretion) and biotransformation of the chemicals due to the different modes of exposure. These metabolic differences between zebrafish and mammals may result in differences in the metabolic breakdown of specific compounds or even in their binding efficacy or targeting capacities (Saad *et al.*, 2016).

Additionally, solubility issues in the zebrafish growth medium may limit the concentration of potential toxicants and specific applications may be required to emulate exposure in humans. In this instance, dermal exposure during embryonic stages may not recapitulate the concentrations of human exposure, instead exposure during adolescent or adult stages of zebrafish will allow for oral route exposure since they swallow water to breathe and thus will be able to achieve appropriate exposure levels even without full solubilization of the drug or chemical (Saad *et al.*, 2016).

CHAPTER 2: IDENTIFICATION AND PREDICTION OF POSTERIOR LATERAL LINE DISRUPTORS

2.1 INTRODUCTION

Environmental chemicals pose risks to human health, especially if exposure occurs during pregnancy and/or early development of an individual. Because tens of thousands of industrial and agricultural chemicals are present on the market and may end up in the environment, there is an urgent need for rapid and reliable screening models to identify the most hazardous ones. We use zebrafish as one such model based on that they share about 71% of their genes with humans (Howe *et al.*, 2013), have high fecundity, and that the small size of embryos enables high throughput screening and live, non-invasive phenotypic observations of chemical-induced insults. In addition, many transgenic zebrafish lines expressing fluorescence in particular cells, tissues or organs are available facilitating straightforward visualization of tissue-specific malformations.

2.1.1 Lateral Line Development in Zebrafish

The lateral line is a system of tactile sense organs, present in all aquatic vertebrates. It consists of mechanoreceptors called neuromasts (**Figure 2.1**), which are structurally, functionally and molecularly similar to the human inner ear hair cells (Whitfield, 2002; Nicolson, 2005). The mature neuromast consists at its core of a group of fifteen to twenty sensory hair cells that respond to the deflection of their cilia. Immediately surrounding the hair cells are the support cells, which in turn are surrounded by the mantle cells that line the neuromast. The processes of directed collective cell migration, existence and maintenance of cell polarity, postembryonic remodeling and regeneration are all vital biological processes that are encompassed in lateral line development. This makes the zebrafish lateral line an excellent *in vivo* model to study these processes. The lateral line in zebrafish is divided into the anterior lateral line (ALL) and the posterior lateral line (PLL), as they arise from two separate primordia (**Figure 2.1**). The ALL also differs from the PLL with

respect to the molecular signals that drive migration of the primordium (Gompel *et al.*, 2001). The PLL placode originates just posterior of the otic vesicle and starts migrating posteriorly at eighteen to twenty hpf. The placode divides into a small anterior group of around twenty cells that differentiate to sensory neurons to form the PLL ganglion, and a large group of around one hundred cells that forms the first PLL primordium (primI) (Ghysen and Dambly-Chaudière, 2007). The primordium completes its migration anterio-posteriorly along the horizontal myoseptum to the tail at about forty hpf, depositing five groups of cells, the protoneuromasts, each at a distance of five to six somites in its wake. PrimI then fragments and forms two to three-terminal neuromasts upon reaching the tip of the tail (Gompel *et al.*, 2001; Nuñez *et al.*, 2009). The protoneuromasts differentiate into mature neuromasts a few hours after deposition. As the primordium migrates, axons from the PLL ganglion concurrently connect. Glial cells then migrate along the axons to form the myelinated PLL nerve. A second primordium, primII, ascends at about the time primI has finished its migration. PrimII deposits neuromasts between primI neuromasts at a distance of approximately two somites along the horizontal myoseptum. At four dpf, the PLL comprises about seven to eight mature neuromasts excluding the terminal neuromasts (Ledent, 2002; Ghysen and Dambly-Chaudière, 2007). Thus, the PLL's reproducible pattern, ease of experimental accessibility, and its potential to shed light on important developmental mechanisms make it a very promising system for developing high throughput screens for chemicals interfering with fundamental biological processes.

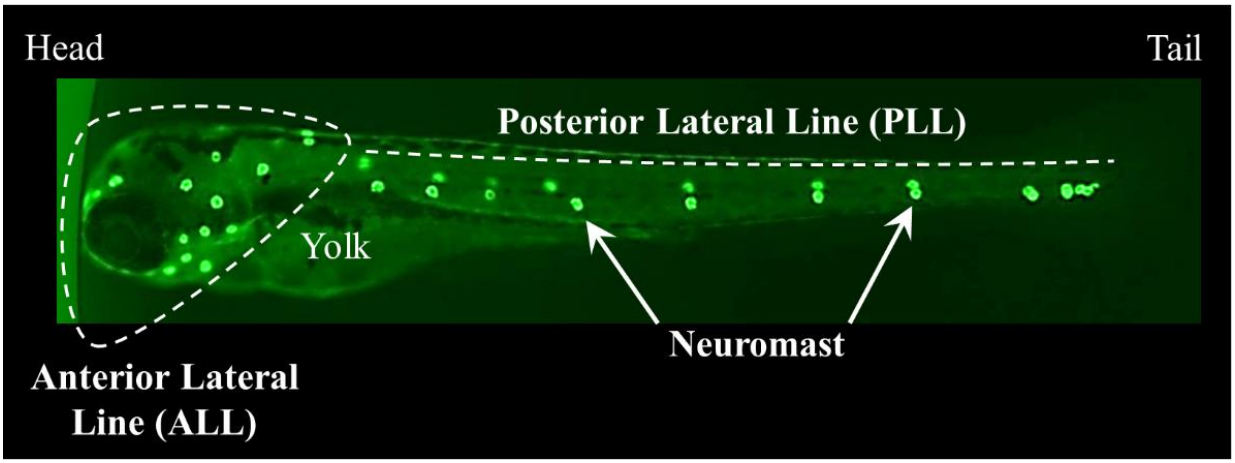

Figure 2.1 Lateral line system of zebrafish at four dpf. *Tg (neuromast:GFP)* larva expressing GFP in the neuromast support cells, was imaged laterally. The two main branches of the lateral line are ALL, anterior lateral line in the head region, and PLL, posterior lateral line in the trunk region.

2.1.2 Zebrafish Screening

Here we have used the zebrafish PLL system as an *in vivo* model to screen for chemicals that adversely affect neuromast development, migration or survival. We used embryos of a transgenic zebrafish line that express GFP in neuromasts to screen 292 unique chemicals of the ToxCast Phase I library. The identified PLL disruptors (PLLDs) were correlated to chemical data of the CompTox Dashboard, which suggested novel mechanisms of action for posterior lateral line disruption. The correlations predicted that serotonin signaling is required for normal PLL development; a hypothesis that was investigated *in vivo*.

2.2 RESULTS

2.2.1 Identification of Novel Posterior Lateral Line Disruptors

To visualize the PLL we used a transgenic zebrafish line expressing GFP in neuromasts, (GW57A (Kondrychyn *et al.*, 2011), here referred to as *Tg (neuromast:GFP)* (**Figure 2.2 B**). Compared to the *cldnb:GFP* transgenic line (**Figure 2.2. A**), with established GFP expression in the mature

neuromasts, as well as in the migrating primordium and the head region (Haas and Gilmour, 2006), *Tg (neuromast:GFP)* has a high GFP-expression in only the support cells of mature neuromasts (Pinto-Teixeira *et al.*, 2015). Visualization of the development of neuromasts by time-lapse microscopy using this line shows that the first PLL neuromast becomes positioned at the boundary between somites 6 and 7 (I-1), and the following ones at somites 13/14 (I-2), 19/20 (I-3), 24/25 (I-4), and 28/29 (I-5) (**Figure 2.2**). The next wave of PLL neuromasts are positioned between the initially deposited neuromasts at approximated every two somites (**Figure 2.2**).

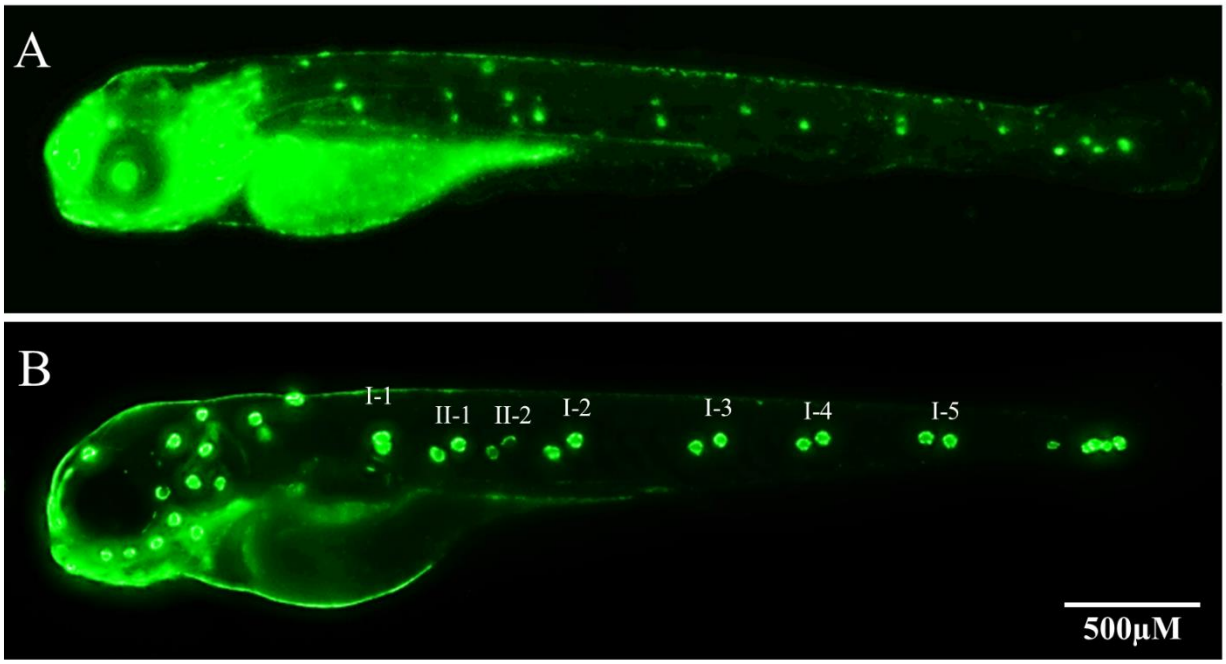

Figure 2.2 *Tg (cldnb:GFP)* vs *Tg (neuromast:GFP)*. The same pattern of neuromasts is observed in the PLL of four dpf zebrafish larvae of A. *Tg (cldnb:GFP)* line that expressed GFP in both PLL primordium and mature neuromasts vs B. *Tg (neuromast:GFP)* line that expresses GFP in only mature neuromasts. All five PrimI neuromasts, I-1 to I-5, as well at the first two neuromasts of PrimII, II-1 and II-2 are seen by this stage of development. The paired neuromasts are localized one on each side of the larvae.

To identify compounds that perturb PLL development in zebrafish, we performed screening of EPA's ToxCast Phase I chemical library. *Tg (neuromast:GFP)* zebrafish embryos were treated with three different concentrations of each chemical (Appendix Table 1) from four hpf to four dpf.

Some of the chemical exposures caused yolk edema, heart edema, and whole embryo malformations. The chemicals and the concentrations causing such general malformations were omitted from the study, and chemicals causing perturbations of the PLL neuromast pattern specifically were recorded. Our initial screen identified that exposure to 46 out of 292 unique chemicals resulted in fewer PLL neuromasts being deposited (Appendix Table 2) by visual determination. These chemicals were then re-screened in follow-up experiments with a higher number of replicates (Appendix Table 2). Twenty-two compounds were confirmed to alter the number of PLL neuromasts deposited; in a dose-dependent manner compared to vehicle (DMSO) treated larvae (**Figure 2.3**). These compounds, their lowest effect levels (LELs) and their dose-response graphs are summarized in **Table 2.1**.

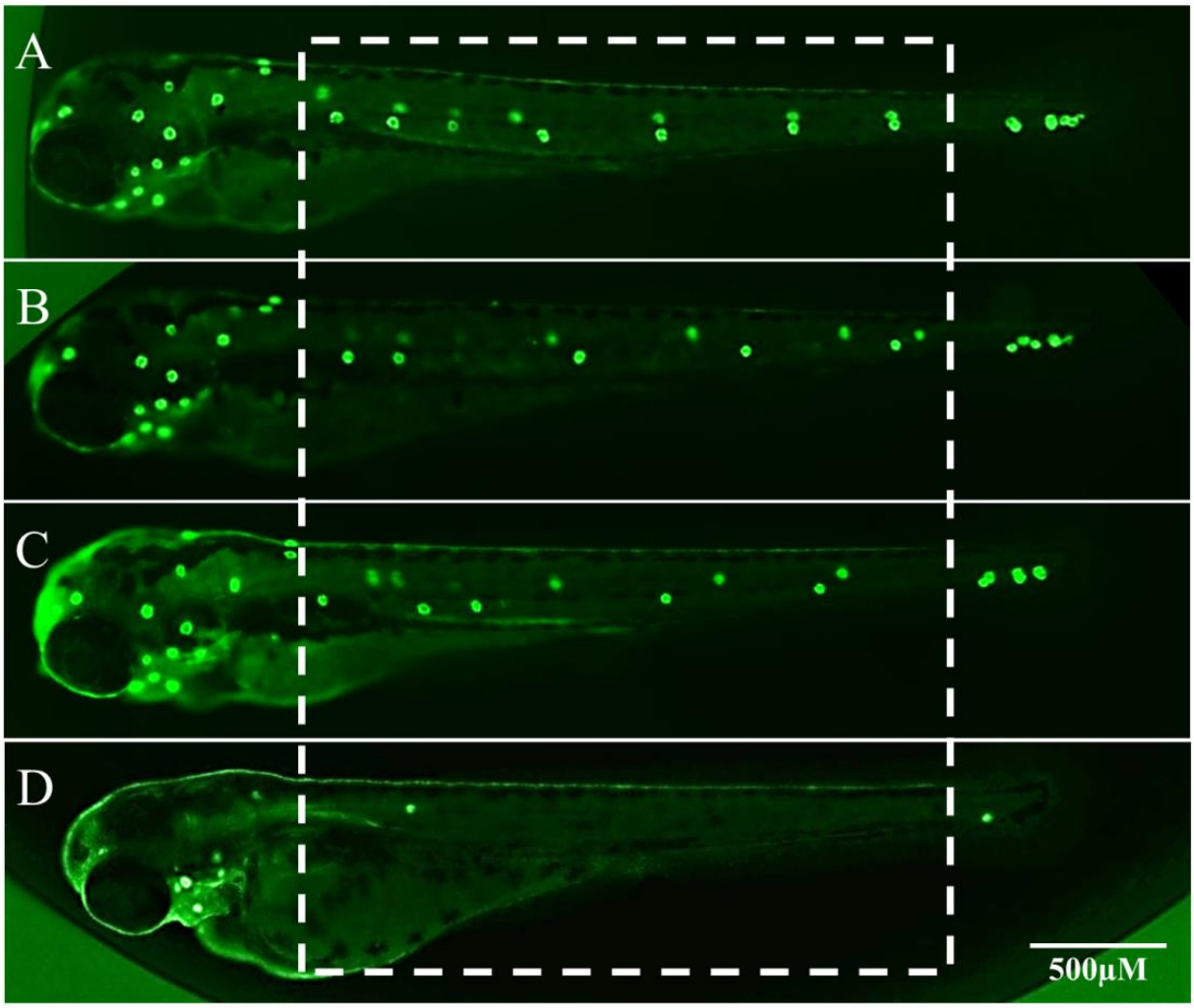

Figure 2.3 Example images of effects caused by the 22 confirmed PLLDs. Images of four dpf *Tg (neuromast:GFP)* larvae exposed to PLLDs from five hpf. The neuromasts enclosed within the dashed white boxes were assessed for variations in the number of neuromasts compared to vehicle-treated embryos; A. Vehicle (DMSO); B. 1 µM Ethylene Thiourea; C. 10 µM Propanil; D. 20 µM Bisphenol A

Table 2.1. Confirmed zebrafish PLLD's identified through ToxCast PhI library screen. Graphs are plotted as Percentage of embryos [with reduced neuromasts (dark green) or dead (light green)] vs Chemical concentration (M)

S.No	Chemical	LEL (µM)	Dose Response Graphs
1	Pryaclostrobin	0.01	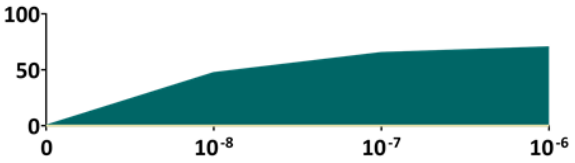
2	Cymoxanil	0.5	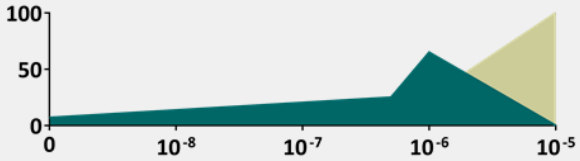
3	Fluoxastrobin	0.5	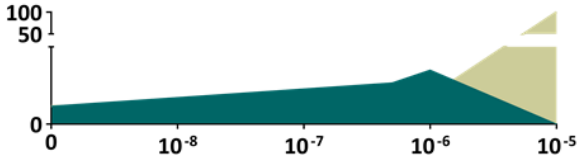
4	Anilazine	1	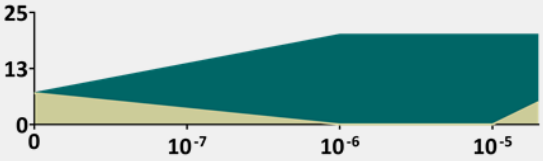
5	Azoxystrobin	1	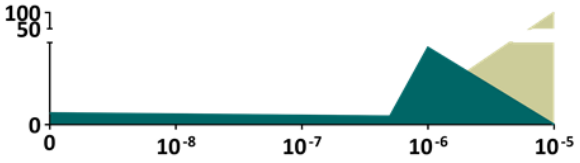
6	Bisphenol A	1	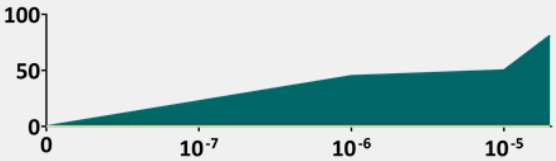
7	Butralin	1	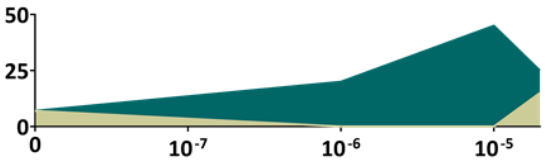
8	Ethoprop	1	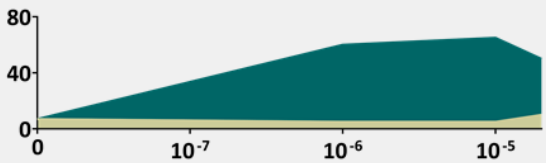

Table 2.1. cntd. Confirmed zebrafish PLLD's identified through ToxCast PhI library screen. Graphs are plotted as Percentage of embryos [with reduced neuromasts (dark green) or dead (light green)] vs Chemical concentration (M)

S.No	Chemical	LEL (µM)	Dose Response Graphs
9	Ethylene Thiourea	1	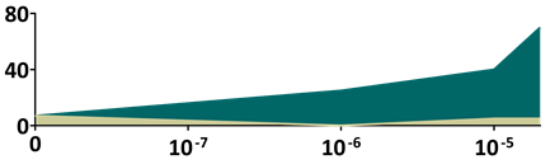
10	Fenitrothion	1	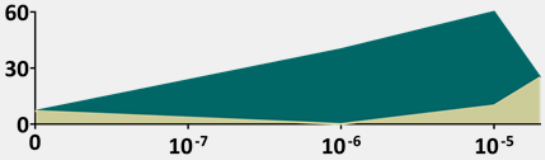
11	Fluometuron	1	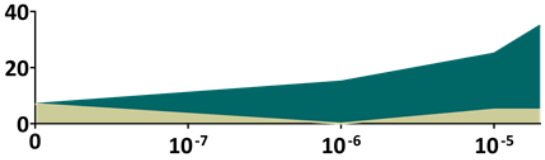
12	Iodosulfuron-methyl-sodium	1	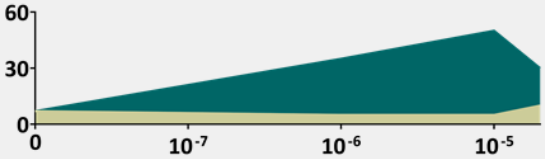
13	Prochloraz	1	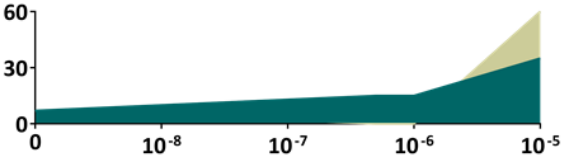
14	Thidiazuron	1	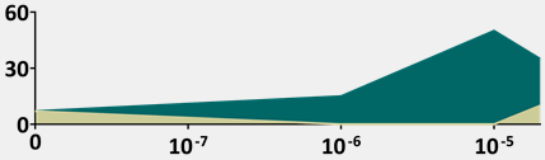
15	Vinclozolin	1	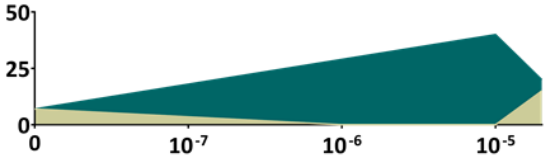
16	Azamethiphos	10	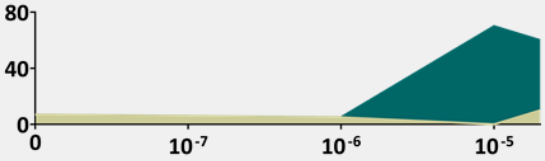

Table 2.1. cntd. Confirmed zebrafish PLLD's identified through ToxCast PhI library screen. Graphs are plotted as Percentage of embryos [with reduced neuromasts (dark green) or dead (light green)] vs Chemical concentration (M)

S.No	Chemical	LEL (µM)	Dose Response Graphs
17	Formetanate Hydrochloride	10 µM	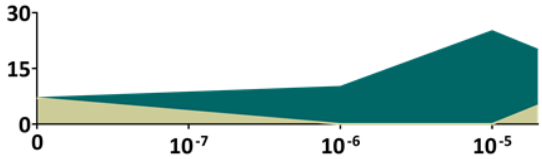
18	Imazapic	10 µM	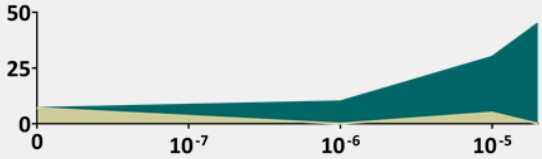
19	Propanil	10 µM	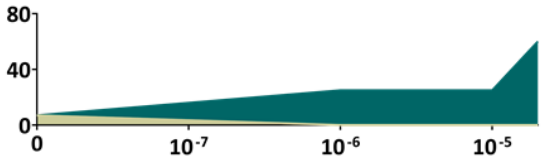
20	Spiroxamine	10 µM	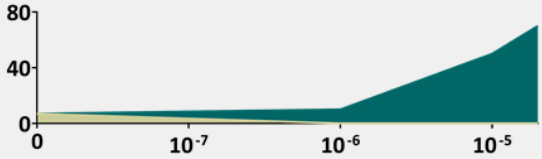
21	Thiabendazole	10 µM	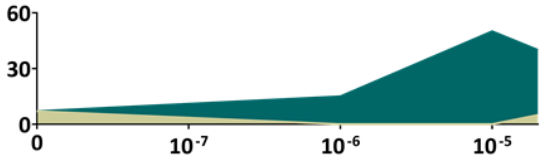
22	Difenoconazole	20 µM	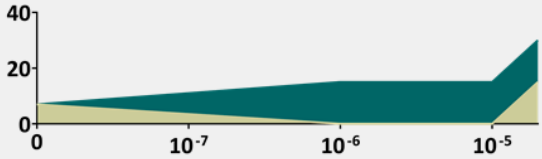

2.2.2 Identification of Altered Pathways through Computational Toxicology

We used the PLL screening results to identify ToxCast *in vitro* assays that correlate with the identified zebrafish PLL disruptors by univariate correlation analysis. **Figure 2.4** shows the

workflow of ToxCast analysis. Thirteen assays significantly correlated with the twenty-two PLL disruptors. Appendix Table 3 shows the list of assays with their true positive and p-values. These assays included five serotonin-related assays (SLC18A2, MAO-A, HTR7, CYP2D1, ADRA2B), two CYP450 assays not related to serotonin (CYP2A1 and CYP2C13), and assays for an enzyme (TPO), two nuclear receptors (RAR and FXR (NR1H4)) and three other receptors (TSPO, SIGMAR1, and PLAUR).

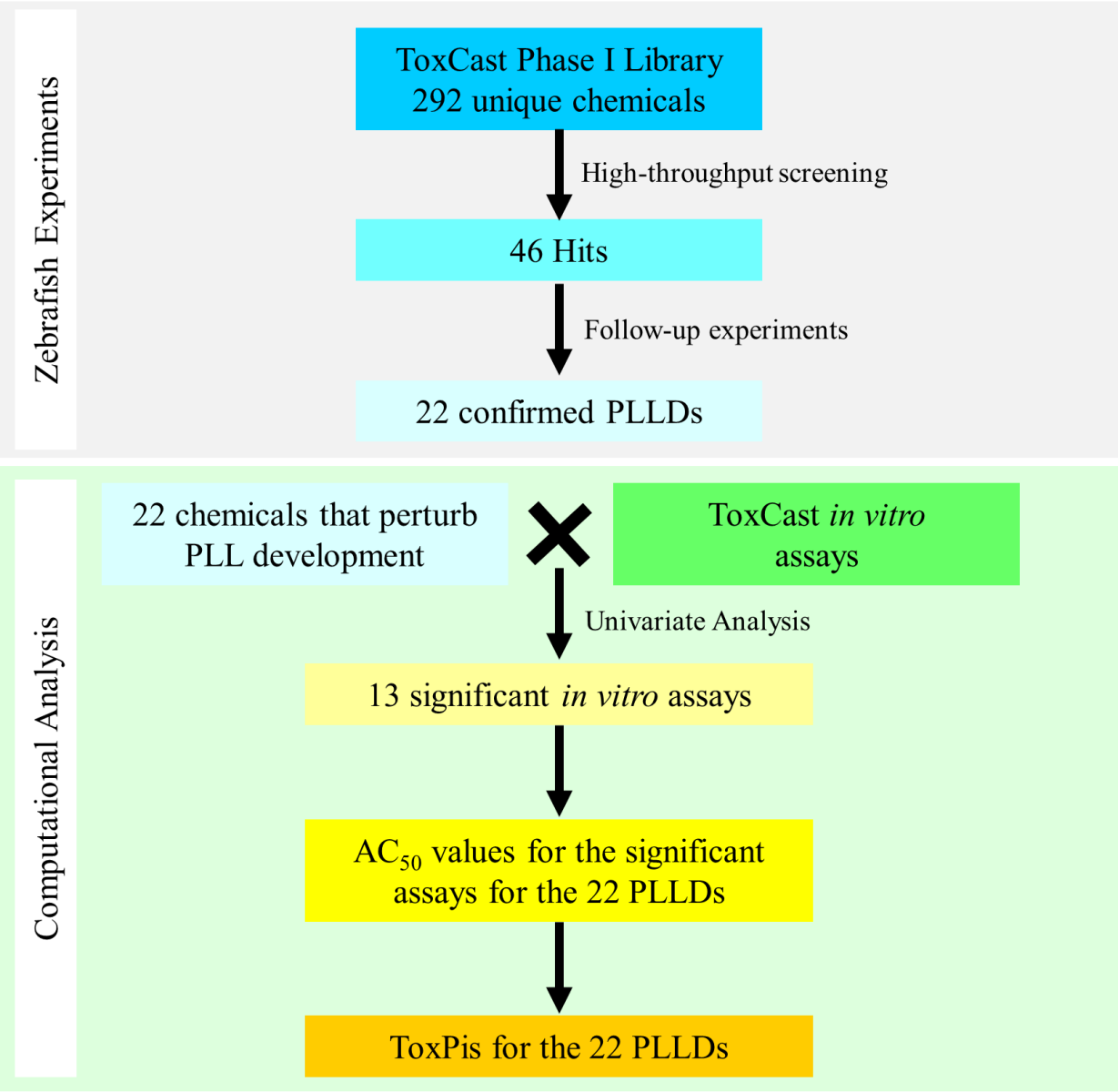

Figure 2.4 Workflow of the ToxCast analysis. Zebrafish high-throughput screening of 292 ToxCast Phase I compounds identified 46 compounds causing PLL disruption. These 46 compounds were re-screened in a low-throughput manner, which confirmed 22 PLL disruptors. ToxCast univariate correlation analysis was performed for the confirmed PLLD compounds. Thirteen assays were correlated with the PLLD effects. ToxPi profiles were created for the 22 chemicals.

The AC_{50} values for each chemical and assay were obtained from the CompTox Dashboard (Appendix Table 5) and were used to create PLL disruptor bioactivity profiles using the ToxPi tool (Reif *et al.*, 2010; Marvel *et al.*, 2018) (**Figure 2.5**). The bioactivity profiles showed that at least

six of the 22 PLLDs affected each of the serotonin assays, and 13 chemicals affected at least one of the serotonin assays, indicating a strong correlation for alterations in serotonin signaling interfering with neuromast positioning. While twenty-one PLL disruptors affected at least one of the correlating thirteen assays, one chemical (iodosulfuron-methyl-sodium) did not affect any of the assays, suggesting that this compound perturbs PLL development through pathways not yet tested for in Tox21.

The ToxPi tool calculates a ToxPi score, which relates to the number of assays perturbed by each chemical and its AC_{50} for each assay. A chemical with a high score is interpreted as a potent chemical interfering with many assays at low AC_{50}s. We used this score to rank the PLL disruptors; the highest score of 0.82 was noted for difenoconazole followed by 0.75 for prochloraz and 0.69 for bisphenol A (**Figure 2.5**).

Figure 2.5 ***In vitro*** **assay signatures for confirmed PLLDs identified through univariate correlation analysis.** ToxPis and potency scores for each of the 22 compounds were confirmed to be PLL development disruptors, generated by running the PLLD hit list against ToxCast in vitro biochemical assays. Only assays that have at least five or more of the 22 compounds as hits with a p-value <0.05 were shortlisted. Bigger pie slices show more potency at lower concentrations. All serotonin pathway compounds are represented by purple/pink slices.

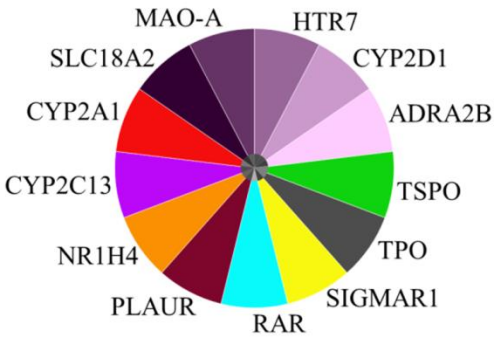

Difenoconazole
0.8193

Prochloraz
0.7486

Bisphenol A
0.6922

Thidiazuron
0.6153

Propanil
0.5926

Fenitrothion
0.4010

Azoxystrobin
0.3829

Pyraclostrobin
0.3712

Spiroxamine
0.3265

Anilazine
0.3101

Ethoprop
0.2946

Butralin
0.2695

Fluometuron
0.2287

Fluoxastrobin
0.2076

Formetanate Hydrochloride
0.1840

Thiabendazole
0.1351

Vinclozolin
0.1249

Azamethiphos
0.1219

EthyleneThiourea
0.1218

Cymoxanil
0.1100

Imazapic
0.0546

Iodosulfuron-methyl-sodium
0.0000

2.2.3 Serotonin Signaling is Required for Normal Posterior Lateral Line Development

The univariate correlation analysis described above suggests that perturbations of serotonin signaling result in alteration of neuromast numbers. To investigate this hypothesis, we selected four compounds (para-chlorophenylalanine (PCPA), methylene blue, fluoxetine, and clorgyline) that are known to affect mammalian serotonin levels. Exposure of *Tg (neuromast:GFP)* embryos to either of the serotonin modulators resulted in altered neuromast numbers in a dose-dependent manner (**Figure 2.6** and **Figure 2.7**) (Appendix Table 4). In serotonin immunostained whole larvae exposed to clorgyline and methylene blue, we observed an increased expression of serotonin, especially in the choroid plexus (**Figure 2.8**). In contrast, larvae exposed to PCPA had decreased serotonin staining (**Figure 2.8**). In fluoxetine-treated larvae, we observed less serotonin staining generally in the brain, but slightly higher staining in the choroid plexus (**Figure 2.8**).

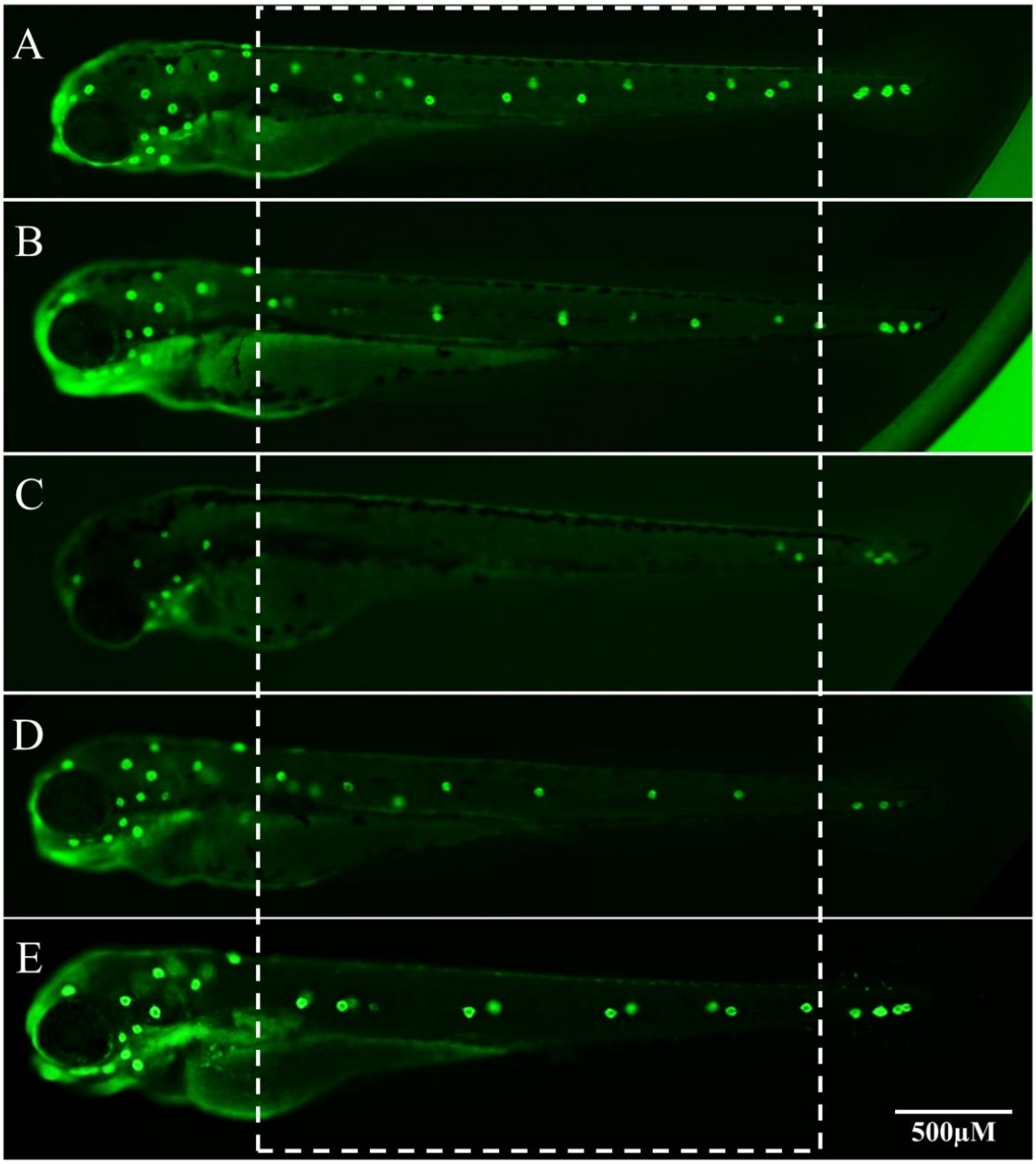

Figure 2.6 Serotonin modulators interfere with PLL development. Images of four dpf *Tg (neuromast:GFP)* larvae exposed to serotonin modulators from five hpf. The neuromasts enclosed within the dashed white boxes were assessed for variations from the vehicle-treated embryos; A. Vehicle (E3); B. 1 µM Methylene Blue; C. 10 µM Fluoxetine; D. 20 µM PCPA; E. 1 µM Clorgyline

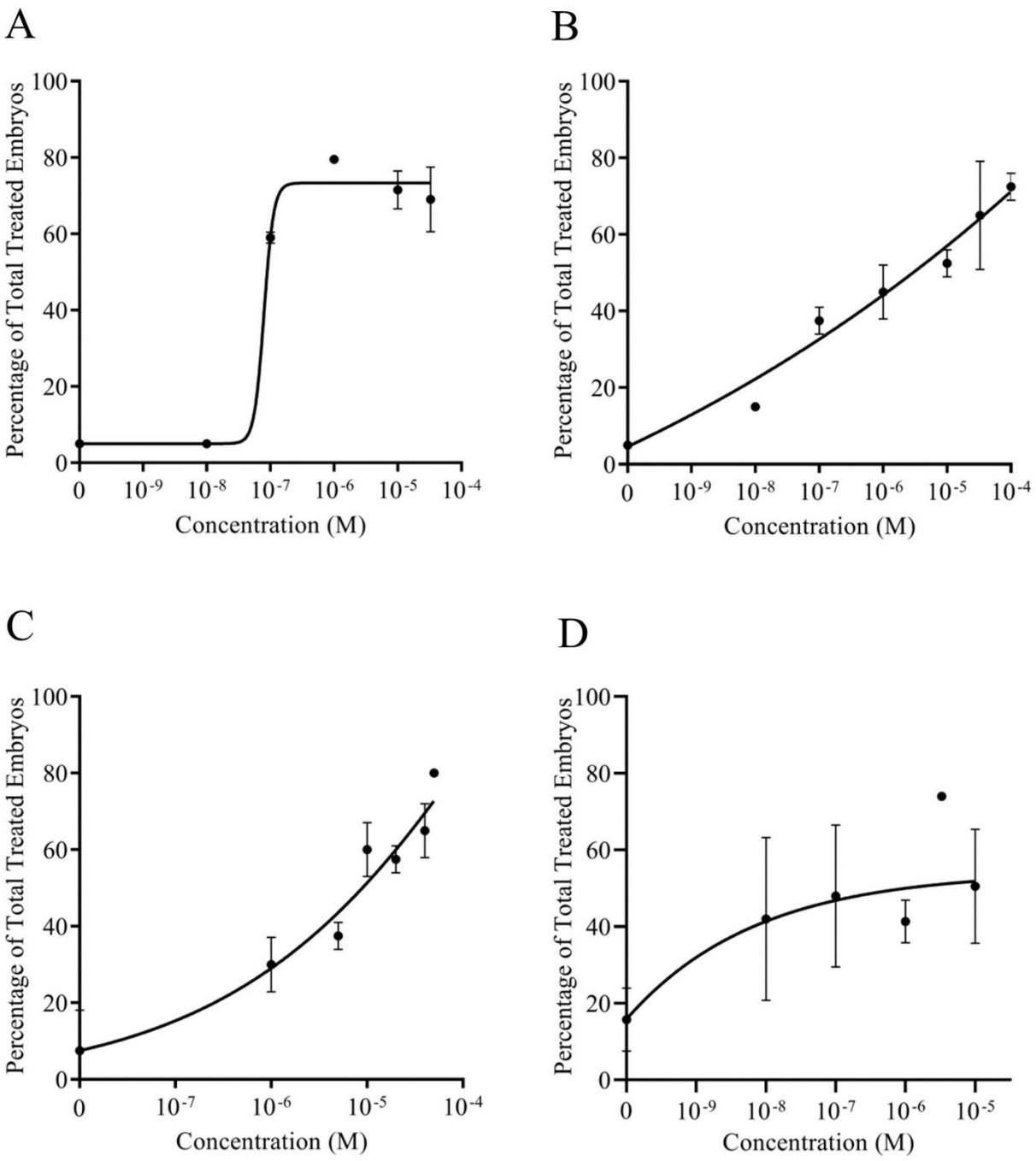

Figure 2.7 Serotonin modulators affect PLL development in a dose-dependent manner. Graphs show the percentage of zebrafish larvae with disrupted PLL development vs concentration of serotonin modulators. n=20 per concentration. Embryos were exposed to chemicals from five hpf. Effects were assessed at four dpf. A. Methylene Blue; B. Fluoxetine; C. PCPA; D. Clorgyline

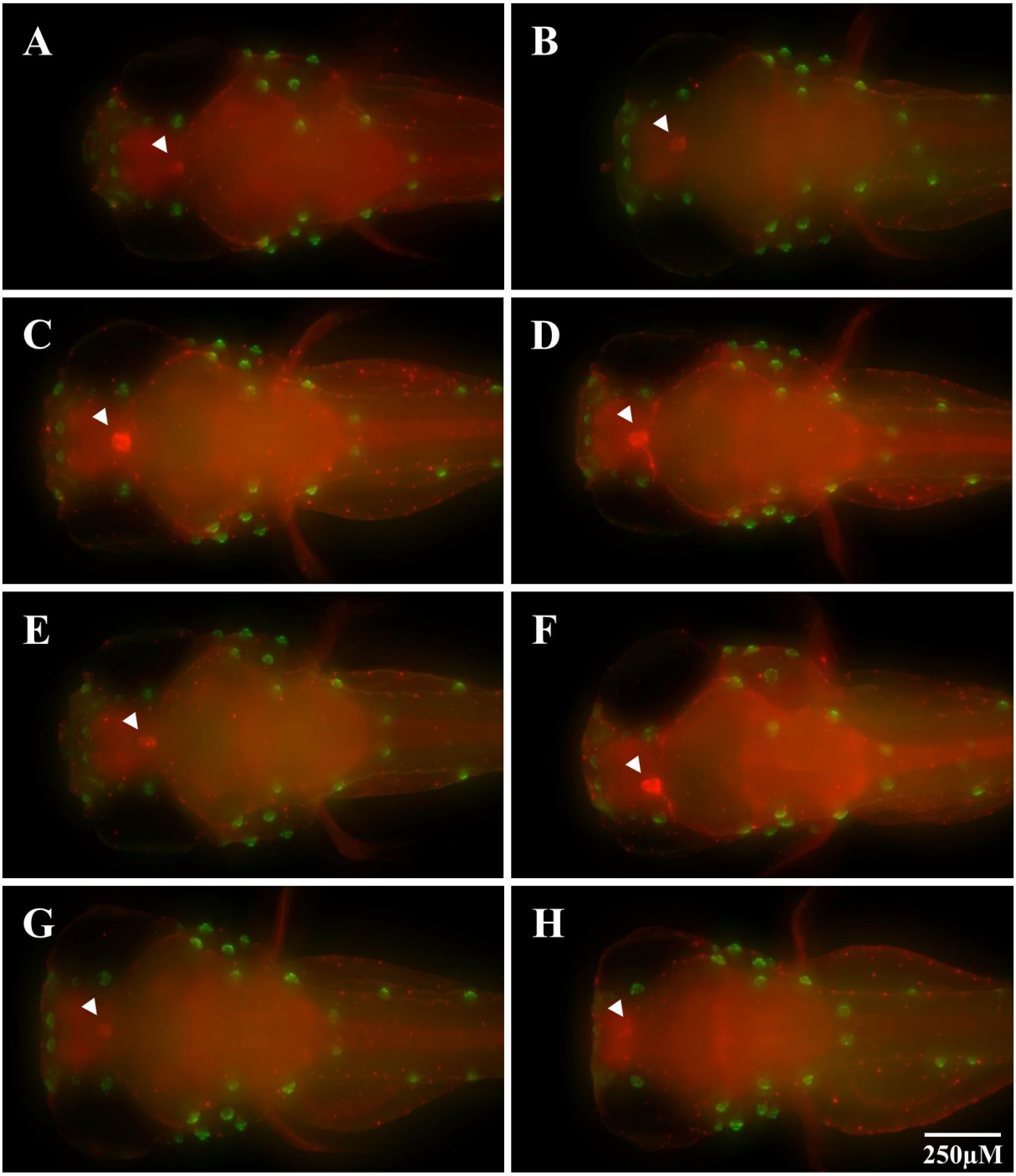

Figure 2.8 Serotonin modulators affect zebrafish serotonin levels. Dorsal view of 5-HT immunostained four dpf *Tg (neuromast:GFP)* zebrafish larvae exposed to serotonin modulators. Embryos were exposed to chemicals from five hpf to four dpf. Larvae were then fixed, immunostained for serotonin and imaged. The white arrowheads point to the choroid plexus. A. Vehicle (E3); B. Fluoxetine 33 µM; C. Clorgyline 1 µM; D. Clorgyline 3.3 µM; E. Methylene Blue 1 µM; F. Methylene Blue 10 µM; G. pCPA 10 µM; H. pCPA 20 µM.

2.2.4 Toxicity Prediction Based on ToxCast Assay Targets

The five serotonergic related assays from the univariate analysis were used to predict new PLLDs. The chemicals that have been tested for these assays and their respective AC_{50} values were extracted from ToxCast data. The ToxPi ranking tool was used to rank these compounds based on their ToxPi score. About 500 compounds were ranked (**Figure 2.9**). To evaluate the prediction, the top nine compounds, three compounds with the lowest score, and three compounds with a zero score were tested in zebrafish (**Figure 2.9**).

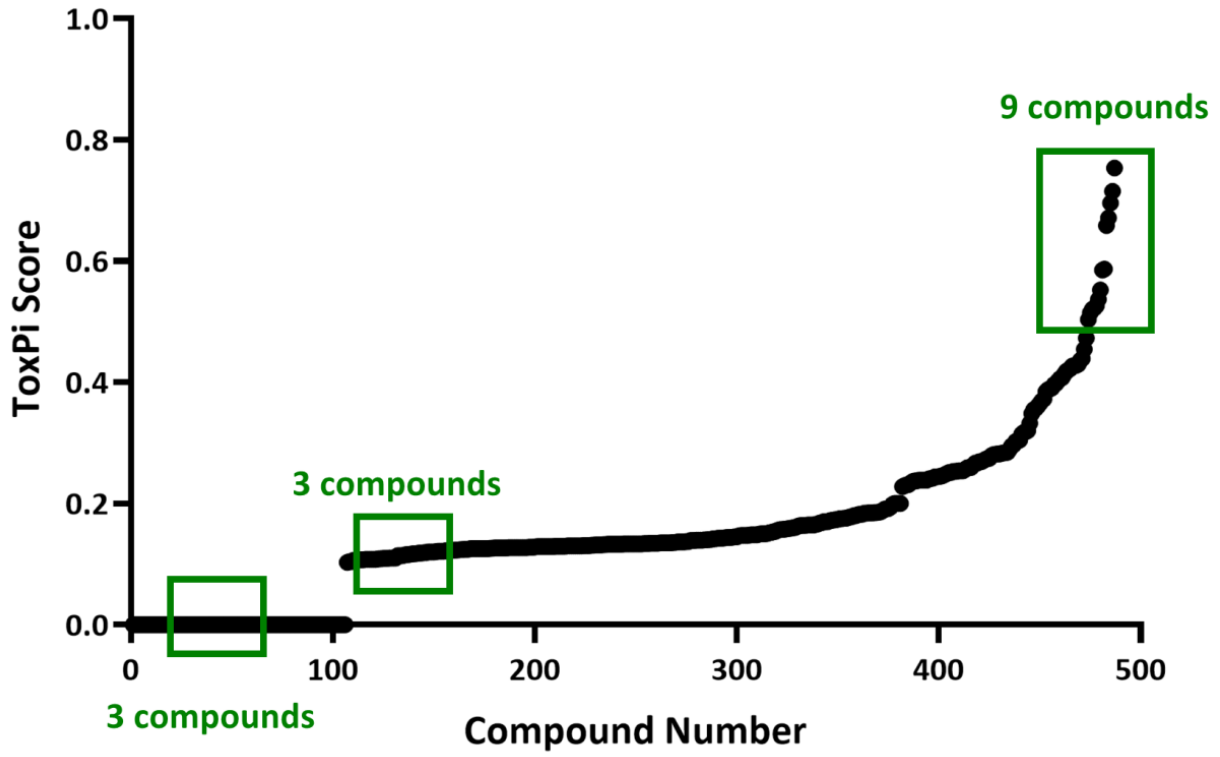

Figure 2.9 Prioritizing predicted PLLD chemicals to be tested based on their ToxPi scores. AC_{50} values were obtained and ToxPi scores were calculated for all compounds tested in the five serotonin assays identified through univariate analysis.

Among the top eleven compounds, three compounds had already been identified as PLLDs from our HTS and follow-up screening and were highly correlated to all five serotonin assays (**Table 2.2**). Those compounds were difenoconazole, prochloraz, and thidiazuron, and among them prochloraz was retested.

Table 2.2. Prediction of new PLLD compounds. The 5 ToxCast *in vitro* serotonin pathway assays retained were used to identify putative PLLDs. ToxPi tool was used to rank the new compounds based on their AC_{50} values for the 5 serotonin pathway related assays

S. No.	Chemical	ToxPi Score
High Prediction Score		
1	Prochloraz	0.72
2	Forchlorfenuron	0.67
3	Flusilazole	0.66
4	Clorophene	0.52
5	Pentamidine isethionate	0.59
6	Gentian Violet	0.54
7	AVE6324	0.53
8	Dodecylbenzenesulfonic acid	0.52
9	Didecyldimethylammonium chloride	0.50
Low Prediction Score		
1	Decane	0.30
2	CP-608039	0.13
3	CP-471358	0.12
Unscored		
1	Malic acid	0
2	CP-283097	0
3	CI-1029	0

The other eight compounds were tested and found to cause PLLD effects in zebrafish in a dose response manner (**Figure 2.10**). Among them, forchlorfenuron, flusilazole, and clorophene were ToxCast Phase I compounds that were not detected during HTS. Pentamidine isethionate, Gentian Violet, AVE6324, dodecylbenzenesulfonic acid, and didecyldimethylammonium chloride were among the ToxCast Phase II compounds. The PLLD effect percentages of these compounds were graphed and compared with that of the vehicle for statistical significance (**Figure 2.10**). All nine compounds had percentage effects higher than 20% which is the vehicle (DMSO) cut off value (**Figure 2.10 A-I**). Among them, prochloraz, fusilazole, and gentian violet were statistically significant (**Figure 2.10 A, B, E**) (unpaired student's T-test, $p < 0.05$, 95% CI). The three chemicals with the least ToxpPi scores did not have any significant effects on PLL (**Figure 2.10 J-L**). All three compounds with a zero-score caused PLL disruption at higher percentages than the vehicle-treated embryos. The results indicated an increased percentage of embryos with perturbed PLL with increasing doses for all the compounds (**Figure 2.10 M-O**).

Figure 2.10 Effects of PLLDs predicted using serotonin pathway assays in zebrafish. *Tg (neuromast:GFP)* embryos were exposed to increasing concentrations of (A-I) high prediction score PLLDs, (J-L) low prediction score PLLDs and (M-O) unscored PLLDs. Y-axis represents percentage of affected embryos and X-axis represents concentration of tested compound (M). The percentage PLLD effects (dark green), and dead percentage (light green) are shown. Statistical significance was determined using unpaired Student's t-test compared to vehicle treatment (*p <0.05, **p <0.01, ***p <0.001, ****p <0.0001).

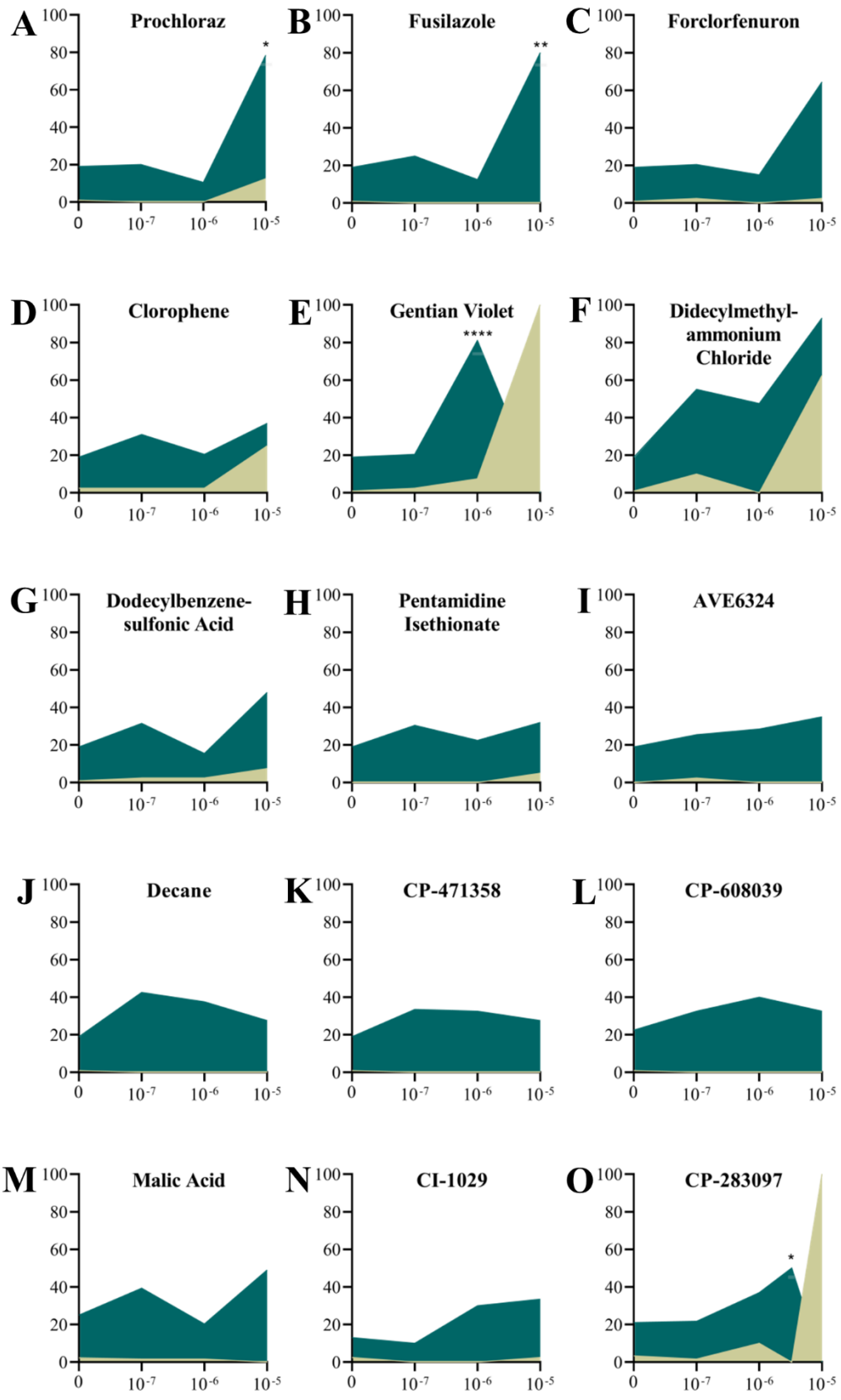
A
Prochloraz
*
B
Fusilazole
**
C
Forclorfenuron
D
Clorophene
E
Gentian Violet
****
F
Didecylmethyl-
ammonium
Chloride
G
Dodecylbenzene-
sulfonic Acid
H
Pentamidine
Isethionate
I
AVE6324
J
Decane
K
CP-471358
L
CP-608039
M
Malic Acid
N
CI-1029
O
CP-283097
*
100
80
60
40
20
0
0
10-7
10-6
10-5

In conclusion, based on the correlation of data between phenotypic high-throughput *in vivo* screening of all ToxCast Phase I chemicals and high throughput screening of *in vitro* assays, we predicted and differentiated PLL disruptors from non-PLL disruptors.

2.3 DISCUSSION

2.3.1 Identification of Novel Posterior Lateral Line Disruptors

We here describe the use of the zebrafish model to screen for posterior lateral line disruptors (PLLDs), and we use computational toxicology to decipher mechanisms of action for such disruptors. We first screened 292 chemicals of the ToxCast phase I chemical library and identified 22 chemicals that altered the number of neuromasts in the PLL after exposure (**Table 2.1**). We next performed univariate correlation analysis to identify *in vitro* ToxCast assays that are affected by those same 22 chemicals. Of the 13 *in vitro* assays identified, several assays are directly or indirectly involved in serotonin production, metabolism, or signaling. The role of serotonin in neuromast development was tested by exposing the embryos to known serotonin modulating compounds, such as clorgyline and PCPA, which confirmed a role for serotonin in PLL development.

Because of their structural resemblance to mammalian hair cells of the inner ear, the zebrafish lateral line has been used for large library screens to identify chemicals that protect against ototoxicity; compounds belonging to the benzothiophene carboxamides family and several FDA approved drugs were identified as being protective (Owens *et al.*, 2008; Ou *et al.*, 2009; Vlasits *et al.*, 2012). On a molecular level, neuromast primordium migration parallels the migration of cancer

cells during metastasis relying on chemokine receptors, such as CXCR4 and CXCR7 and their ligand CXCL12. Based on this notion, the whole zebrafish organism was used in high throughput chemical screening to identify small-molecule modulators of PLL migration, which identified several compounds that both inhibited neuromast migration, breast cancer cell migration *in vitro*, as well as metastasis of the highly metastatic mouse mammary tumor cell line 4T1 *in vivo* in mice (Gallardo *et al.*, 2015). These studies show that because of molecular and structural conservation between mammals and zebrafish, findings in the latter organism often can be extrapolated to mammals. Along this line of reasoning, chemicals that perturb neuromast development in zebrafish may pose risks to mammals, although mammals do not have neuromasts per se. Further research will be required to investigate whether the PLLDs identified here perturb mammalian tissues or cells, such as inner ear hair cells.

2.3.2 Identification of Altered Pathways Through Computational Toxicology

Through computational toxicology, several assays were suggested to be affected by the PLLDs; serotonin-related assays being the most obvious ones. The neurotransmitter serotonin in mammals is present in the digestive system, blood and throughout the central nervous system. Serotonin is produced within axon terminals in a two-step process from the essential amino acid L-tryptophan with the rate-limiting step being hydroxylation of tryptophan by the enzyme tryptophan hydroxylase (Nichols and Nichols, 2008). Serotonin is then packed into vesicles by transporter proteins for release into the synapse in response to an action potential to activate postsynaptic receptors (Lawal and Krantz, 2013). The serotonin receptor family is the largest neurotransmitter G-protein coupled (GPCR) family with 13 distinct genes encoding for its receptors. Besides, there is one ligand-gated ion channel, the 5-HT3 receptor (Barnes and Sharp, 1999; Nichols and Nichols,

2008). The presynaptic serotonin autoreceptors (5-HT1A and 5-HT1B receptors) respond to the presence of synaptic serotonin to regulate synthesis and release within the presynaptic axon terminal. Free serotonin is extracted from the synapse by the serotonin reuptake protein (SERT) in the presynaptic membrane. It is then either repackaged into vesicles for release into the synapse or degraded through deamination by monoamine oxidase A (MAO-A) (Nichols and Nichols, 2008). One of the metabotropic serotonin GPCR, the 5-HT_7 receptor (HTR_7) ToxCast *in vitro* assay had seven out of the 22 PLLDs as hits, which is a strong indication of serotonin's role in PLL development. HTR_7 has the highest affinity for serotonin (Barnes and Sharp, 1999; Bin Wei *et al.*, 2019) and is expressed in the hypothalamus, thalamus, hippocampus and the cerebral cortex in the CNS (Bard *et al.*, 1993; Barnes and Sharp, 1999; Nichols and Nichols, 2008; Bin Wei *et al.*, 2019). HTR_7 is involved in regulating sleep, circadian rhythms, body temperature and has also been indicated as playing a role in depression (Barnes and Sharp, 1999; Nichols and Nichols, 2008; Bin Wei *et al.*, 2019). Seven of the PLLDs also affected the CYP2D1 assay. CYP2D1 is a rat cytochrome P450 enzyme that is homologous to the human CYP2D6 (83% homology) (Miksys *et al.*, 2000; Zhou *et al.*, 2019). It is important for the metabolism of neurotransmitters and neuroactive steroids as well as centrally acting drugs such as monoamine oxidase inhibitors, tricyclic antidepressants, vasodilators (Dutheil, Beaune and Loriot, 2008). In the brain, CYP2D1 catalyzes the formation of serotonin by O-demethylation of 5-methoxytyptamine (5-MT) as an alternative pathway to the classic serotonin synthesis (by tryptophan hydroxylation) pathway (Dutheil, Beaune and Loriot, 2008; Haduch *et al.*, 2013; Singh *et al.*, 2015). Selective serotonin reuptake receptor inhibitors (SSRI's) such as fluoxetine and paroxetine are potent inhibitors of CYP2D1's activity. Eight PLLDs affected the Monoamine Oxidase A (MAO-A)-assay. MAO-A is an enzyme located in the outer mitochondrial membrane which preferentially catalyzes the

oxidative deamination of monoamine neurotransmitters (serotonin, norepinephrine, and dopamine) with the highest affinity for serotonin (Bortolato and Shih, 2011). MAO-A has a key role in the inception, and advancement of embryonic neurodevelopment and neuropsychiatric disorders. Consequently, MAO inhibitors are potent anti-depressants and act by increasing neurotransmitter levels, such as serotonin. Six PLLDs affected the *ADRA2B* gene assay. Adrenoceptor α_{2B} (AR-α_{2B}) encoded by the *ADRA2B* gene is a GPCR, mediating the physiological actions of endogenous catecholamines, norepinephrine, and epinephrine (Lomasney *et al.*, 1990; Nicholas *et al.*, 1991; Weiskopf and Todd, 2000). Presynaptic AR-α_2 also modulates the release of serotonin at the serotonergic nerve terminals (Ma, Rajakumaraswamy and Maze, 2005). Six PLLD compounds affected the Solute Carrier Family 18 Member A2 (*SLC18A2*) assay. The *SLC18A2* genes encode the protein vesicular monoamine transporter 2 (VMAT2). VMAT2 is an ATP-dependent vesicular transporter for monoamines with the highest affinity for serotonin. It is responsible for the active transport of neurotransmitters into secretory vesicles for exocytotic release. Numerous environmental pollutants act by inhibiting VMAT activity, including the organochlorine pesticide heptachlor and polychlorinated biphenyls (PCBs) (Lawal and Krantz, 2013). Just below our cutoff value for correlating assays was the assay for Nuclear Factor 1A (NF1A), a transcription factor that regulates expression of the $5HT_3$ receptor, which is the serotonin-gated ion channel (in contrast to the other serotonin receptors that are GPCRs). The fact that all these serotonin-related ToxCast assays are affected by PLLDs identified by us indicates that serotonin is important for normal PLL development, and if perturbations occur, neuromast numbers will become altered.

The other large group of correlating *in vitro* ToxCast assays contained assays for hormone and steroid signaling. These assays included the retinoic acid receptor (RAR), farnesoid X receptor α (FXRα, NR1H4), and thyroperoxidase (TPO), a hemoprotein that plays a key role in thyroid hormone synthesis (T3 and T4). Retinoic acid (RA) and thyroid hormone both have multitudes of effects during embryonic development. Worth mentioning in this context is that endogenous RA plays a role in the development and maintenance of the Organ of Corti of the inner ear via the RARα and RARγ receptors (Lefebvre *et al.*, 2005; Romand, Dollé and Hashino, 2006). Treatment with exogenous RA significantly increases the number of cells that developed as hair cells in the Organ of Corti (Kelley *et al.*, 1993). For the thyroid hormone system, knockout of thyroid hormone receptor beta in mice causes deafness through malformation of the Tectorial Membrane (Forrest *et al.*, 1996; Winter *et al.*, 2009), an apical membrane of the extracellular matrix, which lies over the Organ of Corti. Another correlating assay was the transmembrane translocator protein (TSPO)-assay. In steroidogenesis, in response to hormonal signals, TSPO forms a multiprotein complex for the import of cholesterol from intracellular stores into mitochondria, which is a rate-determining step in hormonal regulation of steroidogenesis (Batarseh and Papadopoulos, 2010; Rupprecht *et al.*, 2010). Furthermore, assays for CypP450s (CYP2A1 and CYP2C13) correlated to the PLLDs. Both these enzymes are sex-specific and involved in testosterone metabolism. PLLDs also affected the Sigma Nonopioid Intracellular Receptor 1 (SIGMAR1, σ_1R)-assay. SIGMAR1 is a transmembrane chaperone protein localized both at the plasma membrane and endoplasmic reticulum, and it is expressed in neurons and oligodendrocytes in all parts of the brain. SIGMAR1 is responsible for mitochondrial metabolic regulation and promotes mitochondrial energy depletion and apoptosis. In the endoplasmic reticulum, they modulate Ca^{2+} signaling through IP3 receptors. These receptors also regulate ion channels, lipid transport and metabolism,

neurite formation, cellular differentiation, and myelination in the brain (Rousseaux and Greene, 2016). Finally, an assay for PLAUR, the gene that encodes the Urokinase-type Plasminogen Activator (uPA) Receptor (uPAR), correlated to the PLLDs. The PA system has functions in biological processes such as embryogenesis, angiogenesis, cell migration, wound healing, inflammatory response, apoptotic cell death and cancer processes, such as tumor growth, angiogenesis, tumor cell invasion, migration and metastasis (Mahmood, Mihalcioiu, and Rabbani, 2018). However, the specific roles of hormones, steroids, σ_1R and the PA system for neuromast development remain to be investigated.

2.3.3 Serotonin Signaling is Required for Normal Posterior Lateral Line Development

Serotonin modulators such as methylene blue and clorgyline inhibit MAO-A activity either reversibly or irreversibly, respectively, resulting in increased intracellular serotonin (Ramsay, Dunford and Gillman, 2007; Top *et al.*, 2014; Charles and Brandom, 2015; Ooi, Hayden and Pouladi, 2015; Garcia-Miralles *et al.*, 2016). Other serotonin modulators such as PCPA prevent serotonin formation from tryptophan through inhibition of the rate-limiting enzyme tryptophan hydroxylase (Dringenberg *et al.*, 1995; Airhart *et al.*, 2012). The serotonin modulator, fluoxetine is known to affect serotonin levels through a few different mechanisms, the primary one being inhibiting the reuptake of free serotonin through SERT (Crewe *et al.*, 1992; Wong, Bymaster and Engleman, 1995; Barnes and Sharp, 1999; Sangkuhl, Klein and Altman, 2009; Haduch *et al.*, 2013). Upon treatment of zebrafish embryos with these known mammalian serotonin modulators, we observe that they reduce the number of neuromasts deposited in the PLL as well as affect the serotonin levels in zebrafish as seen through immunostaining. This indicates that the levels of serotonin are controlled in a similar way in fish and mammals. As expected, treatment with

methylene blue and clorgyline increased serotonin levels, whereas PCPA decreased serotonin staining. In fluoxetine treated embryos, we observed a general decrease in brain serotonin staining compared to the vehicle treatment except in choroid plexus either because of the serotonin negative feedback loop or as seen in mammalian studies, acute dosing of SSRI's doesn't produce an increase in synaptic serotonin (Bel and Artigas, 1993; Briley and Moret, 1993; Benmansour *et al.*, 2002; Sangkuhl, Klein and Altman, 2009). The region with the strongest increase in serotonin staining after treatment with MAO-A inhibitors, methylene blue, and clorgyline, was observed to be the choroid plexus. More specifically, serotonin staining highlighted the diencephalic choroid plexus at the most dorsal portion of the third ventricle, just anterior to the pineal gland, which contains serotonergic neurons. The choroid plexus is known to act as a sink for excess neurotransmitters in the brain (Kaslin and Panula, 2001; Henson *et al.*, 2014). It is, thus, reasonable to assume that an excess of serotonin in the brain by MAO-A inhibitor treatment would result in serotonin drain through the diencephalic choroid plexus. Furthermore, the choroid plexus epithelial cells have developmentally evolved from neuroepithelial cells. Neuroepithelial cells, distributed over the whole skin surface in young zebrafish larvae, have previously been identified by serotonin immunolabelling (Coccimiglio and Jonz, 2012). These cells, which are observed in our stained larvae, contain synaptic vesicles and are associated with nerve fibers, just as neuromasts are. These skin neuroepithelial cells sense and respond to hypoxia during early zebrafish embryo development (Coccimiglio and Jonz, 2012). Thus, sensing of the surrounding environment by neuroepithelial cells, such as neuromasts or the skin neuroepithelial cells, may have in common serotonin as a signaling molecule.

At this point, we do not know the exact mechanism by which serotonin contributes to neuromast development. The different aspects of PLL development that serotonin could be involved in are

PLL primordium migration or proliferation, or neuromast differentiation or cell survival, or neuromast nerve innervation, or proper neuromast development and deposition. We would require further studies to tease out which PLL development process is under serotonin control. However, the serotonin levels must be strictly regulated as both increased and decreased serotonin levels affected neuromast numbers. What is also clear is that screening in an *in vivo* model in combination with computational toxicology can both identify toxic chemicals and concurrently discover their modes of action. Furthermore, through such medium-throughput *in vivo* assays, a phenotype-specific profile of correlating ToxCast assays can be obtained. This profile can further be used to rank toxicants tested in the Tox21 project to speed up prioritization of chemicals for further testing *in vivo*, and in the long run, result in an improved risk assessment for human and environmental health.

2.2.4 Toxicity Prediction Based on ToxCast Assay Targets

Based on the *in vitro* assay targets, the identified PLLDs affect multiple pathways of which serotonin was the most obvious. We hypothesized that if a compound affects these serotonergic *in vitro* endpoints, then it could potentially be a PLLD *in vivo*. To test this, ToxCast data for the five serotonergic assays were used. All the ToxCast Phase I and Phase II compounds were ranked based on their bioactivity of the *in vitro* endpoints that correlated with zebrafish PLLDs. Eight of the 11 top-ranked compounds were tested in zebrafish and none of these compounds had been tested in zebrafish during the initial screening. As predicted, exposure to these eight compounds caused PLL disruption in zebrafish in a dose-dependent manner. Exposure to the predicted non-PLLDs (low ranked) did not show any effects on neuromast pattern *in vivo*. Interestingly, all three tested compounds with a zero score for PLL disruption affected neuromast pattern in the PLL in a dose-

dependent manner. The compounds that received a zero score for PLL disruption, did so because they were tested in one or more of the five serotonin-related *in vitro* assays and had no effect. Of all the zero-scored compounds, hundred had been tested in only one of the five serotonin assays, while five compounds including Malic acid, CI-1029, and CP-283097 had been tested in two serotonin assays. Only one compound had been tested in four of the five serotonin assays. All three tested compounds with a zero score for PLL disruption affected neuromast pattern somewhat in the PLL in a dose-dependent manner. This goes to show the importance and need of whole organism toxicity testing required to observe the phenotypic effects of these compounds. Their mechanism of action is yet to be elucidated, but they may be affecting the serotonin pathway through a mechanism that is not yet covered by the ToxCast *in vitro* assays. In conclusion, zebrafish based *in vivo* data in combination with ToxCast *in vitro* data can be utilized to predict the *in vivo* toxicity of novel compounds.

CHAPTER 3: IDENTIFICATION AND PREDICTION OF VASCULAR DISRUPTOR COMPOUNDS

3.1 INTRODUCTION

Disruption of vascular development during embryonic stages in mammals does not just result in severe birth defects, but also reduces fetal survival (Isogai, Horiguchi and Weinstein, 2001). Thalidomide, a drug widely prescribed to pregnant women for morning sickness approximately fifty years ago, was found to cause severe birth defects in over 80% of the babies while also increasing infant mortality (Therapontos *et al.*, 2009). The birth defects caused were shortening or absence of limbs; eye, ear, and facial damage; and malformations of internal organs. Thalidomide was later found to be anti-angiogenic (Therapontos *et al.*, 2009). The specific teratogenic birth defects caused by thalidomide demonstrated the wide range of phenotypic malformations caused by vascular disruption and highlighted the importance of identifying vascular disruption compounds (VDCs) to protect unborn babies from exposure.

3.1.1 Vascular System Development in Zebrafish

The zebrafish has a closed vascular circulatory system just as is seen in higher vertebrates (Gore *et al.*, 2012). The zebrafish vasculature develops through the processes of vasculogenesis and angiogenesis. Vascular development in zebrafish begins with vasculogenesis, which is the formation of completely new blood vessels without relying on pre-existing vessels (Zhong *et al.*, 2001; Hogan and Schulte-Merker, 2017). This process begins at approximately 12 hpf when the angioblasts (endothelial precursor cells) are specified in the lateral plate mesoderm and start migrating to the midline (Kimmel, Warga and Schilling, 1990; Fouquet *et al.*, 1997; Zhong *et al.*, 2001). By 14-15 hpf, these migrating angioblasts start to reach the midline and express endothelial cell markers. By 22 hpf, they give rise to two major blood vessels; the dorsal aorta (DA) and posterior cardinal vein (PCV) along the ventral midline (**Figure 3.1**) (Wilkinson and Van Eeden,

2014). By twenty-six hpf tubulogenesis begins allowing blood flow (Hogan and Schulte-Merker, 2017). Sprouting angiogenesis commences from the DA to give rise to intersegmental vessels (ISV) in the trunk (Bushby *et al.*, 2012; Hogan and Schulte-Merker, 2017). ISV's elongate and migrate dorsally between the vertical somite boundaries and are recognizable by 28 hpf (Wilkinson and Van Eeden, 2014; Hogan and Schulte-Merker, 2017). The ISVs connect laterally to form the dorsal longitudinal anastomosing vessels (DLAVs) just dorsally of the roof of the neural tube (**Figure 3.1**) (Zygmunt *et al.*, 2012). This process is completed by twenty-eight to thirty hpf (Hogan and Schulte-Merker, 2017). By two dpf, most trunk vessels become luminized and blood flow is established (Isogai, Horiguchi and Weinstein, 2001). The processes of vasculogenesis and angiogenesis have been visualized in zebrafish through the use of transgenic fish expressing fluorescence in vascular endothelial or blood cells.

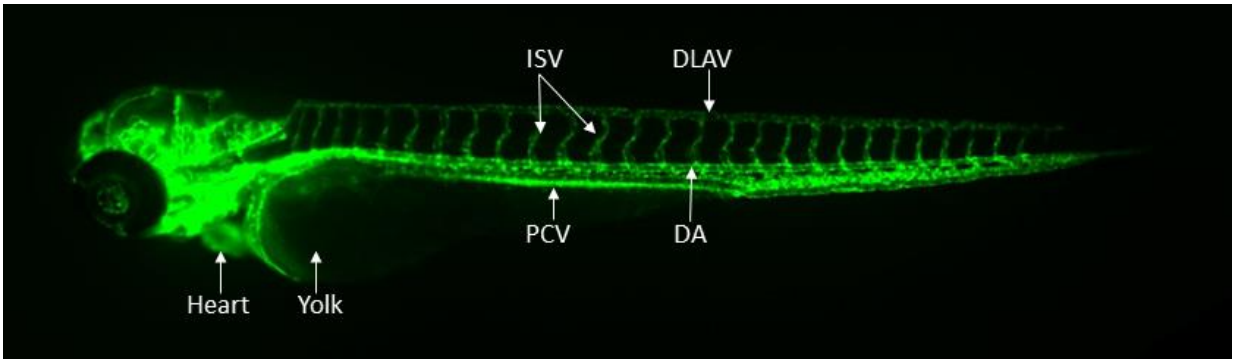

Figure 3.1 Vascular system of zebrafish at four dpf. *Tg (kdrl:EGFP)* larva expressing GFP in the vascular endothelial cells, was imaged laterally. The two main vessels are DA, dorsal aorta and PCV, posterior caudal vein. ISV, intersegmental vessels run between somite boundaries and fuse at the dorsal most region of the body to form DLAV, dorsal longitudinal anastomotic vessels.

3.1.2 Human Umbilical Vascular Endothelial Cells (HUVEC)

The basement membrane (BM) is a specialized extracellular matrix-like material beneath cells (Kalluri, 2003). It is known to be produced by most cell types, but the constituents of BM produced by each cell type are different and this is what gives tissues their specificity and unique structure

(Kalluri, 2003; Arnaoutova and Kleinman, 2010). For endothelial cells, the BM specifically causes the formation of capillary-like tubes. *In vivo,* the vascular BM is responsible for the tube-like barrel structure of blood vessels where it is lined by endothelial cells on the inside and smooth muscle cells on the outside (Madri and Williams, 1983; Kubota *et al.*, 1988; Kalluri, 2003; Arnaoutova and Kleinman, 2010). The major components that distinguish the vascular BM from other BMs are laminins 8 and 10, collagen IV, and nidogens/entactins 1 and 2 (Arnaoutova and Kleinman, 2010).

Understanding of how endothelial cells and BM interact *in vivo* and the factors that contribute to vessel formation has advanced the successful development of angiogenesis assays *in vitro* using endothelial cells derived from various sources, all capable of forming capillary tubes (Folkman and Haudenschild, 1980; Maciag *et al.*, 1982; Madri and Williams, 1983; Arnaoutova and Kleinman, 2010). One source is the endothelial cells derived from human umbilical vein (HUVECs), which are commonly used for these *in vitro* assays (Maciag *et al.*, 1982; Arnaoutova and Kleinman, 2010). HUVECs are typically incubated with BM obtained from a murine tumor cell line that is commercially available as Matrigel (Arnaoutova and Kleinman, 2010). Under these conditions, the HUVECs attach to the matrix, migrate towards each other, align and form tubes within six to twenty hrs (Arnaoutova and Kleinman, 2010). The tubes formed can be assessed through several software programs. This assay is fast, simple, quantitative and robust and can easily be used for *in vitro* mammalian high throughput screening of chemical libraries to identify disruptors of angiogenesis.

Both the *in vivo* zebrafish vascular assay and the *in vitro* HUVEC angiogenesis assay complement each other for toxicity screening in the sense that the zebrafish captures the effects of chemicals at

the whole organism level whereas the HUVECs capture the effects on mammalian systems. Both these systems are amenable to rapid screening methods and in combination can provide a quick, more complete picture of the mechanisms underlying the actions of vascular disruptor compounds in humans.

3.1.3 Screen for Vascular Disruptor Compounds

We previously reported the identification of VDCs in zebrafish embryos and the murine yolk-sac-derived endothelial cell line C166 (McCollum *et al.*, 2017). We screened 175 compounds from the ToxCast phase I chemical library using transgenic fish with GFP expression in the vasculature, which allows for the visualization of vascular structures. We identified several phenotypically different apical endpoints for vascular disruption, including disruption of intersegmental vessel (ISV) structure, failure to condense the caudal vein plexus (CVP), cardiac edema, and blood clots. The identified fish VDCs were rescreened in C166 cells, which can be induced to form endothelial cell tubular networks, similarly to HUVECs. In total 34 compounds were identified to perturb vascular development in zebrafish, and out of these, 22 compounds inhibited tube formation in C166 cells (McCollum *et al.*, 2017).

Based on data mining of EPA's Comptox Chemicals Dashboard (https://comptox.epa.gov/dashboard), HTS *in vitro* assays for specific pathways with evidence to be involved in angiogenic or vasculogenic processes were selected as a VDC profile (Kleinstreuer *et al.*, 2011). Correlation studies of VDCs in zebrafish based on this profile suggests that interference with chemokine signaling, extracellular matrix components, and the vascular endothelial growth factors, particularly VEGFR2, in the ToxCast *in vitro* assays, is indicative of vascular disruption in zebrafish (McCollum *et al.*, 2017). It further suggests that the identification

of chemicals that interfere with these pathways *in vitro* could be predictive of vascular disruption capacity *in vivo*. A correlation study of a larger set of VDCs in zebrafish and other testing systems, identified by screening performed in several laboratories, to HTS results of all ToxCast assays, were conducted to find assays that may be informative of vascular toxicity *in vivo* but were not contained in the initial VDC signature (Tal *et al.*, 2017). Highly correlated novel HTS assays were identified and include an x-box binding protein transcriptional assay and two primary endothelial cell death assays (Tal *et al.*, 2017). However, these studies were based on data of various apical phenotypes of vascular disruption in zebrafish, as well as testing in cells. Because different vascular toxicity phenotypes in zebrafish, such as malformed ISVs and uncondensed CVP, is likely, at least partly, caused by different molecular initiating events, the correlations to pathways may reflect several different and unrelated events.

We here set out to generate and test a more specific VDC profile by focusing on one phenotype only. We selected the disruption of ISVs to represent a phenotypic angiogenesis assay, and among 175 tested ToxCast chemicals, selected the ones that caused ISV perturbations. We investigated the effect of selected ISV Vascular Disruptor Compounds (ISV-VDCs) on zebrafish angiogenesis *in vivo* and human umbilical vascular endothelial cells (HUVEC) tube formation *in vitro*. By univariate correlation analysis, we identified assays that correlated to the ISV-VDCs and used these assays to predict and rank potentially novel vascular disruptors.

3.2 RESULTS

3.2.1 Identification of Novel Vascular Disruptor Compounds (VDC)

McCollum *et al.* from our lab previously screened 175 chemicals of the EPA's ToxCast Phase I library in the *Tg (kdrl:EGFP)mitfa*$^{b692/b6s92}$ embryos of zebrafish to identify VDCs (McCollum *et al.*, 2017). Out of all the VDCs identified, ten chemicals specifically caused ISV disruption (ISV-VDCs) (**Table 3.1**).

Table 3.1. The 10 ISV-VDCs identified in the initial screen of 175 compounds from the ToxCast Phase I library

S. No.	Chemical	LEL (µM)
1	Pyraclostrobin	0.01
2	Rotenone	0.01
3	Trifloxystrobin	0.01
4	Acibenzolar-S-methyl	0.1
5	Dicofol	0.1
6	(Z,E)-Fenpyroximate	0.25
7	Pyridaben	0.25
8	Niclosamide	0.5
9	Diniconazole	6
10	Tebupirimfos	30

3.2.2 VDC Exposure Causes Dose-Dependent ISV Perturbation *in vivo* and *in vitro*

We selected five potent compounds among the 10 ISV-VDCs identified to analyze dose-dependent toxicity. *Tg (kdrl:EGFP)mitfa*$^{b692/b692}$ embryos were exposed to increasing concentrations of fenpyroximate, pyraclostrobin, pyridaben, rotenone, and trifloxystrobin. All five compounds showed a dose-dependent increase in toxicity (**Figure 3.2**).

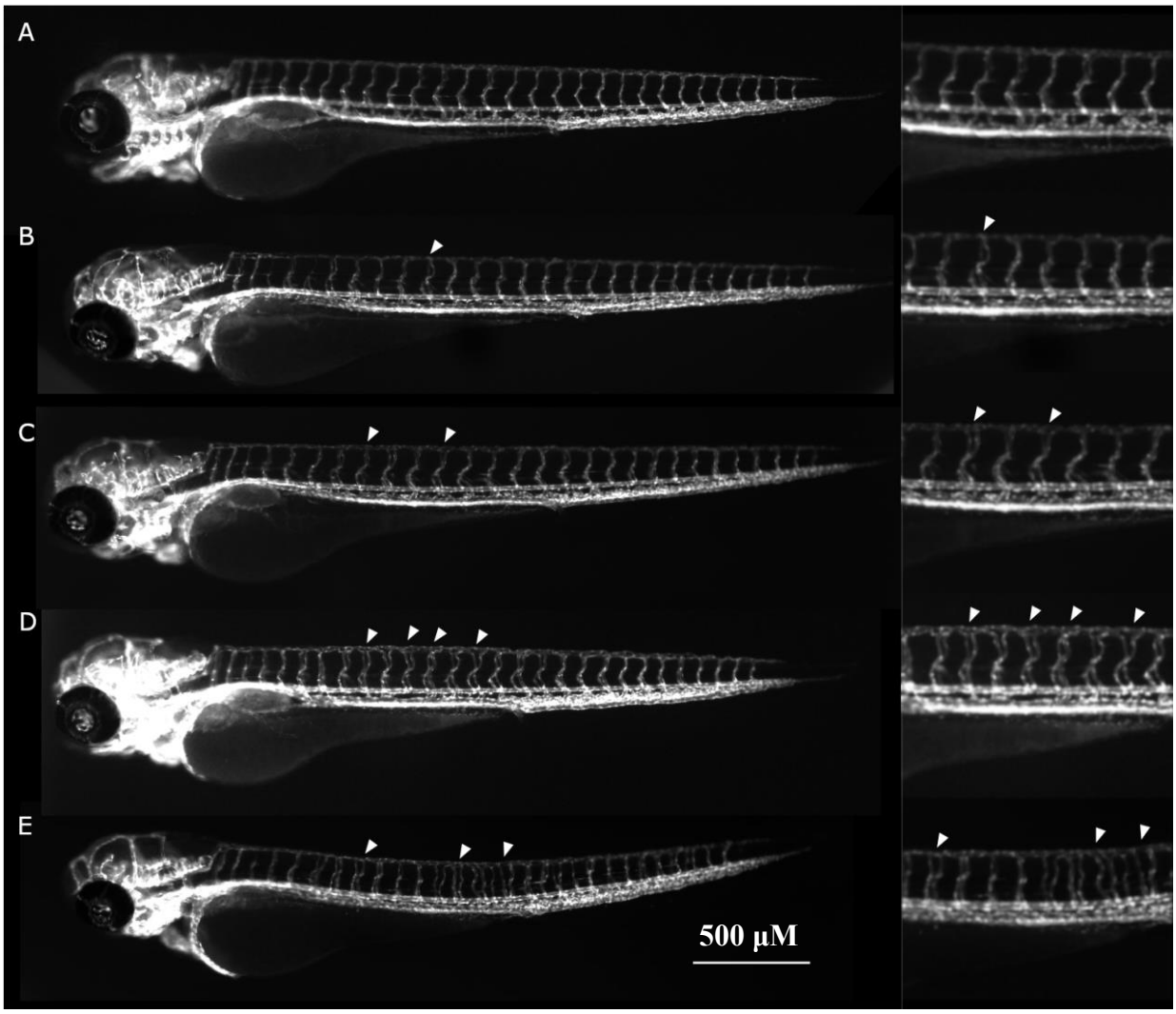

Figure 3.2 Rotenone causes ISV effects in a dose-dependent manner. *Tg (kdrl:EGFP)* larvae were exposed from approximately five hpf to four dpf. The arrowheads point to areas of perturbed ISV formation and the right panel shows these areas at higher magnification. (A) Vehicle treated larvae; (B) 1 nM, (C) 10 nM, (D) 30 nM and (E) 100 nM of rotenone treated larvae. We observed increased ISV perturbations with increasing rotenone concentrations.

Secondly, the percentage of affected embryos out of the treated clutch also increased with increasing concentrations for all five chemicals tested. This was depicted as the percentage effect, which followed a concentration-dependent pattern (**Figure 3.3**).

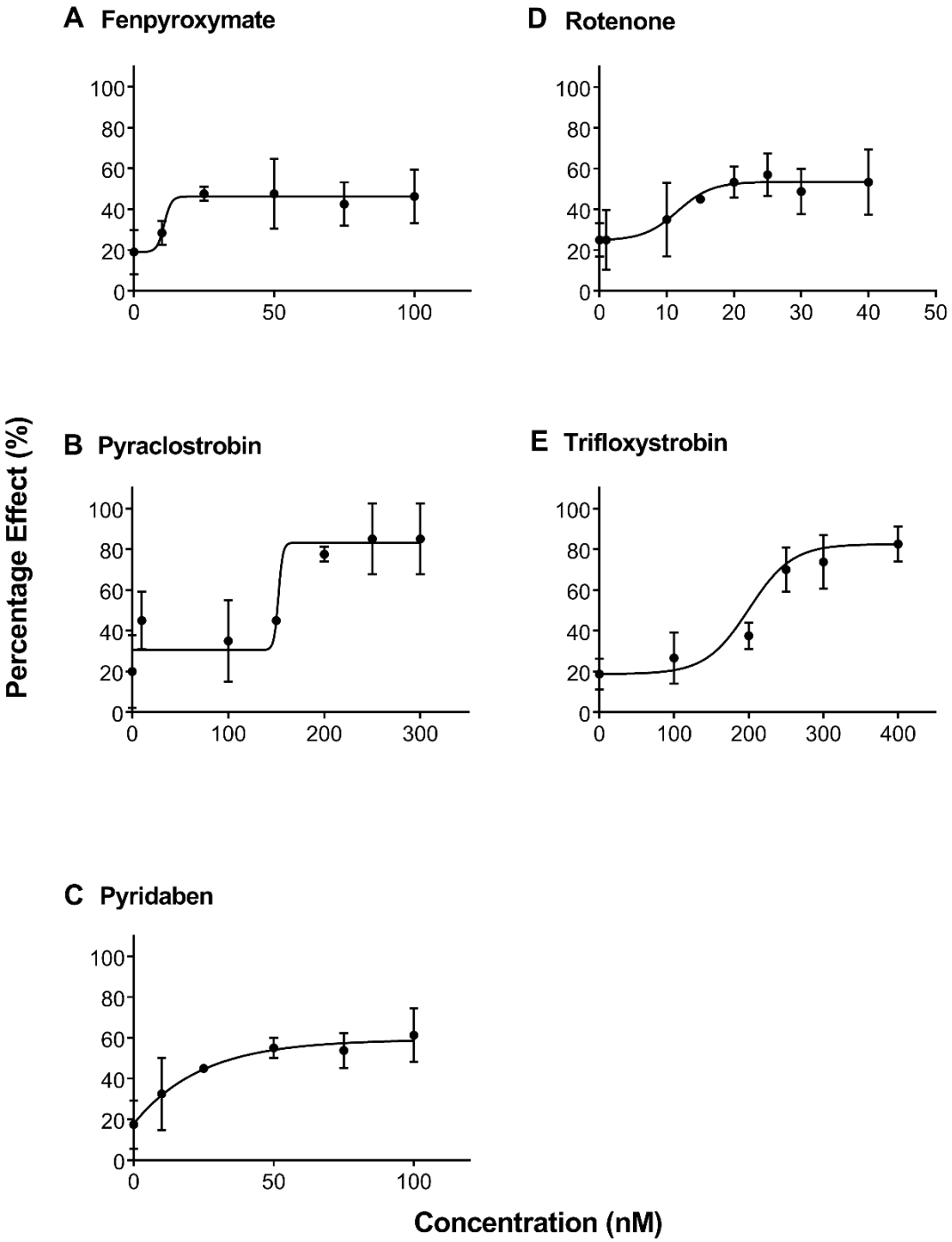

Figure 3.3 VDCs cause ISV effects in a dose-dependent manner. The graphs display the percentage of treated larvae having ISV effects vs the treatment concentration in nM. (A) Fenpyroximate, (B) Pyraclostrobin, (C) Pyridaben, (D) Rotenone, and (E) Trifloxystrobin. All chemicals tested affected an increasing number of embryos with increasing concentrations.

For example, with increasing concentrations of rotenone, increasing numbers of non-overlapping intersegmental vessels and more severe ISV effects, including short, thin and unevenly spaced ISVs, were obtained (**Figure 3.2 B-E**). In addition, with increasing concentrations, the proportion of affected embryos also increased for all five chemicals tested (**Figure 3.3**).

Next we tested the effects of the five potent compounds *in vitro*. We investigated the capacity of the compounds to disrupt tube formation in human primary umbilical vein endothelial cells (HUVECs). We analyzed the tube formation by time-lapse microscopy over 24 hrs, which allows for visualization of both tube formation and break down. All parameters for tube formation were analyzed using the ImageJ angiogenesis analyzer plugin (**Figure 3.5 A'-D'**). As seen in zebrafish, four of the ISV-VDCs also disrupted HUVEC tube formation (**Figure 3.4**) in a dose-dependent manner (**Figure 3.5 B-D**). The total mesh area, which represents the total area of networks formed was significantly decreased from as early as two hrs post-seeding for the 50 µM concentrations of fenpyroximate, pyraclostrobin, and pyridaben, as well as for 0.1 µM rotenone, and did not recover to vehicle control levels even 24 hrs post-seeding (**Figure 3.6**). The VEGFR2 receptor inhibitor, PTK787, was used as a positive control. A heat map was created to represent the other quantified parameters at eight hrs post-seeding (**Figure 3.7**). No effect on tube formation was observed with exposure to trifloxystrobin at the highest concentration tested (100 µM). At higher concentrations, the chemical precipitated out of the solution, and could not be tested. In conclusion, out of five potent ISV-VDCs with activity *in vivo* in zebrafish embryos, four perturbed tube formation *in vitro* in HUVECs.

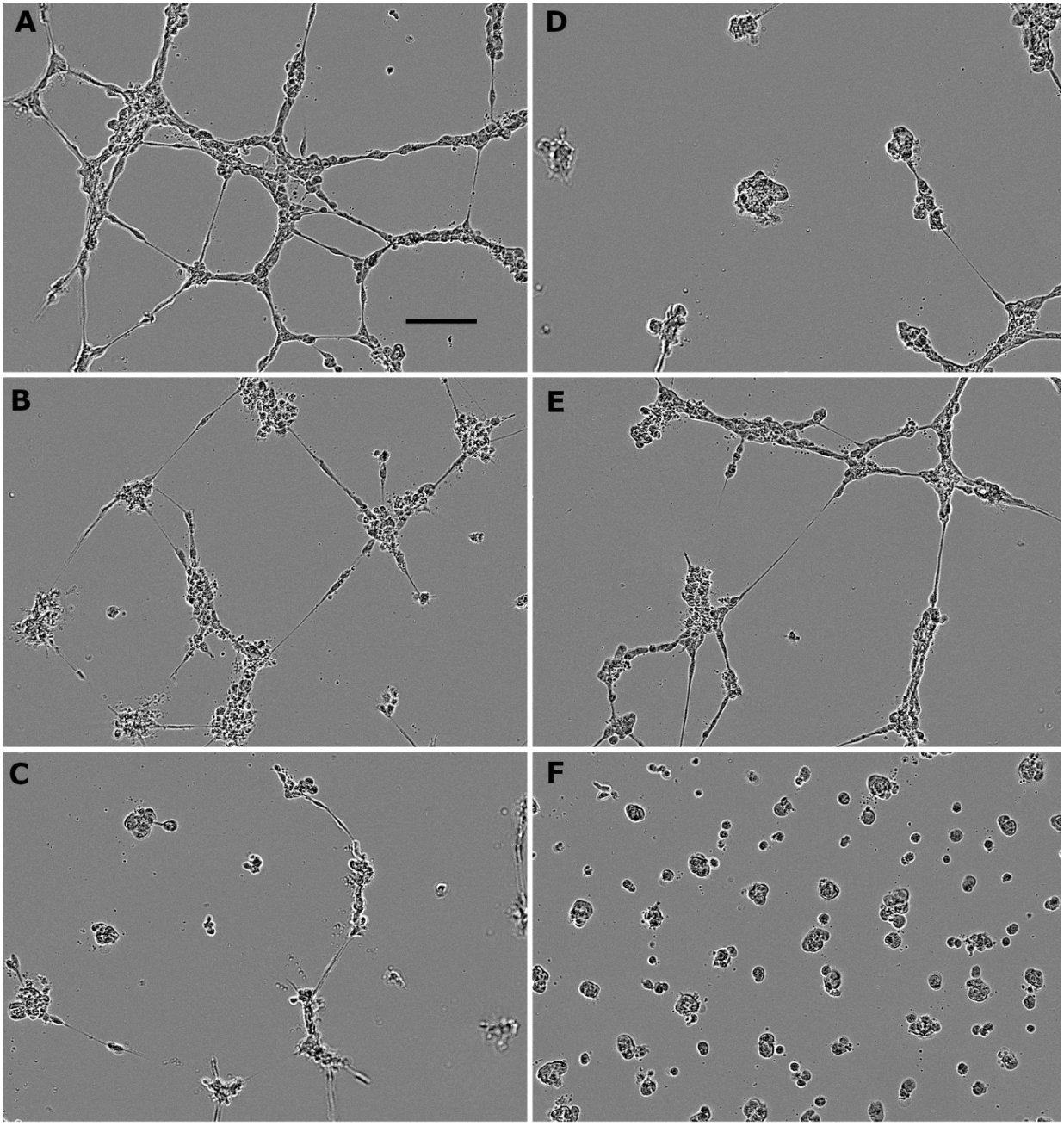

Figure 3.4 All VDCs tested affected HUVEC tube formation. HUVECs were pre-treated with the chemical and seeded on Matrigel to allow for tube formation. The assay was imaged after eight hrs of seeding. Scale bar 100 µm. (A) Vehicle, (B) 50 µM PTK, (C) 10 µM Fenpyroximate, (D) 10 µM Pyraclostrobin, (E) 10 µM Pyridaben, and (F) 10 µM Rotenone.

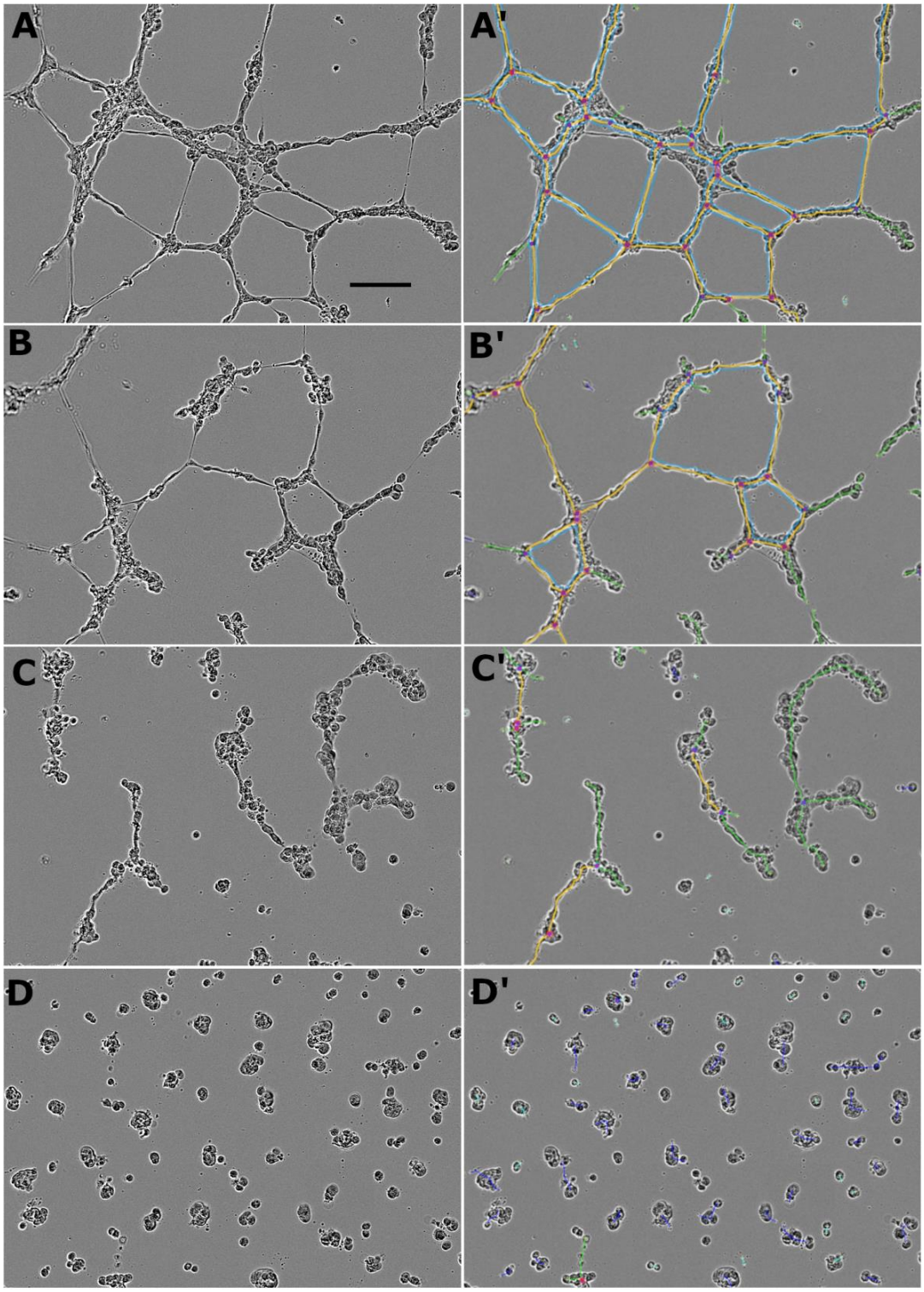

Figure 3.5 The VDCs perturb HUVEC tube formation in a dose-dependent manner. HUVECs were pre-treated with the compound, seeded and then imaged eight hrs post-seeding. Scale bar 100 µm. (A, A') Vehicle treatment; (B, B') 0.1 µM, (C, C') 1 µM and (D, D') 10 µM Rotenone treatment. (A'-D') The networks were mapped using angiogenesis analyzer.

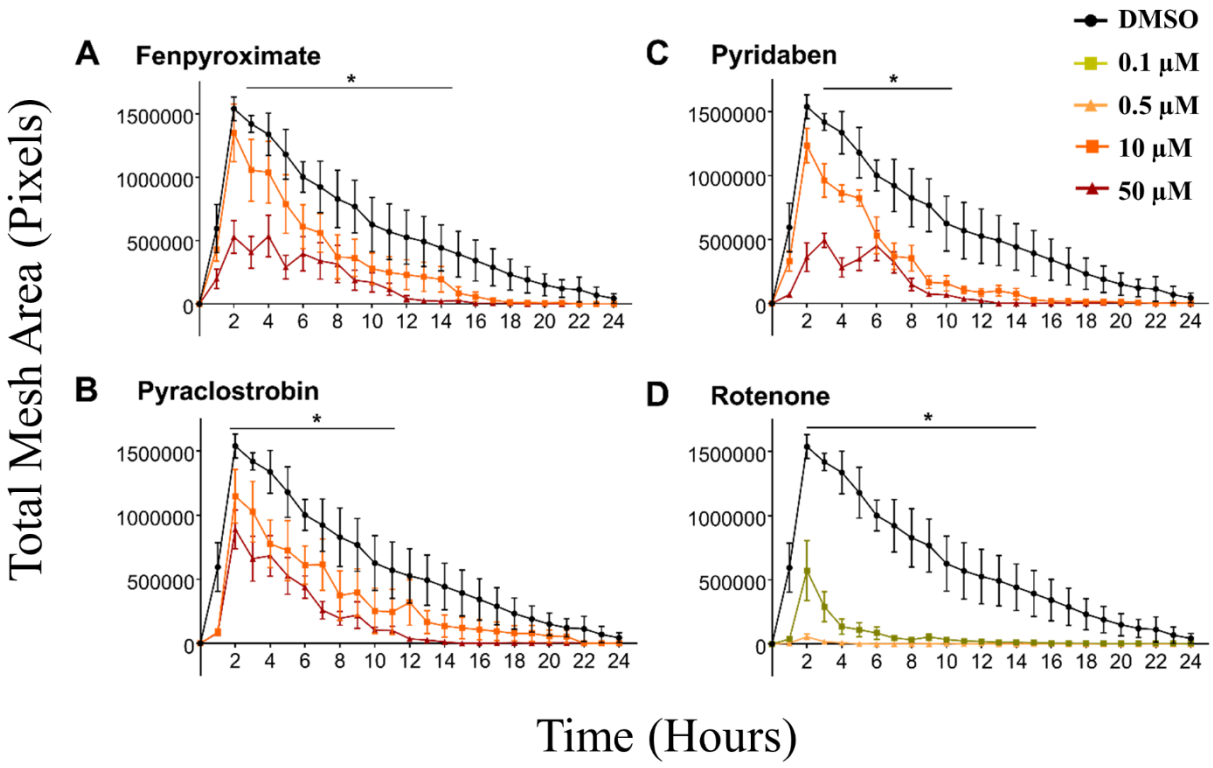

Figure 3.6 VDCs reduced the total mesh area of HUVEC tube formation assay. HUVEC exposed to chemicals, seeded in Matrigel and imaged every hour for 24 hrs post-seeding with IncuCyte ZOOM. The mesh area was measured using ImageJ angiogenesis analyzer. (A) Fenpyroximate, (B) Pyraclostrobin, (C) Pyridaben, and (D) Rotenone.

Figure 3.7 VDCs disrupt HUVEC tube formation. A heat map of the different parameters of tube formation at eight hrs post-seeding as measured by angiogenesis analyzer. For each category, the mean values of the vehicle treatment were set to 100 as the baseline value. Green color indicates lower than baseline and red color higher.

3.2.3 Putative VDC Signatures for the Identified ISV Disruptors

We used the VDC screening results to identify ToxCast *in vitro* assays that correlate with the ten identified zebrafish ISV-VDC disruptors by univariate correlation analysis. All 900+ assays present in the ToxCast screening program (available at https://comptox.epa.gov/dashboard/) were used to identify the signature putative VDC (pVDC) assay profile (see Appendix Table 6) (Reif *et al.*, 2010). To eliminate the *in vitro* assays for cell stress and cytotoxicity which indicate general toxicity, we applied a z-score, as described by Judson *et al.* (Judson *et al.*, 2016) and in methods. Nineteen different *in vitro* assays were identified, including assays for nuclear receptor signaling (AR, THR and RAR), other transcription factors (Hif1a, Pou2F1, SP1, etc.), as well as signal transduction assays (NfκB) (Appendix Table 6).

The ToxPi tool was used to visualize the bioactivity profiles of the ten chemicals, and to score their potency towards the identified assays. We used this score to rank the VDC disruptors. To visualize the results, the AC_{50} values of the ten ISV-VDCs were obtained towards the 19 assays (Appendix Table 7) and a pVDC signature was generated for each of the ten ISV-VDCs depicting the retained assays (**Figure 3.8**).

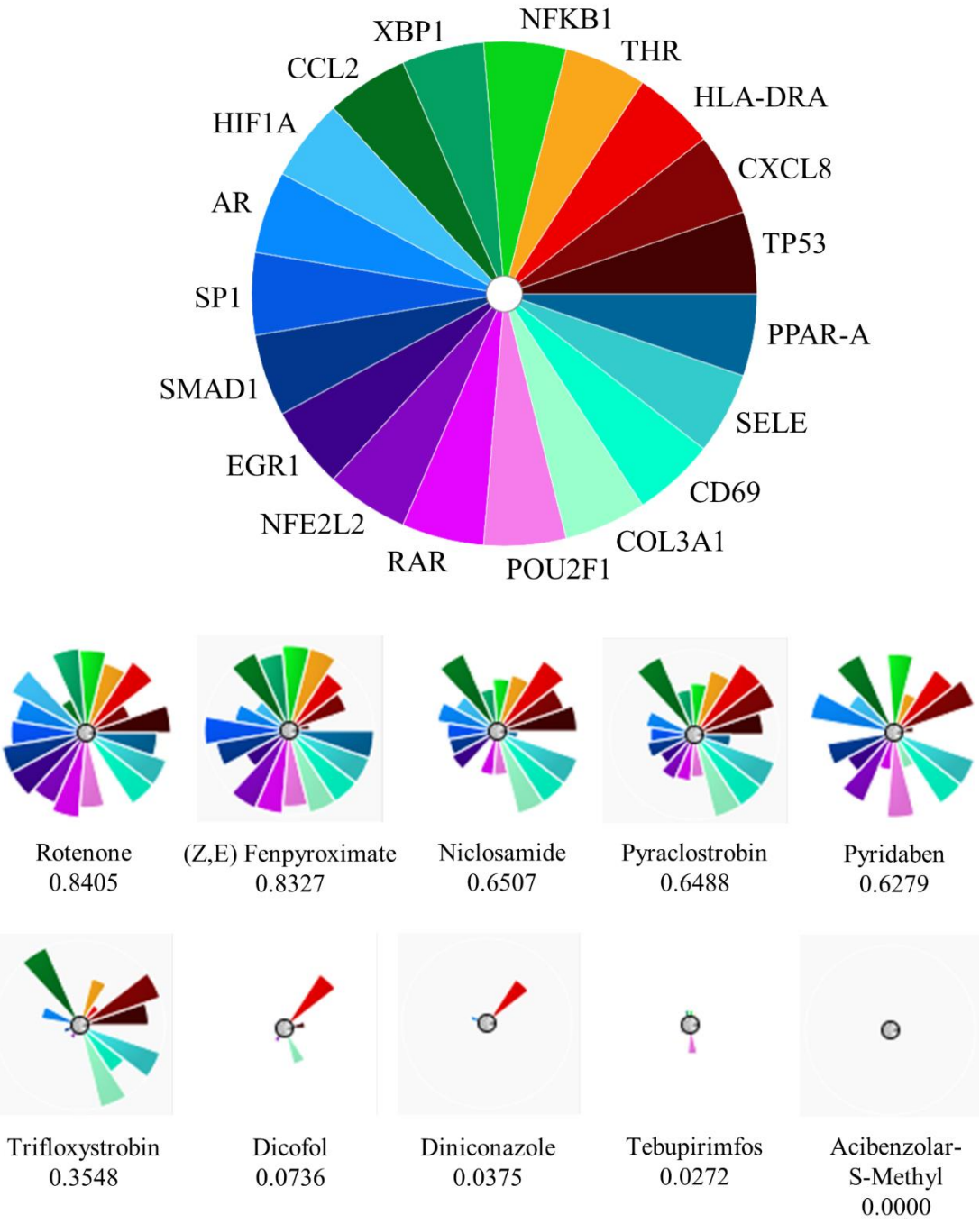

Figure 3.8 *In vitro* assay signatures for confirmed VDCs identified through univariate analysis. ToxPis and potency scores for each of the ten compounds confirmed to perturb ISV development, generated by running the VDC hit list against ToxCast *in vitro* biochemical assays. Only assays where, at least three or more of the ten compounds are active, have a p-value <0.05, and z-score applied were retained. Bigger pie slices show more potency at lower concentrations.

The size of each slice of the ToxPi is proportional to the AC_{50} for that particular in vitro assay and chemical. The chemicals were ranked by their ToxPi score; from rotenone having the highest score (0.8405 out of maximum 1.0) to acibenzolar-S-methyl score having the lowest score (0.0000) of the ten compounds. Acibenzolar-S-methyl did not affect any of the 19 *in vitro* assays identified and may be working through a mechanism not yet covered in the ToxCast *in vitro* assays to cause ISV disruption. All other compounds affected seven of the 19 ToxCast assays; AR, CXCL8, CCL2, CD69, HLA-DRA, THR, and SELE. Most compounds also affected the ToxCast assays for upregulation of NfκB, POU2F1, and activation of nuclear factor (erythroid-derived 2)-like 2 (NFE2L2, Nrf2). In summary, several *in vitro* assays were retained, indicating that these assays reflect molecular pathways required for normal vascular development and that vascular structures become perturbed if these assays are interfered with.

3.2.4 Prediction of Vascular Toxicity of New Compounds

The nineteen assays identified from the univariate analysis were used to predict VDCs. All chemicals that have been tested for these assays and their respective AC_{50} values were extracted from ToxCast dashboard (https://comptox.epa.gov/dashboard/). The ToxPi ranking tool was used to rank these compounds based on their ToxPi score. The extracted documents for each assay were combined into one master spreadsheet, which was uploaded to the ToxPi program to rank all tested chemicals based on their ToxPi score. This created a ranking list for all chemicals tested in ToxCast based on their potential to affect the assays shown in **Figure 3.8**. The top five and bottom two predicted ISV VDCs, and their ToxPi scores are shown in **Table 3.2**. All of these predicted VDC and non-VDCs will be tested for their capacity to perturb ISV development *in vivo* in zebrafish embryos and tube formation *in vitro* in HUVEC cells.

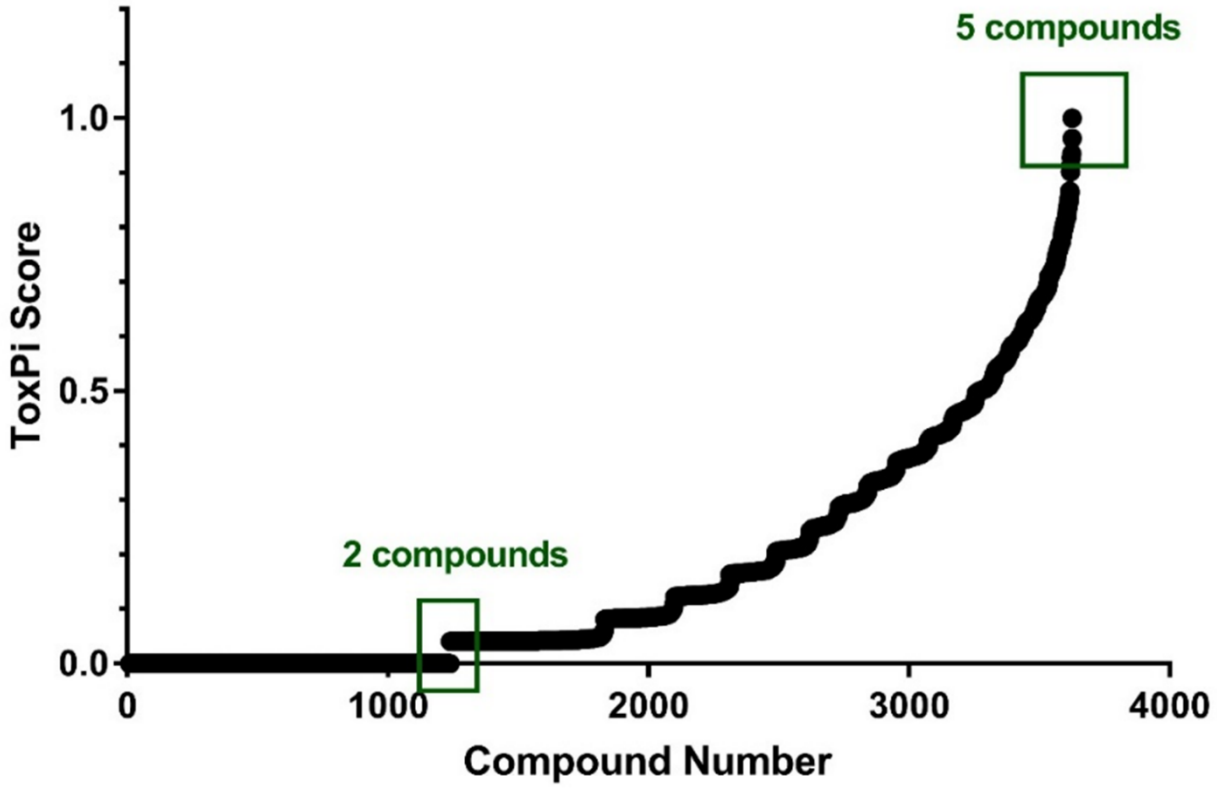

Figure 3.9 Prioritizing predicted VDC chemicals to be tested based on their ToxPi scores. AC_{50} values were obtained and ToxPi scores were calculated for all compounds tested in the thirteen assays identified through univariate analysis.

Table 3.2. Prediction of new VDC compounds. The ToxCast *in vitro* assays retained were used to identify putative VDCs. ToxPi tool was used to rank the new compounds based on their AC_{50} values for the related assays

S. No.	Chemical	ToxPi Score
High Prediction Score		
1	Tebufenpyrad	0.88
2	Triphenyltin hydroxide	0.82
3	Propargite	0.81
4	Tributyltin chloride	0.79
5	Fluoxastrobin	0.72
Low Prediction Score		
1	Mirex	0.04
2	Acetophenone	0.00

Abbreviations: LEL - Lowest effect level

3.3 DISCUSSION

In this study, we describe ten compounds from the ToxCast Phase I chemical library that perturb angiogenesis in zebrafish larvae. Five of these compounds, fenpyroximate, pyridaben and rotenone, which are insecticides, and pyraclostrobin and trifloxystrobin, which are strobulurin fungicides, were selected for further analysis. All five compounds caused perturbations of ISV formation at nM concentrations in zebrafish, rotenone being the most potent one among them. *In vitro* in the HUVEC tube formation assay, four compounds were active (fenpyroximate, pyridaben, rotenone, and pyraclostrobin). Trifloxystrobin did not have any effect on tube formation at the concentrations tested, although it was difficult to test it at high concentrations because it precipitated out of the cell media. Multiple endothelial cell lines are used for tube formation assays, the HUVEC assay being the most widely used one. It measures angiogenesis in human primary

cells and recapitulates all the steps of *in vivo* angiogenesis: adhesion, migration, protease activity, alignment and tube formation (Arnaoutova and Kleinman, 2010). Thus, our results indicate that the VDCs identified in zebrafish, except for trifloxystrobin, could potentially have anti-angiogenic effects in humans as well.

3.3.1 VDCs' Modes of Action Implied from ToxCast Data Correlations

Correlations to ToxCast *in vitro* assay data were performed to propose molecular mechanisms that the identified ISV-VDCs may interfere with. Our ten ISV-VDCs correlated with 19 ToxCast *in vitro* assays, each representing a potential mode of action.

Vascular endothelial growth factor (VEGF) is a key factor for vasculogenesis and angiogenesis across species. It acts through binding to vascular endothelial growth factor receptors (VEGFRs) on vascular endothelial cells (Leung *et al.*, 1989; Neufeld *et al.*, 1994), which results in the expression of genes necessary for normal vascular development. The expression of *VEGF* itself is regulated by multiple transcription factors, such as hypoxia inducible factor 1 alpha (HIF1α), SP1, etc. (Pagès and Pouysségur, 2005). Interestingly, the correlating ToxCast *in vitro* assays identified in this study contained some of these known factors that interact with VEGF signaling (**Figure 3.8**).

There were four nuclear receptor assays that correlated to our VDCs: AR, THR, PPAR-A, and RAR (**Figure 3.8**). Our data suggested that VDCs have antagonistic effects on AR and THR. Androgen receptor (AR) induces angiogenesis by regulating VEGF signaling (Barnabas, Wang and Gao, 2013; Yoshida, Ikeda and Aihara, 2016). Multiple roles of thyroid hormone receptor (THR)-mediated induction of angiogenesis have been described, such as upregulation of vascular

growth factors and integrin-mediated signaling (Davis, Davis and Mousa, 2009). Thus, inhibition of AR and THR could perturb normal vascular development.

Peroxisome proliferator-activated receptor element (PPAR) is used as a ToxCast assay to measure the activity of peroxisome proliferator-activated receptors alpha, delta and gamma (PPARα, PPARδ, and PPARɣ). PPARα is expressed in HUVECs and its activation mediates the transcriptional downregulation of VEGF through inhibition of various transcription factors such as nuclear factor-κB (NFκB) and specificity protein 1 (SP1), both of which have also been indicated in our vascular assay profile (**Figure 3.8**) (Inoue *et al.,* 1998; Meissner *et al.*, 2004; Grau *et al.,* 2006). Our results indicate that PPARα-mediated signaling was upregulated by ISV-VDC exposure (**Figure 3.8**). Retinoic acid receptor (RAR) assays were also reported among the in vitro assays of univariate analysis (**Figure 3.8**). All-trans retinoic acid (atRA) acts via RAR and plays an important role in regulating angiogenesis in early embryonic development and during organogenesis (Saito *et al.*, 2007; Pawlikowski, Wragge and Siegenthaler, 2019). RAR mediates this effect by regulating endogenous VEGF signaling through the VEGFR2 receptor possibly by the transcriptional regulation of hypoxia inducible factor 1α (HIF1α) which is another assay indicated through vascular univariate analysis (**Figure 3.8**) (Saito *et al.*, 2007; Pawlikowski, Wragge and Siegenthaler, 2019). Hypoxia is the key stimulus that induces angiogenesis during embryonic development and induces expression of key angiogenesis factors such as VEGF and stromal derived factor 1 (SDF1; CXCL12) through the transcriptional activity of HIF1α (Lee *et al.*, 2001; Pagès and Pouysségur, 2005; Ramírez-Bergeron *et al.*, 2006; Rey and Semenza, 2010). Hypoxia also induces NFE2L2 (Nrf2) expression, which in turn increases HIF1α expression resulting in increased VEGF expression (Kim *et al.*, 2011). SP1 is another hypoxia-induced

transcription factor that is a major regulator of VEGF expression. SP1's binding to the VEGF promotor is inhibited by interaction with the anti-angiogenic factor P53 (Pagès and Pouysségur, 2005; Teodoro, Evans and Green, 2007). P53 is speculated to exert its anti-angiogenic action by interfering with hypoxia induced regulators of angiogenesis such as Hif1α and SP1, inhibiting pro-angiogenic factors and upregulating anti-angiogenic factors (Teodoro, Evans and Green, 2007). P53 was another assay indicated by the vascular univariate analysis (**Figure 3.8**) Taken together, our data suggest that both PPARα and RAR exert a regulatory effect on VEGF and thus angiogenesis through the regulation of transcriptional factors NFκB, SP1, and HIF1α which are known transcriptional regulators of VEGF and these transcriptional factors can also be regulated by other hypoxia-induced factors such as Nrf2 and P53.

3.3.2 Prediction of Vascular Toxicity of New Compounds

Based on the *in vitro* assay targets, the identified VDCs affect multiple pathways of which many are known to be involved in vascular development. We hypothesized that if a compound affects these vascular *in vitro* endpoints, then it could potentially be a specific ISV-VDC *in vivo*. To rank ToxCast compounds, the nineteen assays were used. All the ToxCast Phase I and Phase II compounds were ranked based on their bioactivity for the *in vitro* endpoints that correlated with zebrafish VDCs. The top five ranked compounds that have not yet been tested for ISV-VDC effects, but will be tested in both zebrafish and HUVEC assays and the results will be compared to two compounds predicted to be non-VDCs. In conclusion, we have now ranked ToxCast compounds based on vascular disruption capacity, and this ranking list can be used to prioritize chemicals for further testing in small animal organisms or rodents. More importantly, we suggest a pipeline for the identification and prediction of toxic compounds. By using a low-to-medium

throughput *in vivo* assay or complex *in vitro* assay to screen a subset of chemicals, a phenotype-specific profile of correlating ToxCast assays can be obtained and further used to rank and predict toxicants tested in the Tox21 project. We propose that using such a pipeline in combination with increasing the number of chemicals tested in Tox21 will significantly speed up prioritization for further testing of the large number of chemicals present in our environment.

CHAPTER 4: MATERIALS AND METHODS

4.1 ZEBRAFISH LINE, HUSBANDRY AND BREEDING

Zebrafish were reared and maintained according to the protocols approved by the Institutional Animal Care and Use Committees at the University of Houston and Indiana University. The fish were housed at 28.5 ℃ on 14h/10h light/dark cycles. For the PLLD project, we used transgenic fish line GW57A (Kondrychyn *et al.*, 2011) (Vladimir Korzh, Institute of Molecular and Cell Biology (IMCB), Singapore) (referred to here as *Tg (neuromast:GFP)*), which has a random transgenic insertion that drives GFP expression in the mature neuromasts. We also used *Tg (cldnb:gfp)*, expressing GFP in neuromasts (Haas and Gilmour, 2006). For the VDC project, We used transgenic fish line *(kdrl:EGFP)mitfa*$^{b692/b692}$ expressing GFP in the vasculature as described previously (McCollum *et al.*, 2017). For all zebrafish lines, natural breeding was used to produce embryos and the collected embryos were kept in Embryo media (E3; 5 mM NaCl, 172 0.17 mMKCl, 0.33 mM CaCl2, 0.33mM MgSO4) at 28.5 ^{o}C.

4.2 CHEMICALS

ToxCast Phase I and Phase II libraries (http://www.epa.gov/ncct/toxcast/chemicals.html) were provided from the National Center for Computational Toxicology of the US EPA under a Material Transfer Agreement. For the PLLD project, the serotonin modular compounds were used to assist for PLLD effects. These compounds were methylene blue and 4-Chloro-DL-phenylalanine (PCPA) purchased from Alfa Aesar (Haverhill, MA); Fluoxetine hydrochloride and N-Methyl-N-propargyl-3-(2,4-dichlorophenoxy) propylamine hydrochloride (Clorgyline) purchased from Sigma-Aldrich (St. Louis, MO). The stock solutions were prepared in dH_2O. For the VDC project, the five most potent compounds found to cause ISV effect were selected for in-depth studies. These compounds were fenpyroximate (CAS # 111812-58-9), pyraclostrobin (CAS # 175013-18-0),

pyridaben (CAS # 96489-71-3), rotenone (CAS # 83-79-4) and trifloxystrobin (CAS # 141517-21-7). The compounds were purchased from Sigma-Aldrich (St. Louis, MO). The stock solutions were prepared and appropriate dilutions were made in DMSO (Sigma-Aldrich, St. Louis, MO).

4.3 CHEMICAL EXPOSURES IN ZEBRAFISH

For PLLD project, we first performed the high throughput screen for the ToxCast Phase I chemicals with the *Tg (neuromast:GFP)* fish line, which allows for visualization of the developed neuromasts. Harvested embryos were manually sorted and placed in 96 well plates, one embryo per well in 100 µl of E3, and were treated from approximately four hpf with chemicals at 0.2, 2 and 20 µM (n=3/concentration) unless otherwise noted (Appendix Table 1). Test agents were added to wells containing embryos using a Tecan Evo 200 (Tecan, Männedorf, Switzerland) fitted with a pin tool assembly (V&P Scientific, San Diego, CA). All test agents were diluted in DMSO (Sigma-Aldrich, St. Louis, MO) and the final concentration of the vehicle in the assay wells was 0.1%. Embryos were kept at 28.5 °C in the treatment media for four days without chemical renewal.

In the PLLD project, for follow-up experiments, active agents identified from the initial screen (Appendix Table 2) were validated in a low-throughput manner with higher numbers of replicates. The compounds that showed PLL disruptor effects at one concentration but were lethal at the other two doses used for HTS were also re-screened at lower doses. The same fish line, conditions and chemical concentrations as HTS were maintained unless otherwise noted (Appendix Table 2), except the embryos were placed in six well plates (n=20/concentration/well) and treated in 3 ml of

E3. The compounds identified as validated hits in the follow-up screen were designated as PLL disruptors.

To test the predicted compounds in the PLLD project, the same methodology was used as the low-throughput screen. Appendix Table 8 shows the treatment concentrations for these compounds.

To test serotonin pathway modulators in the PLLD project, embryos were manually sorted and placed in six well plates, 20 embryos per well in 3 mL of E3 per well, and were treated from approximately four hpf with increasing concentrations (Appendix Table 4) of either methylene blue, PCPA, fluoxetine or clorgyline (n=20/concentration). All test agents were diluted in E3 and embryos were kept at 28.5 °C in the treatment media for four days without chemical renewal.

In the VDC project, to determine dose-response curves for the five most potent ISV-VDCs, *Tg (kdrl:EGFP)mitfa*$^{b692/b692}$ embryos were collected and placed in six well plates (n=20/well) in 3 ml of embryo media (E3; 5 mM NaCl, 0.17 mM KCl, 0.33 mM $CaCl_2$, 0.33 mM $MgSO_4$) at 28.5 ^{o}C. Embryos were treated approximately at three hpf. The final concentration of the vehicle (DMSO) was 0.1% and the embryos were maintained in the treatment until four dpf without renewal of E3 or compounds. The VEGFR2 inhibitor PTK787 (Sigma-Aldrich, St. Louis, MO) was used as a positive control (Tal *et al.*, 2014).

4.4 ZEBRAFISH FLUORESCENCE IMAGING

To image the initial HTS screen in the PLLD project, the embryos were anesthetized at four dpf by directly dispensing 4 µL of 0.04% MS-222 (Western Chemical Inc., Ferndale, WA) to the individual wells using a Thermo Multidrop Combi (Thermo Scientific, Waltham, MA). Lateral

fluorescence images of the embryos were taken with a GE Healthcare IN Cell 6000 Analyzer (GE Healthcare, Little Chalfont, United Kingdom) automated inverted microscope using a 4x/0.20NA objective. Four fields were collected from each well with a 5% overlap and then computationally stitched together to form a single image that covered the entire well.

In the follow-up screen, serotonin experiments and prediction experiments, the embryos were anesthetized and manually transferred to 96 well plates at four dpf and laterally imaged using fluorescence microscopy (inverted Olympus 1X51 microscope equipped with the cellSens Dimension software, 4X objective, and Olympus XM10 camera (Olympus, Center Valley, PA) or Leica DMi8 automated fluorescence microscope equipped with the Leica LASX software, Leica DFC9000 GT camera using a 5X objective).

Time-lapse imaging was performed on a Nikon A1S Confocal microscope (Nikon Instruments Inc., Melville, NY) over a span of 56 h.

4.5 ZEBRAFISH DATA ANALYSIS

In the PLLD project, all the images were visually analyzed to identify the chemicals that altered the number of PLL neuromasts as compared to vehicle treated embryos. The criteria used to identify active compounds in the HTS were compounds that reduced PLL neuromasts: in a dose response pattern; in two or three embryos (out of three replicates) at two or three concentrations; or in at least one embryo across all three concentrations. For the follow-up screening, serotonin modulator treatments, and predicted PLLD treatments, we considered a chemical as a PLL disruptor if it decreased the number of PLL neuromasts in a dose dependent manner. All dose-response graphs were plotted using GraphPad Prism version 7 (GraphPad Software, La Jolla,

CA). The percentage of affected embryos by exposure to the predicted PLLDs were compared to that of the controls using un-paired Student's t-test (95% CI). The mean percentage of affected control (DMSO) embryos was used as a cut-off value.

In the VDC project, images of zebrafish larvae were visually analyzed for the ISV effects. The percentage effect for each concentration of chemicals was calculated from at least three independent experiments and the dose-response curves were plotted using GraphPad Prism version 7 (GraphPad Software, La Jolla, CA).

To quantify network formation in the HUVEC assay in chapter 3, Avi files were extracted as image sequences and analyzed with a customized version of Angiogenesis Analyzer https://imagej.nih.gov/ij/macros/toolsets/Angiogenesis%20Analyzer.txt programmed for ImageJ software (https://imagej.nih.gov/ij/).The statistical analysis of HUVEC vascular networks was performed with three replicates using Student's t-test.

4.6 UNIVARIATE CORRELATION ANALYSIS AND TOXPI SIGNATURES

Univariate correlation analysis was used to associate the zebrafish PLLDs and VDCs separately to ToxCast *in vitro* assay data (Judson *et al.*, 2010). Data for over 900 different *in vitro* assays have been collected for all the ToxCast Phase I chemicals, including AC_{50}s; the concentrations at half-maximal response. Data for each of these assays were compared with the zebrafish PLLDs and VDCs. We examined hit correspondence (*in vitro* assay activity correlated with zebrafish activity) using a chi-squared test. Associations were retained if true positives ≥5 for PLLDs and ≥3 for VDCs (chemicals positive for both zebrafish PLLDs or VDCs and *in vitro* assays) with the chi-squared p-value being <0.05. The AC_{50} values for each PLLD or VDC for each identified

assay/end point were downloaded from EPA's iCSS ToxCast Dashboard (https://comptox.epa.gov/dashboard/) and fed to the ToxPi program V2.2 to generate separated ToxPi profiles for the PLLDs and VDC. Visually, ToxPi is represented as component slices of a unit circle, with each slice representing information on a retained *in vitro* assay that correlated to the PLLDs and VDCs. *In vitro* assays retained for ToxPi profiles were equally weighed.

The identified assays that were retained from the univariate correlation analysis were used to extract and rank chemicals for potential PLLD or ISV VDC capacity. AC_{50} data for chemicals that affected each retained *in vitro* assay were downloaded from EPA's dashboard. These data were downloaded as one CSV document/chemical and combined to generate a spreadsheet showing all chemicals and all assay AC_{50}s. The combined spreadsheets were uploaded to the ToxPi program, and the "ranking tool" was used to rank the chemicals for their potential PLLD or ISV VDC capacity based on their computed ToxPi score, which reflects the potency of the chemicals' effect on the ToxCast assays.

4.7 WHOLE MOUNT SEROTONIN IMMUNOHISTOCHEMISTRY

Whole mount immunohistochemistry for serotonin expression in larval zebrafish was carried out in accordance with a previous study by Ulhaq and Kishida (Ulhaq and Kishida, 2018). Four dpf *Tg (neuromast:GFP)* larvae treated with serotonin effectors as described above were fixed overnight at 4 °C in 4% paraformaldehyde (PFA) (n=20 per treatment). After fixation, larvae were washed in PBS three times for five mins each time. Permeabilization was achieved by incubation of larvae in deionized water for 60 mins at room temperature followed by 100% acetone for eight mins at -20 °C. Larvae were then rinsed once in deionized water, then twice in 1X PBS

(phosphate buffered saline; prepared in dH_20 from commercially available tablets). Blocking solution was prepared with 10% inactivated horse serum diluted in PBT (1X PBS containing 0.3% TritonX-100) (v/v). Larvae were incubated in blocking solution for three hrs at room temperature. Blocking solution was replaced with primary antibody of rabbit polyclonal anti-5HT (5-hydroxytryptamine or serotonin) (ImmunoStar) diluted at 1:500 in 10% horse serum in PBT (v/v) for two days at 4 °C. Larvae were washed with PBSTX (1X PBS containing 0.1% Tween-20 and 0.5% TritonX-100) over four hrs at room temperature with a final PBS wash. The larvae were then incubated overnight at 4 °C in a secondary antibody of goat anti-rabbit IgG Alexa Fluor 594 (Life Technologies) diluted 1:100 in 10% horse serum in PBS. Larvae were washed in PBSTX over four hrs with a final wash in PBS before being postfixed overnight in 4% PFA at 4 °C. Larvae were washed with PBS and mounted in 1% low melting agarose on dorsal side in glass bottom petri-dishes for florescence imaging on a Leica DMi8 automated fluorescence microscope.

4.8 HUVEC CULTURE AND TUBE FORMATION ASSAY

Human primary umbilical vein endothelial cells (HUVECs; ATCC, Manassas, VA) were grown in endothelial cell media (vascular cell basal media plus endothelial cell growth kit-VEGF; ATCC, Manassas, VA). Tube formation assay was performed as described previously (Arnaoutova and Kleinman, 2010). Briefly, basement membrane extract (BME) (ATCC, Manassas, VA) was transferred to a 96 well plate (50 µl/well) and incubated at 37 °C for 30 mins to solidify. For chemical treatments, HUVEC cells were detached using 0.05% trypsin-EDTA, isolated and re-suspended in endothelial cell media at a concentration of 1.5×10^5 cells/ml. Aliquots of 400 µl of cell suspension were transferred to micro tubes and mixed with the chemical stock solutions to achieve the desired final concentrations for each chemical. Then 100 µl of the treated cell

suspension was transferred on top of the gelled BME in triplicates. Cells were incubated at 37 °C in a humidified atmosphere containing 5% CO_2 and air for 24 hrs.

4.9 HUVEC IMAGING AND DATA ANALYSIS

IncuCyte® ZOOM (Essen Bioscience, Ann Arbor, MI) live cell analysis system was used for live imaging of HUVEC tube formation over a period of 24 hrs. The phase-contrast images were captured using inverted 10X objective and were saved as time-lapse videos. Angiogenesis analyzer plug-in developed for the ImageJ software (http://image.bio.methods.free.fr/ImageJ/?Angiogenesis-Analyzer-for-ImageJ) was used by the developer, Gilles Carpentier, to quantify the network formation (Chevalier *et al.*, 2014).

CHAPTER 5: FUTURE DIRECTIONS AND CONCLUSIONS

5.1 CONCLUSIONS

The introduction of thousands of untested synthetic chemicals over the last century and the potential risk of environmental contamination and human exposure are emerging as a serious health risk. Diseases caused by these toxicants are preventable but require proper disposal management and extensive testing of these chemicals prior to their release. Given the sheer number of untested synthetic chemicals already in the environment, plus the abundant number being produced currently, new methodologies need to be developed to speed up the testing of these compounds before they reach the commercial market. EPA has started the ToxCast program in an effort to address this issue which screens these chemicals through *in vitro* biochemical assays. These high throughput cell-based screenings of thousands of chemicals have identified several potential toxicants, but these methodologies lack the whole organism data required to accurately identify the phenotypic manifestations of these toxicants. Zebrafish are a unique vertebrate model system that allow for high-throughput phenotypic and/or genetic screening of chemicals that are indicative of mammalian systems due to their high percentage of shared homology with human genetics and development processes. Their rapid development and low-cost husbandry allow for short-term, cost-effective toxicant screening. This animal model's unique development allows for both *in vitro* and *in vivo* analysis aspects to be covered in a single system. The abundance of transgenic zebrafish and the ability to perform live imaging for phenotypic malformations makes this an ideal model system for the rapid identification of potential toxicants. We used *in vivo* zebrafish embryo teratogenicity screens in combination with pathway-based *in vitro* data to identify environmental chemicals that cause specific developmental malformations and their mechanisms of action.

The PLL of teleost consists of mechanosensory organs called neuromasts, which facilitate the sensing of changes in water movement. The neuromasts develop and function very similarly to the human inner ear hair cells. We here set out to identify chemicals that perturb the development of the zebrafish PLL and study the mechanism by which they act. Using transgenic zebrafish expressing GFP in neuromasts we screened two hundred and ninety-two unique chemicals of the ToxCast Phase I library and found that exposure to twenty-two chemicals altered the number of neuromasts in the PLL of four day old zebrafish larvae. By univariate correlation analysis, we identified thirteen ToxCast *in vitro* assays that are affected by the identified PLLDs. Five of the thirteen *in vitro* assays were related to different aspects of serotonin signaling. Some of the serotonin-related genes identified were MAO-A which is responsible for serotonin degradation, HTR7 which is a serotonin receptor and SLC18A2 which is a serotonin packaging and transport protein. By exposure to known serotonin modulators, we confirmed that interference in the serotonergic system resulted in PLL disruption. Not just that, we also used the five serotonin assays identified through univariate analysis to predicted potential PLLDs and were able to confirm that the ranking of untested compounds correlated to their potency to cause PLL disruption. All eight of the top-scored compounds caused PLL disruption in a dose-dependent manner, whereas the 3 compounds with very low scores did not show any effects on PLL development as compared to vehicle treatment. Interestingly, all three tested compounds with a zero rank were found to interfere with PLL development. This further goes to show the importance of toxicity testing in whole-organism models because just the *in vitro* assays would have missed this association. Thus, we conclude that serotonin is required for proper PLL development and that screening in an *in vivo* model in combination with computational toxicology is an effective pipeline both for the identification of toxic chemicals and for the concurrent discovery of modes of action of chemicals.

We investigated in-depth previously identified VDCs that particularly caused ISV malformations *in vivo* in zebrafish and disrupted tube formation *in vitro* in the murine endothelial cell line, C166. The in-depth analysis was carried out both *in vivo* in zebrafish and *in vitro* in human umbilical cord endothelial cells (HUVECs). All of the ISV-VDCs tested caused ISV and tube formation-disruption in a dose-dependent manner. Upon univariate analysis of the ten ISV-VDCs, ToxCast data correlations identified that these chemicals alter signaling of nuclear receptors like AR, THR, RAR and transcription factors like HIF1α, POU2F1 causing vascular perturbations. All of these genes are known to play a role in mammalian vascular development. Using the ToxPi tool, the ToxCast *in vitro* assays that correlated with the identified ISV-VDCs were used to predict other chemicals that may have toxicity *in vivo* in zebrafish and *in vitro* in HUVECs. It remains to be seen how these chemicals affect ISV development in zebrafish and tube formation in HUVECs. In conclusion, the ISV-VDCs identified through the initial chemical screen can be used to create a pVDC signature assay profile and were also found to cause ISV disruption in zebrafish and interfere with tube-formation in HUVECs in a dose-dependent manner. The pVDC assay profile can also be used to predict other VDCs with potential *in vivo* effects through the ranking of chemicals that have been tested *in vitro* in the identified ToxCast assays.

Most of the identified molecular mechanisms are conserved among vertebrates, suggesting that these chemicals could potentially be harmful to humans and other mammals. Thus, the zebrafish is a promising model system to perform initial chemical screens to prioritize chemicals and predict their molecular targets that will require further mammalian testing. Through our work, we have only just begun to scratch the surface of the potential held by the zebrafish model system. Their mapped genome, high degree of homology to humans, amenability to rapid screening and ease of genetic manipulation will allow the zebrafish model system to open new avenues for toxicity testing and chemical risk assessment.

5.2 FUTURE DIRECTIONS

The zebrafish animal model has been used extensively in the study of disease onset, progression, and associated phenotypic changes. In this analysis, we provide a synopsis of both the posterior lateral line and vascular disruption caused by environmental toxicants using a reliable first-pass screening model for the classification of chemicals according to their teratogenic effects in the zebrafish animal model system. These posterior lateral line and vascular studies identify specific developmental deformities associated with exposure to the environmental toxicants and describe specific teratogenic effects on zebrafish neuromast and vascular systems. Overall, this will help rapidly screen through the vast number of environmental chemicals for their teratogenic effects that not only apply to aquatic vertebrates but also translate into mammals either by directly identifying the phenotypic effect they cause as seen in the VDC project or identifying the molecular pathways they work through as seen in the PLLD project.

5.2.1 Posterior Lateral Line Disruptors

For the PLLD project, we still need to understand the exact mechanism by which serotonin interference causes perturbations in the PLL during development since serotonin is not a pathway that has previously been indicated for this role. To do this, we would start by conducting serotonin rescue experiments following exposure to PCPA which reduces serotonin production. To test the hypothesis, exogenous serotonin would compensate for PCPA's action and rescue the reduced neuromast phenotype up to a certain concentration of serotonin until homeostasis is achieved. Increasing serotonin levels past this concentration would again result in detrimental effects on PLL development similar to effects caused by methylene blue and clorgyline, both of which increase serotonin levels by preventing its breakdown.

We are yet to understand if the PLLDs are affecting the PLL primordium or hair cell survival in neuromasts. Therefore, we would test these compounds in the *Tg (cldnb:GFP)* line which expresses GFP in the PLL primordium, to count the number of cells and the migration speed of the primordium after exposure (Haas and Gilmour, 2006). We would test the effect of PLLDs on neuromast hair cells by immunostaining with the hair cell-specific marker HCS1 and then run a TUNEL assay for apoptosis detection (López-Schier and Hudspeth, 2006).

Another aspect that remains to be explored is the effect of PLLDs on PLL innervation. We would examine the effects of PLLD exposure in a double transgenic line of *Et (T2KHG)39d* and *Tg (cxcr4b:mRFP)* which will express GFP in the lateral line neurons and RFP in the neuromasts, respectively (Faucherre *et al.*, 2009; Wada *et al.*, 2013).

It is also important to identify how the other pathways indicated in PLL disruption through univariate analysis are involved. This can be tested through RNA extraction and RT-qPCR of zebrafish larvae exposed to the most potent PLLDs to test if these genes are indeed affected in the zebrafish. Following this confirmation, it would be useful to perform RNA sequencing to understand how and if these different mechanisms are interconnected to manifest into the phenotypic effects we see.

Furthermore, the lateral line in teleost mediates behavioral orientation to water currents (rheotaxis) for surface feeding, schooling behavior, obstacle avoidance, and subsurface detection of prey (Chitnis, Nogare and Matsuda, 2012). Since the PLLDs identified affect zebrafish PLL development, they could also result in behavioral changes in the fish that are important for its health and survival, especially since the serotonin system is involved. We would test this

hypothesis by testing the most potent identified PLLDs in behavioral assays such as the rheotaxis assay (Olive *et al.*, 2016) or the novel tank test assay (Giacomini *et al.*, 2016; Kysil *et al.*, 2017).

Since neuromasts are molecularly, structurally and functionally similar to the human inner ear hair cells (Whitfield, 2002; Nicolson, 2005), we hypothesize that the PLLDs identified would also interfere with mammalian inner ear hair cell development. To test our hypothesis that these results would translate well into mammalian systems, we would like to test our most potent identified PLLDs on the *in vitro* inner ear organoid assay developed by the Karl Koehler lab (Koehler *et al.*, 2017).

5.2.2 Vascular Disruptor Compounds

For the VDC project, we are still to elucidate the mode of action for the chemicals identified and to tease out the mechanism involved in disrupting angiogenesis processes. The embryos treated with the four compounds (rotenone, pyridaben, pyraclostrobin, and fenpyroximate) that were confirmed as VDCs in both the zebrafish and HUVEC dose-response experiments, were subjected to RNA extraction and RNA sequencing to identify the mechanism of action for each compound and the common pathways affected by them that relate to vascular development. The bioinformatics analysis of the sequencing data is currently in process.

Furthermore, testing the predicted VDC compounds in both zebrafish and HUVECs for angiogenesis disruption and tube formation disruption, respectively, will establish our screening method as a reliable way to predict other vascular teratogens.

Since we have already established that the identified ISV-VDCs from the initial screen not only disrupt ISV formation in zebrafish but also tube formation in the mammalian HUVECs, the

translation of this screen from zebrafish to mammalian systems is evident phenotypically. In addition to this, the univariate analysis also identified many pathways that are already known to be involved in vascular development. To further test the translation of results seen in zebrafish, we would test some of the most potent VDC compounds identified within *in vivo* mammalian studies.

5.2.3 The Future

Overall, our pipeline to establish the zebrafish model as a predictor of specific teratogenic effects caused by environmental toxicants, not only identified the phenotypic effects caused and identified the known pathways involved in those processes but also identified new mechanisms of action for these compounds. These results also translate well into *in vitro* mammalian systems; thus, our methodology can be used to:

1. Identify lead compounds that require further *in vivo* mammalian testing
2. Shorten risk assessment time for industrial chemicals
3. Reduce the cost of toxicity testing
4. Identify the target pathways to be tested for mammalian studies
5. Establish other such screens to identify and predict compounds causing specific teratogenicity

APPENDIX

Appendix Table 1. The list of ToxCastPhI chemicals and the concentrations used for the HTS

CASRN	Chemical Name	Concentrations Tested
21564-17-0	2-(Thiocyanomethylthio)benzothiazole	20µM, 2µM, 0.2µM
2971-36-0	2,2-Bis(4-hydroxyphenyl)-1,1,1-trichloroethane	20µM, 2µM, 0.2µM
94-75-7	2,4-Dichlorophenoxyacetic acid	20µM, 2µM, 0.2µM
109-86-4	2-Methoxyethanol	20µM, 2µM, 0.2µM
94-74-6	2-Methyl-4-chlorophenoxyacetic acid	20µM, 2µM, 0.2µM
122-99-6	2-Phenoxyethanol	20µM, 2µM, 0.2µM
90-43-7	2-Phenylphenol	20µM, 2µM, 0.2µM
55406-53-6	3-Iodo-2-propynyl-N-butylcarbamate	20µM, 2µM, 0.2µM
94-82-6	4-(2,4-Dichlorophenoxy)butyric acid	20µM, 2µM, 0.2µM
71751-41-2	Abamectin	12µM, 1.2µM, 0.12µM
30560-19-1	Acephate	20µM, 2µM, 0.2µM
135410-20-7	Acetamiprid	20µM, 2µM, 0.2µM
34256-82-1	Acetochlor	20µM, 2µM, 0.2µM
135158-54-2	Acibenzolar-S-methyl	20µM, 2µM, 0.2µM
50594-66-6	Acifluorfen	20µM, 2µM, 0.2µM
15972-60-8	Alachlor	20µM, 2µM, 0.2µM
116-06-3	Aldicarb	20µM, 2µM, 0.2µM
584-79-2	Allethrin	20µM, 2µM, 0.2µM
834-12-8	Ametryn	20µM, 2µM, 0.2µM
33089-61-1	Amitraz	20µM, 2µM, 0.2µM
101-05-3	Anilazine	20µM, 2µM, 0.2µM
3337-71-1	Asulam	20µM, 2µM, 0.2µM
1912-24-9	Atrazine	20µM, 2µM, 0.2µM
35575-96-3	Azamethiphos	20µM, 2µM, 0.2µM
86-50-0	Azinphos-methyl	20µM, 2µM, 0.2µM
131860-33-8	Azoxystrobin	20µM, 2µM, 0.2µM
22781-23-3	Bendiocarb	20µM, 2µM, 0.2µM
1861-40-1	Benfluralin	20µM, 2µM, 0.2µM
17804-35-2	Benomyl	20µM, 2µM, 0.2µM
741-58-2	Bensulide	20µM, 2µM, 0.2µM
25057-89-0	Bentazone	20µM, 2µM, 0.2µM
149877-41-8	Bifenazate	20µM, 2µM, 0.2µM
82657-04-3	Bifenthrin	20µM, 2µM, 0.2µM
80-05-7	Bisphenol A	20µM, 2µM, 0.2µM
10043-35-3	Boric acid	20µM, 2µM, 0.2µM
188425-85-6	Boscalid	20µM, 2µM, 0.2µM
314-40-9	Bromacil	20µM, 2µM, 0.2µM
1689-84-5	Bromoxynil	16µM, 1.6µM, 0.16µM
69327-76-0	Buprofezin	20µM, 2µM, 0.2µM

Appendix Table 1. cntd. The list of ToxCastPhI chemicals and the concentrations used for the HTS

CASRN	Chemical Name	Concentrations Tested
23184-66-9	Butachlor	20µM, 2µM, 0.2µM
134605-64-4	Butafenacil	20µM, 2µM, 0.2µM
33629-47-9	Butralin	20µM, 2µM, 0.2µM
2008-41-5	Butylate	20µM, 2µM, 0.2µM
191906	Captafol	20µM, 2µM, 0.2µM
133-06-2	Captan	19.7µM, 2µM, 0.2µM
63-25-2	Carbaryl	20µM, 2µM, 0.2µM
5234-68-4	Carboxin	20µM, 2µM, 0.2µM
128639-02-1	Carfentrazone-ethyl	20µM, 2µM, 0.2µM
54593-83-8	Chlorethoxyfos	20µM, 2µM, 0.2µM
1698-60-8	Chloridazon	20µM, 2µM, 0.2µM
2675-77-6	Chloroneb	20µM, 2µM, 0.2µM
1897-45-6	Chlorothalonil	20µM, 2µM, 0.2µM
101-21-3	Chlorpropham	20µM, 2µM, 0.2µM
5598-15-2	Chlorpyrifos oxon	19.9µM, 2µM, 0.2µM
5598-13-0	Chlorpyrifos-methyl	20µM, 2µM, 0.2µM
87818-31-3	Cinmethylin	20µM, 2µM, 0.2µM
105512-06-9	Clodinafop-propargyl	20µM, 2µM, 0.2µM
74115-24-5	Clofentezine	20µM, 2µM, 0.2µM
81777-89-1	Clomazone	20µM, 2µM, 0.2µM
101-10-0	Cloprop	20µM, 2µM, 0.2µM
1702-17-6	Clopyralid	20µM, 2µM, 0.2µM
57754-85-5	Clopyralid-olamine	20µM, 2µM, 0.2µM
120-32-1	Clorophene	20µM, 2µM, 0.2µM
210880-92-5	Clothianidin	20µM, 2µM, 0.2µM
56-72-4	Coumaphos	20µM, 2µM, 0.2µM
420-04-2	Cyanamide	20µM, 2µM, 0.2µM
21725-46-2	Cyanazine	20µM, 2µM, 0.2µM
120116-88-3	Cyazofamid	20µM, 2µM, 0.2µM
113136-77-9	Cyclanilide	20µM, 2µM, 0.2µM
1134-23-2	Cycloate	20µM, 2µM, 0.2µM
68359-37-5	Cyfluthrin	20µM, 2µM, 0.2µM
122008-85-9	Cyhalofop-butyl	19.9µM, 2µM, 0.2µM
57966-95-7	Cymoxanil	20µM, 2µM, 0.2µM
52315-07-8	Cypermethrin	20µM, 2µM, 0.2µM
94361-06-5	Cyproconazole	19.9µM, 2µM, 0.2µM
121552-61-2	Cyprodinil	20µM, 2µM, 0.2µM
66215-27-8	Cyromazine	20µM, 2µM, 0.2µM
1596-84-5	Daminozide	20µM, 2µM, 0.2µM
533-74-4	Dazomet	20µM, 2µM, 0.2µM

Appendix Table 1. cntd. The list of ToxCastPhI chemicals and the concentrations used for the HTS

CASRN	Chemical Name	Concentrations Tested
1007-28-9	Deisopropylatrazine	20µM, 2µM, 0.2µM
117-81-7	Di(2-ethylhexyl) phthalate	20µM, 2µM, 0.2µM
333-41-5	Diazinon	20µM, 2µM, 0.2µM
962-58-3	Diazoxon	20µM, 2µM, 0.2µM
84-74-2	Dibutyl phthalate	20µM, 2µM, 0.2µM
1918-00-9	Dicamba	20µM, 2µM, 0.2µM
1194-65-6	Dichlobenil	20µM, 2µM, 0.2µM
120-36-5	Dichlorprop	20µM, 2µM, 0.2µM
62-73-7	Dichlorvos	10µM, 1µM, 0.1µM
51338-27-3	Diclofop-methyl	20µM, 2µM, 0.2µM
99-30-9	Dicloran	20µM, 2µM, 0.2µM
145701-21-9	Diclosulam	20µM, 2µM, 0.2µM
115-32-2	Dicofol	20µM, 2µM, 0.2µM
141-66-2	Dicrotophos	20µM, 2µM, 0.2µM
119446-68-3	Difenoconazole	20µM, 2µM, 0.2µM
43222-48-6	Difenzoquat metilsulfate	20µM, 2µM, 0.2µM
87674-68-8	Dimethenamid	20µM, 2µM, 0.2µM
60-51-5	Dimethoate	20µM, 2µM, 0.2µM
110488-70-5	Dimethomorph	20µM, 2µM, 0.2µM
131-11-3	Dimethyl phthalate	20µM, 2µM, 0.2µM
75-60-5	Dimethylarsinic acid	20µM, 2µM, 0.2µM
83657-18-5	Diniconazole-M	20µM, 2µM, 0.2µM
122-39-4	Diphenylamine	20µM, 2µM, 0.2µM
136-45-8	Dipropyl pyridine-2,5-dicarboxylate	20µM, 2µM, 0.2µM
6385-62-2	Diquat dibromide monohydrate	10µM, 1µM, 0.1µM
298-04-4	Disulfoton	8.9µM, 0.9µM, 0.1µM
97886-45-8	Dithiopyr	19.9µM, 2µM, 0.2µM
330-54-1	Diuron	20µM, 2µM, 0.2µM
155569-91-8	Emamectin benzoate	20µM, 2µM, 0.2µM
115-29-7	Endosulfan	20µM, 2µM, 0.2µM
66230-04-4	Esfenvalerate	20µM, 2µM, 0.2µM
55283-68-6	Ethalfluralin	20µM, 2µM, 0.2µM
16672-87-0	Ethephon	20µM, 2µM, 0.2µM
26225-79-6	Ethofumesate	20µM, 2µM, 0.2µM
13194-48-4	Ethoprop	20.6µM, 2µM, 0.2µM
96-45-7	Ethylene thiourea	20µM, 2µM, 0.2µM
153233-91-1	Etoxazole	13.2µM, 1.3µM, 0.13µM
2593-15-9	Etridiazole	20µM, 2µM, 0.2µM
131807-57-3	Famoxadone	20.1µM, 2µM, 0.2µM
161326-34-7	Fenamidone	20µM, 2µM, 0.2µM

Appendix Table 1. cntd. The list of ToxCastPhI chemicals and the concentrations used for the HTS

CASRN	Chemical Name	Concentrations Tested
161326-34-7	Fenamidone	20µM, 2µM, 0.2µM
22224-92-6	Fenamiphos	20µM, 2µM, 0.2µM
60168-88-9	Fenarimol	20µM, 2µM, 0.2µM
114369-43-6	Fenbuconazole	20µM, 2µM, 0.2µM
126833-17-8	Fenhexamid	20µM, 2µM, 0.2µM
122-14-5	Fenitrothion	20µM, 2µM, 0.2µM
66441-23-4	Fenoxaprop-ethyl	20µM, 2µM, 0.2µM
72490-01-8	Fenoxycarb	20µM, 2µM, 0.2µM
39515-41-8	Fenpropathrin	20µM, 2µM, 0.2µM
111812-58-9	Fenpyroximate (Z,E)	20µM, 2µM, 0.2µM
55-38-9	Fenthion	20µM, 2µM, 0.2µM
120068-37-3	Fipronil	20.1µM, 2µM, 0.2µM
69806-50-4	Fluazifop-butyl	20µM, 2µM, 0.2µM
79241-46-6	Fluazifop-P-butyl	20.1µM, 2µM, 0.2µM
79622-59-6	Fluazinam	20µM, 2µM, 0.2µM
131341-86-1	Fludioxonil	20µM, 2µM, 0.2µM
142459-58-3	Flufenacet	20µM, 2µM, 0.2µM
188489-07-8	Flufenpyr-ethyl	20µM, 2µM, 0.2µM
62924-70-3	Flumetralin	20µM, 2µM, 0.2µM
98967-40-9	Flumetsulam	20µM, 2µM, 0.2µM
87546-18-7	Flumiclorac-pentyl	20µM, 2µM, 0.2µM
103361-09-7	Flumioxazin	20µM, 2µM, 0.2µM
2164-17-2	Fluometuron	20µM, 2µM, 0.2µM
361377-29-9	Fluoxastrobin	20µM, 2µM, 0.2µM
69377-81-7	Fluroxypyr	20µM, 2µM, 0.2µM
81406-37-3	Fluroxypyr-meptyl	20µM, 2µM, 0.2µM
85509-19-9	Flusilazole	20µM, 2µM, 0.2µM
117337-19-6	Fluthiacet-methyl	20µM, 2µM, 0.2µM
66332-96-5	Flutolanil	20µM, 2µM, 0.2µM
133-07-3	Folpet	20µM, 2µM, 0.2µM
68157-60-8	Forchlorfenuron	20µM, 2µM, 0.2µM
23422-53-9	Formetanate hydrochloride	20.1µM, 2µM, 0.2µM
98886-44-3	Fosthiazate	20µM, 2µM, 0.2µM
79983-71-4	Hexaconazole	20µM, 2µM, 0.2µM
51235-04-2	Hexazinone	20µM, 2µM, 0.2µM
78587-05-0	Hexythiazox	20µM, 2µM, 0.2µM
119515-38-7	Icaridin	20µM, 2µM, 0.2µM
35554-44-0	Imazalil	20µM, 2µM, 0.2µM
114311-32-9	Imazamox	20µM, 2µM, 0.2µM
104098-48-8	Imazapic	20µM, 2µM, 0.2µM

Appendix Table 1. cntd. The list of ToxCastPhI chemicals and the concentrations used for the HTS

CASRN	Chemical Name	Concentrations Tested
81334-34-1	Imazapyr	20µM, 2µM, 0.2µM
81335-37-7	Imazaquin	20µM, 2µM, 0.2µM
81335-77-5	Imazethapyr	20µM, 2µM, 0.2µM
138261-41-3	Imidacloprid	20µM, 2µM, 0.2µM
173584-44-6	Indoxacarb	16µM, 1.6µM, 0.16µM
144550-36-7	Iodosulfuron-methyl-sodium	20µM, 2µM, 0.2µM
36734-19-7	Iprodione	20µM, 2µM, 0.2µM
42509-80-8	Isazofos	20µM, 2µM, 0.2µM
82558-50-7	Isoxaben	20µM, 2µM, 0.2µM
141112-29-0	Isoxaflutole	20µM, 2µM, 0.2µM
77501-63-4	Lactofen	20µM, 2µM, 0.2µM
58-89-9	Lindane	20µM, 2µM, 0.2µM
330-55-2	Linuron	20µM, 2µM, 0.2µM
1634-78-2	Malaoxon	20µM, 2µM, 0.2µM
121-75-5	Malathion	20µM, 2µM, 0.2µM
123-33-1	Maleic hydrazide	20µM, 2µM, 0.2µM
2234562	Mancozeb	20µM, 2µM, 0.2µM
12427-38-2	Maneb	10µM, 1µM, 0.1µM
24307-26-4	Mepiquat chloride	20µM, 2µM, 0.2µM
104206-82-8	Mesotrione	20.3µM, 2µM, 0.2µM
57837-19-1	Metalaxyl	20µM, 2µM, 0.2µM
10265-92-6	Methamidophos	20µM, 2µM, 0.2µM
6734-80-1	Methan-sodium hydrate	20µM, 2µM, 0.2µM
950-37-8	Methidathion	20µM, 2µM, 0.2µM
16752-77-5	Methomyl	20µM, 2µM, 0.2µM
72-43-5	Methoxychlor	19.9µM, 2µM, 0.2µM
161050-58-4	Methoxyfenozide	20µM, 2µM, 0.2µM
556-61-6	Methyl isothiocyanate	20µM, 2µM, 0.2µM
298-00-0	Methyl parathion	20µM, 2µM, 0.2µM
6317-18-6	Methylene bis(thiocyanate)	20µM, 2µM, 0.2µM
51218-45-2	Metolachlor	20µM, 2µM, 0.2µM
21087-64-9	Metribuzin	20µM, 2µM, 0.2µM
7786-34-7	Mevinphos	20µM, 2µM, 0.2µM
113-48-4	MGK-264	20µM, 2µM, 0.2µM
NOCAS_34742	Milbemectin (mixture of >=70 percent Milbemcin A4, & <=30 percent Milbemycin A3)	19.5µM, 2µM, 0.2µM
2212-67-1	Molinate	20µM, 2µM, 0.2µM
4376-20-9	Mono(2-ethylhexyl) phthalate	20.3µM, 2µM, 0.2µM
131-70-4	Monobutyl phthalate	20µM, 2µM, 0.2µM

Appendix Table 1. cntd. The list of ToxCastPhI chemicals and the concentrations used for the HTS

CASRN	Chemical Name	Concentrations Tested
6923-22-4	Monocrotophos	20µM, 2µM, 0.2µM
4376-18-5	Monomethyl phthalate	20µM, 2µM, 0.2µM
88671-89-0	Myclobutanil	20µM, 2µM, 0.2µM
134-62-3	N,N-Diethyl-3-methylbenzamide	20µM, 2µM, 0.2µM
300-76-5	Naled	20µM, 2µM, 0.2µM
15299-99-7	Napropamide	20µM, 2µM, 0.2µM
50-65-7	Niclosamide	10µM, 1µM, 0.1µM
1929-82-4	Nitrapyrin	20µM, 2µM, 0.2µM
27314-13-2	Norflurazon	20µM, 2µM, 0.2µM
116714-46-6	Novaluron	10µM, 1µM, 0.1µM
19044-88-3	Oryzalin	20µM, 2µM, 0.2µM
19666-30-9	Oxadiazon	20µM, 2µM, 0.2µM
23135-22-0	Oxamyl	20µM, 2µM, 0.2µM
42874-03-3	Oxyfluorfen	20µM, 2µM, 0.2µM
6153-64-6	Oxytetracycline dihydrate	20µM, 2µM, 0.2µM
76738-62-0	Paclobutrazol	20µM, 2µM, 0.2µM
56-38-2	Parathion	10µM, 1µM, 0.1µM
40487-42-1	Pendimethalin	20µM, 2µM, 0.2µM
219714-96-2	Penoxsulam	20µM, 2µM, 0.2µM
82-68-8	Pentachloronitrobenzene	20µM, 2µM, 0.2µM
1763-23-1	Perfluorooctane sulfonic acid	20µM, 2µM, 0.2µM
335-67-1	Perfluorooctanoic acid	20µM, 2µM, 0.2µM
52645-53-1	Permethrin	20µM, 2µM, 0.2µM
2310-17-0	Phosalone	20µM, 2µM, 0.2µM
6607	Picloram	20µM, 2µM, 0.2µM
51-03-6	Piperonyl butoxide	20.2µM, 2µM, 0.2µM
23103-98-2	Pirimicarb	20µM, 2µM, 0.2µM
29232-93-7	Pirimiphos-methyl	20µM, 2µM, 0.2µM
23031-36-9	Prallethrin	19.9µM, 2µM, 0.2µM
67747-09-5	Prochloraz	20µM, 2µM, 0.2µM
29091-21-2	Prodiamine	20µM, 2µM, 0.2µM
41198-08-7	Profenofos	10µM, 1µM, 0.1µM
1610-18-0	Prometon	20µM, 2µM, 0.2µM
7287-19-6	Prometryn	20µM, 2µM, 0.2µM
25606-41-1	Propamocarb hydrochloride	20µM, 2µM, 0.2µM
709-98-8	Propanil	20µM, 2µM, 0.2µM
2312-35-8	Propargite	20µM, 2µM, 0.2µM
139-40-2	Propazine	20µM, 2µM, 0.2µM
31218-83-4	Propetamphos	20µM, 2µM, 0.2µM
60207-90-1	Propiconazole	20µM, 2µM, 0.2µM

Appendix Table 1. cntd. The list of ToxCastPhI chemicals and the concentrations used for the HTS

CASRN	Chemical Name	Concentrations Tested
114-26-1	Propoxur	20µM, 2µM, 0.2µM
181274-15-7	Propoxycarbazone-sodium	20µM, 2µM, 0.2µM
23950-58-5	Propyzamide	20µM, 2µM, 0.2µM
123312-89-0	Pymetrozine	20µM, 2µM, 0.2µM
175013-18-0	Pyraclostrobin	20µM, 2µM, 0.2µM
129630-19-9	Pyraflufen-ethyl	20µM, 2µM, 0.2µM
96489-71-3	Pyridaben	20µM, 2µM, 0.2µM
53112-28-0	Pyrimethanil	20µM, 2µM, 0.2µM
95737-68-1	Pyriproxyfen	20µM, 2µM, 0.2µM
123343-16-8	Pyrithiobac-sodium	20µM, 2µM, 0.2µM
84087-01-4	Quinclorac	20µM, 2µM, 0.2µM
124495-18-7	Quinoxyfen	20µM, 2µM, 0.2µM
76578-14-8	Quizalofop-ethyl	17.2µM, 1.7µM, 0.17µM
10453-86-8	Resmethrin	20µM, 2µM, 0.2µM
83-79-4	Rotenone	20µM, 2µM, 0.2µM
28434-00-6	S-Bioallethrin	20µM, 2µM, 0.2µM
74051-80-2	Sethoxydim	20.1µM, 2µM, 0.2µM
759-94-4	S-Ethyl dipropylthiocarbamate	20µM, 2µM, 0.2µM
122-34-9	Simazine	20µM, 2µM, 0.2µM
148477-71-8	Spirodiclofen	20µM, 2µM, 0.2µM
118134-30-8	Spiroxamine	20µM, 2µM, 0.2µM
122836-35-5	Sulfentrazone	20µM, 2µM, 0.2µM
87-90-1	Symclosene	20µM, 2µM, 0.2µM
112410-23-8	Tebufenozide	20µM, 2µM, 0.2µM
119168-77-3	Tebufenpyrad	20µM, 2µM, 0.2µM
96182-53-5	Tebupirimfos	20µM, 2µM, 0.2µM
34014-18-1	Tebuthiuron	20µM, 2µM, 0.2µM
79538-32-2	Tefluthrin	20µM, 2µM, 0.2µM
149979-41-9	Tepraloxydim	20µM, 2µM, 0.2µM
5902-51-2	Terbacil	20µM, 2µM, 0.2µM
112281-77-3	Tetraconazole	19.9µM, 2µM, 0.2µM
7696-12-0	Tetramethrin	20µM, 2µM, 0.2µM
148-79-8	Thiabendazole	20µM, 2µM, 0.2µM
111988-49-9	Thiacloprid	20µM, 2µM, 0.2µM
153719-23-4	Thiamethoxam	20µM, 2µM, 0.2µM
117718-60-2	Thiazopyr	20µM, 2µM, 0.2µM
51707-55-2	Thidiazuron	20µM, 2µM, 0.2µM
28249-77-6	Thiobencarb	20µM, 2µM, 0.2µM
59669-26-0	Thiodicarb	20µM, 2µM, 0.2µM
23564-05-8	Thiophanate-methyl	20µM, 2µM, 0.2µM

Appendix Table 1. cntd. The list of ToxCastPhI chemicals and the concentrations used for the HTS

CASRN	Chemical Name	Concentrations Tested
23564-05-8	Thiophanate-methyl	20µM, 2µM, 0.2µM
137-26-8	Thiram	20µM, 2µM, 0.2µM
87820-88-0	Tralkoxydim	20µM, 2µM, 0.2µM
43121-43-3	Triadimefon	20µM, 2µM, 0.2µM
55219-65-3	Triadimenol	20µM, 2µM, 0.2µM
2303-17-5	Tri-allate	20µM, 2µM, 0.2µM
78-48-8	Tribufos	20µM, 2µM, 0.2µM
52-68-6	Trichlorfon	20µM, 2µM, 0.2µM
55335-06-3	Triclopyr	20.4µM, 2µM, 0.2µM
3380-34-5	Triclosan	20.4µM, 2µM, 0.2µM
141517-21-7	Trifloxystrobin	20µM, 2µM, 0.2µM
199119-58-9	Trifloxysulfuron-sodium	20µM, 2µM, 0.2µM
68694-11-1	Triflumizole	20µM, 2µM, 0.2µM
1582-09-8	Trifluralin	20µM, 2µM, 0.2µM
76-87-9	Triphenyltin hydroxide	20µM, 2µM, 0.2µM
131983-72-7	Triticonazole	19.9µM, 2µM, 0.2µM
50471-44-8	Vinclozolin	20µM, 2µM, 0.2µM
156052-68-5	Zoxamide	20.1µM, 2µM, 0.2µM

Appendix Table 2. The list of positive compounds altering PLL neuromast numbers as identified from HTS and their follow-up screen concentrations

S. No.	CASRN	Chemical Name	Concentrations Tested
1	135158-54-2	Acibenzolar-S-methyl	20µM, 10µM, 1µM
2	101-05-3	Anilazine	20µM, 10µM, 1µM
3	35575-96-3	Azamethiphos	20µM, 10µM, 1µM
4	86-50-0	Azinphos-methyl	5µM, 1µM, 0.75µM
5	131860-33-8	Azoxystrobin	10µM, 1µM, 0.5µM
6	80-05-7	Bisphenol A	20µM, 10µM, 1µM
7	33629-47-9	Butralin	20µM, 10µM, 1µM
8	63-25-2	Carbaryl	20µM, 10µM, 1µM
9	1698-60-8	Chloridazon	20µM, 10µM, 1µM
10	5598-15-2	Chlorpyrifos oxon	0.75µM, 0.5µM, 0.1µM
11	5598-13-0	Chlorpyrifos-methyl	20µM, 10µM, 1µM
12	105512-06-9	Clodinafop-propargyl	5µM, 1µM, 0.5µM
13	57966-95-7	Cymoxanil	10µM, 1µM, 0.5µM
14	119446-68-3	Difenoconazole	20µM, 10µM, 1µM
15	298-04-4	Disulfoton	8.9 µM, 4.5µM, 0.45µM
16	115-29-7	Endosulfan	1µM, 0.5µM, 0.1µM
17	13194-48-4	Ethoprop	20µM, 10µM, 1µM
18	96-45-7	Ethylene thiourea	20µM, 10µM, 1µM
19	153233-91-1	Etoxazole	20µM, 10µM, 1µM
20	122-14-5	Fenitrothion	20µM, 10µM, 1µM
21	2164-17-2	Fluometuron	20µM, 10µM, 1µM
22	361377-29-9	Fluoxastrobin	10µM, 1µM, 0.5µM
23	23422-53-9	Formetanate hydrochloride	20µM, 10µM, 1µM
24	104098-48-8	Imazapic	20µM, 10µM, 1µM
25	144550-36-7	Iodosulfuron-methyl-sodium	20µM, 10µM, 1µM
26	82558-50-7	Isoxaben	20µM, 10µM, 1µM
27	77501-63-4	Lactofen	0.5µM, 0.1µM, 0.05µM
28	1634-78-2	Malaoxon	1µM, 0.5µM, 0.1µM
29	950-37-8	Methidathion	15µM, 10µM, 1µM
30	72-43-5	Methoxychlor	1µM, 0.5µM, 0.1µM
31	556-61-6	Methyl isothiocyanate	20µM, 10µM, 1µM
32	50-65-7	Niclosamide	10µM, 1µM, 0.5µM
33	82-68-8	Pentachloronitrobenzene	5µM, 1µM, 0.5µM
34	1763-23-1	Perfluorooctane sulfonic acid	5µM, 1µM, 0.75µM
35	67747-09-5	Prochloraz	10µM, 1µM, 0.5µM
36	709-98-8	Propanil	20µM, 10µM, 1µM
37	23950-58-5	Propyzamide	20µM, 10µM, 1µM

Appendix Table 2. cntd. The list of positive compounds altering PLL neuromast numbers as identified from HTS and their follow-up screen concentrations

S. No.	CASRN	Chemical Name	Concentrations Tested
38	175013-18-0	Pyraclostrobin	1μM, 0.1μM, 0.01μM
39	28434-00-6	S-Bioallethrin	1μM, 0.5μM, 0.1μM
40	118134-30-8	Spiroxamine	20μM, 10μM, 1μM
41	148-79-8	Thiabendazole	20μM, 10μM, 1μM
42	51707-55-2	Thidiazuron	20μM, 10μM, 1μM
43	78-48-8	Tribufos	15μM, 10μM, 1μM
44	55335-06-3	Triclopyr	20.4μM, 10.2μM, 1.02μM
45	3380-34-5	Triclosan	10.2μM, 5.1μM, 1.02μM
46	50471-44-8	Vinclozolin	20μM, 10μM, 1μM

Appendix Table 3. The list of assays identified through Univariate Analysis of PLLDs with number of true positive and p-value for each assay

S. No	Assay	Biological Endpoint	Gene Target	True Positives	p-value
1	NVS_ADME_rCYP2A1	CYP450	Cyp2a1	9	0.001
2	NVS_ENZ_rMAOAC	Mitochondrial disruption up	Maoa	6	0.001
3	NVS_GPCR_rmAdra2B	GPCR	Adra2b	5	0.005
4	NVS_OR_gSIGMA_NonSelective	Ion channel	Sigmar1	5	0.006
5	NVS_TR_rVMAT2	Transporter	Slc18a2	5	0.008
6	ATG_DR5_CIS_up	Nuclear receptor ATG	RARA RARB RARG	10	0.013
7	BSK_BE3C_uPAR_up	Extracellular matrix up	PLAUR	6	0.017
8	NVS_GPCR_h5HT7	GPCR	HTR7	6	0.028
9	NVS_MP_rPBR	Mitochondrial disruption up	Tspo	9	0.030
10	OT_FXR_FXRSRC1_1440	Nuclear receptor OT	NR1H4	10	0.036
11	NVS_ADME_rCYP2D1	CYP450	Cyp2d1	6	0.042
12	NCCT_TPO_AUR_dn	TPO	TPO	10	0.043
13	NVS_ADME_rCYP2C13	CYP450	Cyp2c13	6	0.048

Appendix Table 4. Treatment concentrations used for the serotonin pathway affecting compounds

CASRN	General Name	Chemical Name	Concentrations Tested
17780-75-5	Clorgyline	N-Methyl-N-propargyl-3-(2,4-dichlorophenoxy)propylamine hydrochloride	0.01µM, 0.1µM, 1µM, 10µM, 33µM, 100µM
122965-43-9	Methylene Blue	Methylene Blue	0.1µM, 1µM, 10µM, 33µM, 100µM
7424-00-2	PCPA	4-Chloro-DL-phenylalanine	1µM, 5µM, 10µM, 20µM, 40µM, 50µM
56296-78-7	Fluoxetine	Fluoxetine Hydrochloride	0.01µM, 0.1µM, 1µM, 10µM, 33µM, 100µM

Appendix Table 5. ToxPi input file for AC_{50} values of all 22 PLLDs towards the 13 assays identified through univariate analysis

S. No.	Chemical	CYP2D1	ADRA2B	SLC8A2	MAO-A	HTR7
1	Anilazine	NA	NA	21.4	NA	NA
2	Bisphenol A	11.4	28.4	11.8	NA	22.1
3	Ethylene thiourea	NA	NA	NA	NA	NA
4	Fluometuron	NA	NA	NA	30.7	NA
5	Thiabendazole	NA	NA	NA	14.1	NA
6	Propanil	6.4	14.4	27.0	18.2	NA
7	Vinclozolin	NA	NA	NA	NA	NA
8	Prochloraz	1.1	3.9	12.9	11.0	19.3
9	Butralin	NA	NA	NA	NA	NA
10	Cymoxanil	NA	NA	NA	NA	NA
11	Difenoconazole	0.6	5.6	19.6	1.9	3.1
12	Formetanate hydrochloride	NA	NA	NA	0.5	NA
13	Azoxystrobin	6.6	NA	NA	NA	4.0
14	Ethoprop	NA	NA	NA	NA	NA
15	Fenitrothion	NA	NA	NA	9.8	NA
16	Pyraclostrobin	2.0	NA	NA	NA	1.0
17	Thidiazuron	9.4	16.4	5.9	5.3	7.9
18	Spiroxamine	NA	30.6	NA	NA	10.0
19	Imazapic	NA	NA	NA	NA	NA
20	Fluoxastrobin	NA	NA	NA	NA	NA
21	Iodosulfuron-methyl-sodium	NA	NA	NA	NA	NA
22	Azamethiphos	NA	NA	NA	NA	NA

Appendix Table 5. cntd. ToxPi input file for AC_{50} values of all 22 PLLDs towards the 13 assays identified through univariate analysis

S. No.	Chemical	SIGMAR1	RAR	FXR	PLAUR	TPO
1	Anilazine	NA	81.8	NA	0.2	5.3
2	Bisphenol A	0.6	11.9	32.6	NA	0.5
3	Ethylene thiourea	NA	NA	NA	0.6	7.8
4	Fluometuron	NA	7.9	NA	NA	NA
5	Thiabendazole	NA	NA	NA	0.0	NA
6	Propanil	13.4	NA	43.6	NA	34.6
7	Vinclozolin	NA	NA	34.1	NA	NA
8	Prochloraz	12.1	2.5	17.7	NA	NA
9	Butralin	NA	6.1	31.6	0.0	NA
10	Cymoxanil	NA	NA	46.0	NA	53.7
11	Difenoconazole	1.3	2.1	4.2	NA	38.9
12	Formetanate hydrochloride	NA	81.7	NA	NA	20.9
13	Azoxystrobin	NA	3.9	19.4	NA	NA
14	Ethoprop	NA	13.1	88.9	0.0	46.6
15	Fenitrothion	4.4	NA	31.4	NA	5.0
16	Pyraclostrobin	NA	0.5	1.8	NA	NA
17	Thidiazuron	NA	19.5	NA	6.3	36.0
18	Spiroxamine	0.0	3.8	NA	2.1	NA
19	Imazapic	NA	35.5	NA	NA	NA
20	Fluoxastrobin	NA	0.6	11.5	NA	NA
21	Iodosulfuron-methyl-sodium	NA	NA	NA	NA	NA
22	Azamethiphos	NA	11.1	NA	NA	9.6

Appendix Table 5. cntd. ToxPi input file for AC_{50} values of all 22 PLLDs towards the 13 assays identified through univariate analysis

S. No.	Chemical	TSPO	CYP2A1	CYP2C13
1	Anilazine	1.4	NA	NA
2	Bisphenol A	15.3	2.8	2.4
3	Ethylene thiourea	NA	NA	NA
4	Fluometuron	14.3	4.4	NA
5	Thiabendazole	NA	NA	NA
6	Propanil	11.3	2.1	6.7
7	Vinclozolin	0.7	NA	NA
8	Prochloraz	0.1	0.5	0.2
9	Butralin	NA	NA	0.7
10	Cymoxanil	NA	NA	NA
11	Difenoconazole	1.8	0.1	1.1
12	Formetanate hydrochloride	NA	NA	NA
13	Azoxystrobin	1.8	4.7	NA
14	Ethoprop	15.4	NA	NA
15	Fenitrothion	41.0	3.9	10.7
16	Pyraclostrobin	0.3	NA	NA
17	Thidiazuron	NA	5.9	7.7
18	Spiroxamine	NA	NA	NA
19	Imazapic	NA	NA	NA
20	Fluoxastrobin	NA	1.5	NA
21	Iodosulfuron-methyl-sodium	NA	NA	NA
22	Azamethiphos	NA	NA	NA

Appendix Table 6. The list of assays identified through Univariate Analysis of ISV-VDCs with number of true positive and p-value for each assay. Z-score was applied for these assays.

S. No	Assay	Biological Endpoint	Gene Target	True Positives	p-value
1	TOX21_p53_BLA_p2_ratio	apoptosis up	TP53	6	0.000
2	TOX21_TR_LUC_GH3_Antagonist	nuclear receptor Tox21 ant	THR	6	0.000
3	ATG_NF_kB_CIS_up	inflammation up	NFKB1	4	0.000
4	ATG_Xbp1_CIS_up	ER stress	XBP1	4	0.001
5	BSK_SAg_MCP1_down	chemokine down	CCL2	4	0.002
6	ATG_HIF1a_CIS_up	hypoxia	HIF1A	3	0.003
7	BSK_SAg_IL8_down	chemokine down	CXCL8	4	0.005
8	TOX21_AR_BLA_Antagonist_ratio	androgen receptor	AR	4	0.005
9	ATG_Sp1_CIS_up	transcription factor	SP1	3	0.006
10	BSK_3C_HLADR_down	inflammation down	HLA-DRA	5	0.013
11	ATG_BRE_CIS_up	transcription factor	SMAD1	4	0.013
12	ATG_EGR_CIS_up	growth factor up	EGR1	3	0.013
13	TOX21_ARE_BLA_agonist_ratio	inflammation up	NFE2L2	4	0.017
14	ATG_DR5_CIS_up	nuclear receptor ATG	RAR	5	0.028
15	ATG_Oct_MLP_CIS_up	transcription factor	POU2F1	5	0.037
16	BSK_hDFCGF_CollagenIII_down	cellular adhesion down	COL3A1	4	0.037
17	BSK_SAg_CD69_down	inflammation down	CD69	3	0.037
18	BSK_SAg_Eselectin_down	inflammation down	SELE	4	0.044
19	ATG_PPRE_CIS_up	ppar signaling	PPAR-A	4	0.047

Appendix Table 7. ToxPi input file for AC_{50} values of 10 ISV-VDCs towards the 19 assays identified through univariate analysis

S. No.	Chemical	TP53	CXCL8	HLA-DRA	THR	NFKB1
1	(Z,E)-Fenpyroximate	0.004	1.0	1.0000000	0.01	0.1
2	Acibenzolar-S-methyl	NA	NA	NA	NA	NA
3	Dicofol	NA	40.0	10.0	78.1	NA
4	Diniconazole	NA	40.0	40.0	60.8	NA
5	Niclosamide	0.2	1.0	1.0	0.2	0.8
6	Pyraclostrobin	1.1	1.0	1.0	0.1	0.9
7	Pyridaben	0.01	1.0	1.0	1.4	0.1
8	Rotenone	0.1	1.0	1.0	0.03	0.1
9	Tebupirimfos	NA	40.0	40.0	52.5	22.6
10	Trifloxystrobin	1.4	1.0	1.0	0.6	37.4

Appendix Table 7. cntd. ToxPi input file for AC_{50} values of 10 ISV-VDCs towards the 19 assays identified through univariate analysis

S. No.	Chemical	XBP1	CCL2	HIF1A	AR	SP1
1	(Z,E)-Fenpyroximate	0.03	1.0	1.2	0.7	0.02
2	Acibenzolar-S-methyl	NA	NA	NA	NA	NA
3	Dicofol	NA	40.0	NA	36.6	NA
4	Diniconazole	NA	40.0	NA	22.4	NA
5	Niclosamide	0.5	1.0	0.6	0.4	0.5
6	Pyraclostrobin	0.4	1.0	NA	1.2	1.0
7	Pyridaben	NA	1.0	0.4	0.05	0
8	Rotenone	0.02	10.0	0.03	0.2	0.04
9	Tebupirimfos	5.4	40.0	NA	46.8	31.8
10	Trifloxystrobin	9.2	1.0	16.2	3.0	NA

Appendix Table 7. cntd. ToxPi input file for AC_{50} values of 10 ISV-VDCs towards the 19 assays identified through univariate analysis

S. No.	Chemical	SMAD1	EGR1	NFE2L2	RAR	POU2F1
1	(Z,E)-Fenpyroximate	0.03	0.7	0.004	0.03	0.03
2	Acibenzolar-S-methyl	NA	NA	NA	NA	NA
3	Dicofol	NA	NA	22.5	NA	NA
4	Diniconazole	NA	NA	53.2	NA	NA
5	Niclosamide	0.6	0.6	NA	0.7	0.6
6	Pyraclostrobin	0.7	1.7	0.3	0.5	0.6
7	Pyridaben	0.07	0.5	0.01	1.1	0.01
8	Rotenone	0.01	0.03	0.01	0.02	0.03
9	Tebupirimfos	56.2	19.9	NA	12.3	2.1
10	Trifloxystrobin	22.6	25.8	23.0	NA	14.2

Appendix Table 7. cntd. ToxPi input file for AC_{50} values of 10 ISV-VDCs towards the 19 assays identified through univariate analysis

S. No.	Chemical	COL3A1	CD69	SELE	PPAR-A
1	(Z,E)-Fenpyroximate	1.0	1.0	1.0	0.03
2	Acibenzolar-S-methyl	NA	NA	NA	NA
3	Dicofol	10	40.0	40.0	NA
4	Diniconazole	NA	40.0	40.0	NA
5	Niclosamide	1.0	1.0	1.0	0.5
6	Pyraclostrobin	1.0	1.0	1.0	0.3
7	Pyridaben	10.0	1.0	1.0	0.8
8	Rotenone	40.0	1.0	1.0	0.1
9	Tebupirimfos	40.0	40.0	40.0	NA
10	Trifloxystrobin	1.0	4.0	1.0	NA

Appendix Table 8. Treatment concentrations of the predicted PLLDs identified through ToxPi Ranking

S. No.	Chemical Name	Concentrations Tested
1	Prochloraz	10µM, 1µM, 0.1µM
2	Forchlorfenuron	10µM, 1µM, 0.1µM
3	Flusilazole	10µM, 1µM, 0.1µM
4	Clorophene	10µM, 1µM, 0.1µM
5	Pentamidine isethionate	10µM, 1µM, 0.1µM
6	Gentian Violet	10µM, 1µM, 0.1µM
7	AVE6324	10µM, 1µM, 0.1µM
8	Dodecylbenzenesulfonic acid	10µM, 1µM, 0.1µM
9	Didecyldimethylammonium chloride	10µM, 1µM, 0.1µM
10	Decane	10µM, 1µM, 0.1µM
11	CP-608039	10µM, 1µM, 0.1µM
12	CP-471358	10µM, 1µM, 0.1µM
13	Malic acid	10µM, 1µM, 0.1µM
14	CP-283097	10µM, 3.3µM, 1µM, 0.1µM
15	CI-1029	10µM, 1µM, 0.1µM

BIBLIOGRAPHY

Airhart, M. J., Lee, D. H., Wilson, T. D., Miller, B. E., Miller, M. N., Skalko, R. G. and Monaco, P. J. (2012) 'Adverse effects of serotonin depletion in developing zebrafish', *Neurotoxicology and Teratology*, 34(1), pp. 152–160.

Ali, S., Champagne, D. L., Spaink, H. P. and Richardson, M. K. (2011) 'Zebrafish embryos and larvae: A new generation of disease models and drug screens', *Birth Defects Research Part C - Embryo Today: Reviews*, 93(2), pp. 115–133.

Arnaoutova, I. and Kleinman, H. K. (2010) 'In vitro angiogenesis: Endothelial cell tube formation on gelled basement membrane extract', *Nature Protocols*, 5(4), pp. 628–635.

Ball, J. S., Stedman, D. B., Hillegass, J. M., Zhang, C. X., Panzica-kelly, J., Coburn, A., Enright, B. P., Tornesi, B., Amouzadeh, H. R., Hetheridge, M., Gustafson, A. L. and Augustine-rauch, K. A. (2014) 'Fishing for teratogens: A consortium effort for a harmonized zebrafish developmental toxicology assay', *Toxicological Sciences*, 139(1), pp. 210–219.

Bard, J. A., Zgombick, J., Adham, N., Vaysse, P., Branchek, T. A. and Weinshank, R. L. (1993) 'Cloning of a novel human serotonin receptor (5-HT7) positively linked to adenylate cyclase', *Journal of Biological Chemistry*, 268(31), pp. 23422–23426.

Barnabas, O., Wang, H. and Gao, X.-M. (2013) 'Role of estrogen in angiogenesis in cardiovascular diseases', *Journal of Geriatric Cardiology : JGC*, 10(4), pp. 377–382.

Barnes, N. M. and Sharp, T. (1999) 'A review of central 5-HT receptors and their function', *Neuropharmacology*, 38(8), pp. 1083–1152.

Batarseh, A. and Papadopoulos, V. (2010) 'Regulation of translocator protein 18 kDa (TSPO) expression in health and disease states', *Molecular and Cellular Endocrinology*, 327(1–2), pp. 1–12.

Bel, N. and Artigas, F. (1993) 'Chronic treatment with fluvoxamine increases extracellular serotonin in frontal cortex but not in raphe nuclei', *Synapse*, 15(3), pp. 243–245.

Benmansour, S., Owens, W. A., Cecchi, M., Morilak, D. A. and Frazer, A. (2002) 'Serotonin clearance in vivo is altered to a greater extent by antidepressant-induced downregulation of the serotonin transporter than by acute blockade of this transporter', *The Journal of Neuroscience : The Official Journal of the Society for Neuroscience*, 22(15), pp. 6766–6772.

Bortolato, M. and Shih, J. C. (2011) *Behavioral outcomes of monoamine oxidase deficiency: Preclinical and clinical evidence*. 1st edn, *International Review of Neurobiology*. 1st edn. Elsevier Inc.

Brignull, H. R., Raible, D. W. and Stone, J. S. (2009) 'Feathers and fins: non-mammalian models for hair cell regeneration', *Brain Research*. 2009/02/24, 1277, pp. 12–23.

Briley, M. and Moret, C. (1993) 'Neurobiological mechanisms involved in antidepressant therapies.', *Clinical Neuropharmacology*, pp. 387–400.

Bugel, S. M., Tanguay, R. L. and Planchart, A. (2014) 'Zebrafish: A marvel of high-throughput biology for 21(st) century toxicology', *Current Environmental Health Reports*, 1(4), pp. 341–352.

Bushby, A. J., Mariggi, G., Armer, H. E. J. and Collinson, L. M. (2012) 'Correlative Light and Volume Electron Microscopy: Using Focused Ion Beam Scanning Electron Microscopy to Image Transient Events in Model Organisms', *Methods in Cell Biology*, 111, pp. 357–382.

Carvan, M. J., Dalton, T. P., Stuart, G. W. and Nebert, D. W. (2006) 'Transgenic Zebrafish as Sentinels for Aquatic Pollution', *Annals of the New York Academy of Sciences*, 919(1), pp. 133–147.

Center for Disease Control and Prevention (2020) 'Facts about Birth Defects'. Available at: https://www.cdc.gov/ncbddd/birthdefects/facts.html.

Charles, B. and Brandom, B. W. (2015) 'Methylene Blue and the Risk of Serotonin Toxicity', *APSF Newsletter*, 30(1), pp. 1–6.

Chevalier, F., Lavergne, M., Negroni, E., Ferratge, S., Carpentier, G., Gilbert-Sirieix, M., Siñeriz,

F., Uzan, G. and Albanese, P. (2014) ‘Glycosaminoglycan mimetic improves enrichment and cell functions of human endothelial progenitor cell colonies’, *Stem Cell Research*, 12(3), pp. 703–715.

Chitnis, A. B., Nogare, D. D. and Matsuda, M. (2012) ‘Building the posterior lateral line system in zebrafish’, *Developmental Neurobiology*, 72(3), pp. 234–255.

Chiu, L. L., Cunningham, L. L., Raible, D. W., Rubel, E. W. and Ou, H. C. (2008) ‘Using the zebrafish lateral line to screen for ototoxicity’, *JARO - Journal of the Association for Research in Otolaryngology*, 9(2), pp. 178–190.

Coccimiglio, M. L. and Jonz, M. G. (2012) ‘Serotonergic neuroepithelial cells of the skin in developing zebrafish: morphology, innervation and oxygen-sensitive properties’, *The Journal of Experimental Biology*, 215, pp. 3881–3894.

Crewe, H. K., Lennard, M. S., Tucker, G. T., Woods, F. R. and Haddock, R. E. (1992) ‘The effect of selective serotonin re-uptake inhibitors on cytochrome P4502D6 (CYP2D6) activity in human liver microsomes’, *British Journal ofCclinical Pharmacology*, 34(3), pp. 262–265.

Dahm, R. and Geisler, R. (2006) ‘Learning from small fry: The zebrafish as a genetic model organism for aquaculture fish species’, *Marine Biotechnology*, 8(4), pp. 329–345.

Davis, P. J., Davis, F. B. and Mousa, S. A. (2009) ‘Thyroid hormone-induced angiogenesis’, *Current Cardiology Reviews*, 5(1), pp. 12–16.

Dix, D. J., Houck, K. A., Martin, M. T., Richard, A. M., Setzer, R. W. and Kavlock, R. J. (2007) ‘The toxcast program for prioritizing toxicity testing of environmental chemicals’, *Toxicological Sciences*, 95(1), pp. 5–12.

Driever, W., Stemple, D., Schier, A. and Solnica-Krezel, L. (1994) ‘Zebrafish: genetic tools for studying vertebrate development’, *Trends in Genetics*, 10(5), pp. 152–159.

Dringenberg, H. C., Hargreaves, E. L., Baker, G. B., Cooley, R. K. and Vanderwolf, C. H. (1995) ‘p-Chlorophenylalanine-induced serotonin depletion: reduction in exploratory locomotion but no

obvious sensory-motor deficits', *Behavioural Brain Research*, 68(2), pp. 229–237.

Dutheil, F., Beaune, P. and Loriot, M. A. (2008) 'Xenobiotic metabolizing enzymes in the central nervous system: Contribution of cytochrome P450 enzymes in normal and pathological human brain', *Biochimie*, 90(3), pp. 426–436.

Environmental Protection Agency (2018) 'Releases of Chemicals', *TRI National Analysis:Release of Chemicals*, (January), pp. 1–22. Available at: https://www.epa.gov/trinationalanalysis/releases-chemicals.

Faucherre, A., Pujol-Martí, J., Kawakami, K. and López-Schier, H. (2009) 'Afferent neurons of the zebrafish lateral line are strict selectors of hair-cell orientation', *PLoS ONE*, 4(2).

Folkman, J. and Haudenschild, C. (1980) 'Angiogenesis in vitro', *Nature*, 288(5791), pp. 551–556.

Forrest, D., Erway, L. C., Ng, L., Altschuler, R. and Curran, T. (1996) 'Thyroid hormone receptor β is essential for development of auditory function', *Nature Genetics*, 13(3), pp. 354–357.

Fouquet, B., Weinstein, B. M., Serluca, F. C. and Fishman, M. C. (1997) 'Vessel Patterning in the Embryo of the Zebrafish: Guidance by Notochord', *Developmental Biology*. Academic Press, 183(1), pp. 37–48.

Gallardo, V. E., Varshney, G. K., Lee, M., Bupp, S., Xu, L., Shinn, P., Crawford, N. P., Inglese, J. and Burgess, S. M. (2015) 'Phenotype-driven chemical screening in zebrafish for compounds that inhibit collective cell migration identifies multiple pathways potentially involved in metastatic invasion', *DMM Disease Models and Mechanisms*, 8(6), pp. 565–576.

Garcia-Miralles, M., Ooi, J., Ferrari Bardile, C., Tan, L. J., George, M., Drum, C. L., Lin, R. Y., Hayden, M. R. and Pouladi, M. A. (2016) 'Treatment with the MAO-A inhibitor clorgyline elevates monoamine neurotransmitter levels and improves affective phenotypes in a mouse model of Huntington disease', *Experimental Neurology*, 278, pp. 4–10.

Ghysen, A. and Dambly-Chaudière, C. (2007) 'The lateral line microcosmos', *Genes and Development*, 21(17), pp. 2118–2130.

Giacomini, A. C. V. V., Abreu, M. S., Giacomini, L. V., Siebel, A. M., Zimerman, F. F., Rambo, C. L., Mocelin, R., Bonan, C. D., Piato, A. L. and Barcellos, L. J. G. (2016) 'Fluoxetine and diazepam acutely modulate stress induced-behavior', *Behavioural Brain Research*, 296, pp. 301–310.

Goldstone, J. V., McArthur, A. G., Kubota, A., Zanette, J., Parente, T., Jönsson, M. E., Nelson, D. R. and Stegeman, J. J. (2010) 'Identification and developmental expression of the full complement of Cytochrome P450 genes in Zebrafish', *BMC Genomics*, 11(1), p. 643.

Gompel, N., Cubedo, N., Thisse, C., Thisse, B., Dambly-Chaudière, C. and Ghysen, A. (2001) 'Pattern formation in the lateral line of zebrafish', *Mechanisms of Development*, 105(1–2), pp. 69–77.

Gore, A. V, Monzo, K., Cha, Y. R., Pan, W. and Weinstein, B. M. (2012) 'Vascular development in the zebrafish', *Cold Spring Harbor Perspectives in Medicine*, 2(5), pp. a006684–a006684.

Gorelick, D. A. and Halpern, M. E. (2011) 'Visualization of estrogen receptor transcriptional activation in zebrafish', *Endocrinology*, 152(7), pp. 2690–2703.

Grau, R., Punzón, C., Fresno, M. and Iñiguez, M. A. (2006) 'Peroxisome-proliferator-activated receptor α agonists inhibit cyclo-oxygenase 2 and vascular endothelial growth factor transcriptional activation in human colorectal carcinoma cells via inhibition of activator protein-1', *Biochemical Journal*, 395(1), pp. 81–88.

Gustafson, A. L., Stedman, D. B., Ball, J., Hillegass, J. M., Flood, A., Zhang, C. X., Panzica-Kelly, J., Cao, J., Coburn, A., Enright, B. P., Tornesi, M. B., Hetheridge, M. and Augustine-Rauch, K. A. (2012) 'Inter-laboratory assessment of a harmonized zebrafish developmental toxicology assay - Progress report on phase I', *Reproductive Toxicology*, 33(2), pp. 155–164.

Haas, P. and Gilmour, D. (2006) 'Chemokine Signaling Mediates Self-Organizing Tissue

Migration in the Zebrafish Lateral Line', *Developmental Cell*, 10(5), pp. 673–680.

Haduch, A., Bromek, E., Sadakierska-Chudy, A., Wójcikowski, J. and Daniel, W. A. (2013) 'The catalytic competence of cytochrome P450 in the synthesis of serotonin from 5-methoxytryptamine in the brain: An in vitro study', *Pharmacological Research*, 67(1), pp. 53–59.

Hamilton, F. (1822) *An account of the fishes found in the river Ganges and its branches*. Edinburgh : Printed for A. Constable and company; [etc., etc.]. Available at: https://www.biodiversitylibrary.org/item/30042.

Henson, H. E., Parupalli, C., Ju, B. and Taylor, M. R. (2014) 'Functional and genetic analysis of choroid plexus development in zebrafish', *Frontiers in Neuroscience*, 8, p. 364.

Hill, A. J., Teraoka, H., Heideman, W. and Peterson, R. E. (2005) 'Zebrafish as a model vertebrate for investigating chemical toxicity', *Toxicological Sciences*, 86(1), pp. 6–19.

Hogan, B. M. and Schulte-Merker, S. (2017) 'How to Plumb a Pisces: Understanding Vascular Development and Disease Using Zebrafish Embryos', *Developmental Cell*, 42(6), pp. 567–583.

Howe, K., Clark, M. D., Torroja, C. F., Torrance, J., Berthelot, C., Muffato, M., Collins, J. E., Humphray, S., McLaren, K., Matthews, L., McLaren, S., Sealy, I., Caccamo, M., Churcher, C., Scott, C., Barrett, J. C., Koch, R., Rauch, G. J., White, S., *et al.* (2013) 'The zebrafish reference genome sequence and its relationship to the human genome', *Nature*, 496(7446), pp. 498–503.

Inoue, I., Shino, K., Noji, S., Awata, T. and Katayama, S. (1998) 'Expression of peroxisome proliferator-activated receptor α (PPARα) in primary cultures of human vascular endothelial cells', *Biochemical and Biophysical Research Communications*, 246(2), pp. 370–374.

Isogai, S., Horiguchi, M. and Weinstein, B. M. (2001) 'The vascular anatomy of the developing zebrafish: An atlas of embryonic and early larval development', *Developmental Biology*, 230(2), pp. 278–301.

Judson, R., Houck, K., Martin, M., Richard, A. M., Knudsen, T. B., Shah, I., Little, S., Wambaugh,

J., Woodrow Setzer, R., Kothiya, P., Phuong, J., Filer, D., Smith, D., Reif, D., Rotroff, D., Kleinstreuer, N., Sipes, N., Xia, M., Huang, R., *et al.* (2016) 'Editor's Highlight: Analysis of the Effects of Cell Stress and Cytotoxicity on In Vitro Assay Activity Across a Diverse Chemical and Assay Space.', *Toxicological Sciences : an official journal of the Society of Toxicology*, 152(2), pp. 323–339.

Judson, R. S., Houck, K. A., Kavlock, R. J., Knudsen, T. B., Martin, M. T., Mortensen, H. M., Reif, D. M., Rotroff, D. M., Shah, I., Richard, A. M. and Dix, D. J. (2010) 'In vitro screening of environmental chemicals for targeted testing prioritization: The toxcast project', *Environmental Health Perspectives*, 118(4), pp. 485–492.

Kalluri, R. (2003) 'Basement membranes: Structure, assembly and role in tumour angiogenesis', *Nature Reviews Cancer*, 3(6), pp. 422–433.

Kaslin, J. and Panula, P. (2001) 'Comparative anatomy of the histaminergic and other aminergic systems in zebrafish (Danio rerio)', *Journal of Comparative Neurology*, 440(4), pp. 342–377.

Kelley, M. W., Xu, X. M., Wagner, M. A., Warchol, M. E. and Corwin, J. T. (1993) 'The developing organ of Corti contains retinoic acid and forms supernumerary hair cells in response to exogenous retinoic acid in culture', *Development*, 119(4), pp. 1041–1053.

Kim, T. H., Hur, E. G., Kang, S. J., Kim, J. A., Thapa, D., Mie Lee, Y., Ku, S. K., Jung, Y. and Kwak, M. K. (2011) 'NRF2 blockade suppresses colon tumor angiogenesis by inhibiting hypoxia-induced activation of HIF-1α', *Cancer Research*, 71(6), pp. 2260–2275.

Kimmel, C. B., Warga, R. M. and Schilling, T. F. (1990) 'Origin and organization of the zebrafish fate map', *Development*, 108(4), pp. 581 LP – 594.

Kleinstreuer, N. C., Judson, R. S., Reif, D. M., Sipes, N. S., Singh, A. V., Chandler, K. J., DeWoskin, R., Dix, D. J., Kavlock, R. J. and Knudsen, T. B. (2011) 'Environmental impact on vascular development predicted by high-throughput screening', *Environmental Health Perspectives*, 119(11), pp. 1596–1603.

Koehler, K. R., Nie, J., Longworth-Mills, E., Liu, X.-P., Lee, J., Holt, J. R. and Hashino, E. (2017) 'Generation of inner ear organoids containing functional hair cells from human pluripotent stem cells', *Nature Biotechnology*, 35(6), pp. 583–589.

Kondrychyn, I., Teh, C., Garcia-Lecea, M., Guan, Y., Kang, A. and Korzh, V. (2011) 'Zebrafish Enhancer TRAP Transgenic Line Database ZETRAP 2.0', *Zebrafish*, 8(4), pp. 181–182.

Kraska, R. C. (2001) 'Industrial chemicals: Regulation of new and existing chemicals (The Toxic Substances Control Act and similar worldwide chemical control laws)', in *Regulatory Toxicology, 2nd Ed.*, pp. 244–276.

Kubota, Y., Kleinman, H. K., Martin, G. R. and Lawley, T. J. (1988) 'Role of laminin and basement membrane in the morphological differentiation of human endothelial cells into capillary-like structures.', *The Journal of Cell Biology*, 107(4), pp. 1589–1598.

Kysil, E. V, Meshalkina, D. A., Frick, E. E., Echevarria, D. J., Rosemberg, D. B., Maximino, C., Lima, M. G., Abreu, M. S., Giacomini, A. C., Barcellos, L. J. G., Song, C. and Kalueff, A. V (2017) 'Comparative Analyses of Zebrafish Anxiety-Like Behavior Using Conflict-Based Novelty Tests', *Zebrafish*, 14(3), pp. 197–208.

Lawal, H. O. and Krantz, D. E. (2013) 'SLC18: Vesicular neurotransmitter transporters for monoamines and acetylcholine', *Molecular Aspects of Medicine*, 34(2–3), pp. 360–372.

Ledent, V. (2002) 'Postembryonic development of the posterior lateral line in zebrafish', *Development*, 129(3), pp. 597 LP – 604.

Lee, O., Green, J. M. and Tyler, C. R. (2015) 'Transgenic fish systems and their application in ecotoxicology', *Critical Reviews in Toxicology*, 45(2), pp. 124–141.

Lee, Y. M., Jeong, C.-H., Koo, S.-Y., Son, M. J., Song, H. S., Bae, S.-K., Raleigh, J. A., Chung, H.-Y., Yoo, M.-A. and Kim, K.-W. (2001) 'Determination of hypoxic region by hypoxia marker in developing mouse embryos in vivo: A possible signal for vessel development', *Developmental Dynamics*, 220(2), pp. 175–186.

Lefebvre, P., Martin, P. J., Billaut, X. and Lefebvre, B. (2005) 'Transciptional Activities of Retinoic Acid Receptors', *Vitamins And Hormones*, 70, pp. 199–264 .

Leung, D. W., Cachianes, G., Kuang, W. J., Goeddel, D. V and Ferrara, N. (1989) 'Vascular endothelial growth factor is a secreted angiogenic mitogen', *Science*, 246(4935), pp. 1306 LP – 1309.

Lieschke, G. J. and Trede, N. S. (2009) 'Fish immunology', *Current Biology*, 19(16), pp. R678–R682.

Lomasney, J. W., Lorenz, W., Allen, L. F., King, K., Regan, J. W., Yang-Feng, T. L., Caron, M. G. and Lefkowitz, R. J. (1990) 'Expansion of the α2-adrenergic receptor family: Cloning and characterization of a human α2-adrenergic receptor subtype, the gene for which is located on chromosome 2', *Proceedings of the National Academy of Sciences of the United States of America*, 87(13), pp. 5094–5098.

López-Schier, H. and Hudspeth, A. J. (2006) 'A two-step mechanism underlies the planar polarization of regenerating sensory hair cells', *Proceedings of the National Academy of Sciences of the United States of America*, 103(49), pp. 18615–18620.

Ma, D., Rajakumaraswamy, N. and Maze, M. (2005) 'α2-adrenoceptor agonists: Shedding light on neuroprotection?', *British Medical Bulletin*, 71, pp. 77–92.

Maciag, T., Kadish, J., Wllkins, L., Stemerman, M. B. and Weinstein, R. (1982) 'Organizational behavior of human umbilical vein endothelial cells', *Journal of Cell Biology*, 94(3), pp. 511–520.

MacRae, C. A. and Peterson, R. T. (2015) 'Zebrafish as tools for drug discovery', *Nature Reviews Drug Discovery*, 14(10), pp. 721–731.

Madri, J. A. and Williams, S. K. (1983) 'Capillary endothelial cell cultures: Phenotypic modulation by matrix components', *Journal of Cell Biology*, 97(1), pp. 153–165.

Mahmood, N., Mihalcioiu, C. and Rabbani, S. A. (2018) 'Multifaceted role of the urokinase-type

plasminogen activator (uPA) and its receptor (uPAR): Diagnostic, prognostic, and therapeutic applications', *Frontiers in Oncology*, 8(24).

Marvel, S. W., To, K., Grimm, F. A., Wright, F. A., Rusyn, I. and Reif, D. M. (2018) 'ToxPi Graphical User Interface 2.0: Dynamic exploration, visualization, and sharing of integrated data models', *BMC bioinformatics*, 19(1), p. 80.

McCollum, C. W., Conde-Vancells, J., Hans, C., Vazquez-Chantada, M., Kleinstreuer, N., Tal, T., Knudsen, T., Shah, S. S., Merchant, F. A., Finnell, R. H., Gustafsson, J.-Å., Cabrera, R. and Bondesson, M. (2017) 'Identification of vascular disruptor compounds by analysis in zebrafish embryos and mouse embryonic endothelial cells', *Reproductive Toxicology (Elmsford, N.Y.)*, 70, p. 60—69.

Meissner, M., Stein, M., Urbich, C., Reisinger, K., Suske, G., Staels, B., Kaufmann, R. and Gille, J. (2004) 'PPARα Activators Inhibit Vascular Endothelial Growth Factor Receptor-2 Expression by Repressing Sp1-Dependent DNA Binding and Transactivation', *Circulation Research*, 94(3), pp. 324–332.

Miksys, S., Rao, Y., Sellers, E. M., Kwan, M., Mendis, D. and Tyndale, R. F. (2000) 'Regional and cellular distribution of CYP2D subfamily members in rat brain', *Xenobiotica*, 30(6), pp. 547–564.

Namdaran, P., Reinhart, K. E., Owens, K. N., Raible, D. W. and Rubel, E. W. (2012) 'Identification of modulators of hair cell regeneration in the zebrafish lateral line', *Journal of Neuroscience*, 32(10), pp. 3516–3528.

National Research Council (2007) *Toxicity Testing in the 21st Century: A Vision and a Strategy*. Washington, DC: The National Academies Press.

National Toxicology Program (2020) 'Toxicology in the 21st Century (Tox21)'. Available at: https://ntp.niehs.nih.gov/results/tox21/index.html.

Neufeld, G., Tessler, S., Gitay-Goren, H., Cohen, T. and Levi, B.-Z. (1994) 'Vascular endothelial

growth factor and its receptors', *Progress in Growth Factor Research*, 5(1), pp. 89–97.

Nicholas, A. P., Pieribone, V. A., Elde, R. and Hökfelt, T. (1991) 'Initial observations on the localization of mRNA for α and β adrenergic receptors in brain and peripheral tissues of rat using in situ hybridization', *Molecular and Cellular Neuroscience*, 2(4), pp. 344–350.

Nichols, D. E. and Nichols, C. D. (2008) 'Serotonin receptors', *Chemical Reviews*, 108(5), pp. 1614–1641.

Nicolson, T. (2005) 'The Genetics of Hearing and Balance in Zebrafish', *Annual Review of Genetics*, 39(1), pp. 9–22.

Nuñez, V. A., Sarrazin, A. F., Cubedo, N., Allende, M. L., Dambly-Chaudière, C. and Ghysen, A. (2009) 'Postembryonic development of the posterior lateral line in the zebrafish', *Evolution and Development*, 11(4), pp. 391–404.

Olive, R., Wolf, S., Dubreuil, A., Bormuth, V., Debrégeas, G. and Candelier, R. (2016) 'Rheotaxis of Larval Zebrafish: Behavioral Study of a Multi-Sensory Process', *Frontiers in Systems Neuroscience*, 10, p. 14.

Ooi, J., Hayden, M. R. and Pouladi, M. A. (2015) 'Inhibition of Excessive Monoamine Oxidase A/B Activity Protects Against Stress-induced Neuronal Death in Huntington Disease', *Molecular Neurobiology*, 52(3), pp. 1850–1861.

Ou, H. C., Cunningham, L. L., Francis, S. P., Brandon, C. S., Simon, J. A., Raible, D. W. and Rubel, E. W. (2009) 'Identification of FDA-approved drugs and bioactives that protect hair cells in the zebrafish (danio rerio) lateral line and mouse (mus musculus) utricle', *JARO - Journal of the Association for Research in Otolaryngology*, 10(2), pp. 191–203.

Owens, K. N., Santos, F., Roberts, B., Linbo, T., Coffin, A. B., Knisely, A. J., Simon, J. A., Rubel, E. W. and Raible, D. W. (2008) 'Identification of Genetic and Chemical Modulators of Zebrafish Mechanosensory Hair Cell Death', *PLoS Genetics*, 4(2), p. e1000020.

Padilla, S., Corum, D., Padnos, B., Hunter, D. L., Beam, A., Houck, K. A., Sipes, N., Kleinstreuer, N., Knudsen, T., Dix, D. J. and Reif, D. M. (2012) 'Zebrafish developmental screening of the ToxCast™ Phase I chemical library', *Reproductive Toxicology*, 33(2), pp. 174–187.

Pagès, G. and Pouysségur, J. (2005) 'Transcriptional regulation of the Vascular Endothelial Growth Factor gene - A concert of activating factors', *Cardiovascular Research*, 65(3), pp. 564–573.

Pawlikowski, B., Wragge, J. and Siegenthaler, J. A. (2019) 'Retinoic acid signaling in vascular development', *Genesis (New York, N.Y. : 2000)*, 57(7–8), pp. e23287–e23287.

Pinto-Teixeira, F., Viader-Llargués, O., Torres-Mejía, E., Turan, M., González-Gualda, E., Pola-Morell, L. and Lopez-Schier, H. (2015) 'Inexhaustible hair-cell regeneration in young and aged zebrafish', *Biology Open*, 4(7), pp. 903–909.

Ramírez-Bergeron, D. L., Runge, A., Adelman, D. M., Gohil, M. and Simon, M. C. (2006) 'HIF-dependent hematopoietic factors regulate the development of the embryonic vasculature', *Developmental Cell*, 11(1), pp. 81–92.

Ramsay, R. R., Dunford, C. and Gillman, P. K. (2007) 'Methylene blue and serotonin toxicity: Inhibition of monoamine oxidase A (MAO A) confirms a theoretical prediction', *British Journal of Pharmacology*, 152(6), pp. 946–951.

Reif, D. M., Martin, M. T., Tan, S. W., Houck, K. A., Judson, R. S., Richard, A. M., Knudsen, T. B., Dix, D. J. and Kavlock, R. J. (2010) 'Endocrine profiling and prioritization of environmental chemicals using ToxCast data', *Environmental Health Perspectives*, 118(12), pp. 1714–1720.

Rey, S. and Semenza, G. L. (2010) 'Hypoxia-inducible factor-1-dependent mechanisms of vascularization and vascular remodelling', *Cardiovascular Research*, 86(2), pp. 236–242.

Richard, A., Judson, R., Houck, K., Grulke, C., Volarath, P., Thillainadarajah, I., Yang, C., Rathman, J., Martin, M., Wambaugh, J., Knudsen, T., Kancherla, J., Kamel, M., Patlewicz, G., Williams, A., Little, S., Crofton, K. and Thomas, R. (2016) 'The ToxCast Chemical Landscape:

Paving the Road to 21st Century Toxicology', *Chemical Research in Toxicology*, 29(8), pp. 1225–1251.

Romand, R., Dollé, P. and Hashino, E. (2006) 'Retinoid signaling in inner ear development', *Journal of Neurobiology*, 66(7), pp. 687–704.

Rousseaux, C. G. and Greene, S. F. (2016) 'Sigma receptors [σ Rs]: Biology in normal and diseased states', *Journal of Receptors and Signal Transduction*, 36(4), pp. 327–388.

Rupprecht, R., Papadopoulos, V., Rammes, G., Baghai, T. C., Fan, J., Akula, N., Groyer, G., Adams, D. and Schumacher, M. (2010) 'Translocator protein (18 kDa) (TSPO) as a therapeutic target for neurological and psychiatric disorders', *Nature Reviews Drug Discovery*, 9(12), pp. 971–988.

Saad, M., Cavanaugh, K., Verbueken, E., Pype, C., Casteleyn, C., Ginneken, C. Van and Cruchten, S. Van (2016) 'Xenobiotic metabolism in the zebrafish: A review of the spatiotemporal distribution, modulation and activity of cytochrome p450 families 1 to 3', *Journal of Toxicological Sciences*, 41(1), pp. 1–11.

Saito, A., Sugawara, A., Uruno, A., Kudo, M., Kagechika, H., Sato, Y., Owada, Y., Kondo, H., Sato, M., Kurabayashi, M., Imaizumi, M., Tsuchiya, S. and Ito, S. (2007) 'All-trans retinoic acid induces in vitro angiogenesis via retinoic acid receptor: Possible involvement of paracrine effects of endogenous vascular endothelial growth factor signaling', *Endocrinology*, 148(3), pp. 1412–1423.

Sangkuhl, K., Klein, T. E. and Altman, R. B. (2009) 'Selective serotonin reuptake inhibitors pathway', *Pharmacogenetics and Genomics*, 19(11), pp. 907–909.

Singh, A., Mudawal, A., Shukla, R. K., Yadav, S., Khanna, V. K., Sethumadhavan, R. and Parmar, D. (2015) 'Effect of Gestational Exposure of Cypermethrin on Postnatal Development of Brain Cytochrome P450 2D1 and 3A1 and Neurotransmitter Receptors', *Molecular Neurobiology*, 52(1), pp. 741–756.

Sipes, N. S., Martin, M. T., Reif, D. M., Kleinstreuer, N. C., Judson, R. S., Singh, A. V, Chandler, K. J., Dix, D. J., Kavlock, R. J. and Knudsen, T. B. (2011) 'Predictive Models of Prenatal Developmental Toxicity from ToxCast High-Throughput Screening Data', *Toxicological Sciences*, 124(1), pp. 109–127.

Tal, T., Kilty, C., Smith, A., LaLone, C., Kennedy, B., Tennant, A., McCollum, C. W., Bondesson, M., Knudsen, T., Padilla, S. and Kleinstreuer, N. (2017) 'Screening for angiogenic inhibitors in zebrafish to evaluate a predictive model for developmental vascular toxicity', *Reproductive Toxicology (Elmsford, N.Y.)*, 70, pp. 70–81.

Tal, T. L., McCollum, C. W., Harris, P. S., Olin, J., Kleinstreuer, N., Wood, C. E., Hans, C., Shah, S., Merchant, F. A., Bondesson, M., Knudsen, T. B., Padilla, S. and Hemmer, M. J. (2014) 'Immediate and long-term consequences of vascular toxicity during zebrafish development', *Reproductive Toxicology*, 48, pp. 51–61.

Teodoro, J. G., Evans, S. K. and Green, M. R. (2007) 'Inhibition of tumor angiogenesis by p53: A new role for the guardian of the genome', *Journal of Molecular Medicine*, 85(11), pp. 1175–1186.

Teraoka, H., Dong, W. and Hiraga, T. (2003) 'Zebrafish as a novel experimental model for developmental toxicology.', *Congenital Anomalies*, 43(2), pp. 123–132.

Therapontos, C., Erskine, L., Gardner, E. R., Figg, W. D. and Vargesson, N. (2009) 'Thalidomide induces limb defects by preventing angiogenic outgrowth during early limb formation', *Proceedings of the National Academy of Sciences of the United States of America*, 106(21), pp. 8573–8578.

Top, W. M. C., Gillman, P. K., de Langen, C. J. and Kooy, A. (2014) 'Fatal methylene blue associated serotonin toxicity', *Netherlands Journal of Medicine*, 72(3), pp. 179–181.

Ulhaq, Z. S. and Kishida, M. (2018) 'Brain Aromatase Modulates Serotonergic Neuron by Regulating Serotonin Levels in Zebrafish Embryos and Larvae', *Frontiers in Endocrinology*, 9, p. 230.

Vlasits, A. L., Simon, J. A., Raible, D. W., Rubel, E. W. and Owen, K. N. (2012) 'Screen of FDA-approved drug library reveals compounds that protect hair cells from aminoglycosides and cisplatin', *Hearing Research*, 294(1–2), pp. 153–165.

Wada, H., Dambly-Chaudière, C., Kawakami, K. and Ghysen, A. (2013) 'Innervation is required for sense organ development in the lateral line system of adult zebrafish', *Proceedings of the National Academy of Sciences of the United States of America*, 110(14), pp. 5659–5664.

Wei, Y. B, McCarthy, M., Ren, H., Carrillo-Roa, T., Shekhtman, T., DeModena, A., Liu, J. J., Leckband, S. G., Mors, O., Rietschel, M., Henigsberg, N., Cattaneo, A., Binder, E. B., Aitchison, K. J. and Kelsoe, J. R. (2019) 'A functional variant in the serotonin receptor 7 gene (HTR7), rs7905446, is associated with good response to SSRIs in bipolar and unipolar depression', *Molecular Psychiatry*.

Weiskopf, R. B. and Todd, M. M. (2000) 'Clinical Uses of alpha 2 -Adrenergic Agonists', *Anesthesiology*, 93(5), pp. 1345–1349.

Whitfield, T. T. (2002) 'Zebrafish as a model for hearing and deafness', *Journal of Neurobiology*, 53(2), pp. 157–171.

Wilkinson, R. N. and Van Eeden, F. J. M. (2014) *The zebrafish as a model of vascular development and disease*. 1st edn, *Progress in Molecular Biology and Translational Science*. 1st edn. Elsevier Inc.

Winter, H., Rüttiger, L., Müller, M., Kuhn, S., Brandt, N., Zimmermann, U., Hirt, B., Bress, A., Sausbier, M., Conscience, A., Flamant, F., Tian, Y., Zuo, J., Pfister, M., Ruth, P., Löwenheim, H., Samarut, J., Engel, J. and Knipper, M. (2009) 'Deafness in TRbeta mutants is caused by malformation of the tectorial membrane', *The Journal of Neuroscience : the official journal of the Society for Neuroscience*, 29(8), pp. 2581–2587.

Wong, D. T., Bymaster, F. P. and Engleman, E. A. (1995) 'Prozac (fluoxetine, lilly 110140), the first selective serotonin uptake inhibitor and an antidepressant drug: Twenty years since its first publication', *Life Sciences*, 57(5), pp. 411–441.

Yoshida, S., Ikeda, Y. and Aihara, K. (2016) ‘Roles of the Androgen – Androgen Receptor System in Vascular Angiogenesis’, *Journal of Atherosclerosis and Thrombosis*, 23(3), pp. 257–265.

Zhong, T., Childs, S., Leu, J. and Fishman, M. (2001) ‘Gridlock Signalling Pathway Fashions the first embryonic artery’, *Nature*, 414, pp. 216–220.

Zhou, H., Yang, L., Wang, C., Li, Z., Ouyang, Z., Shan, M., Gu, J. and Wei, Y. (2019) ‘CYP2D1 gene knockout reduces the metabolism and efficacy of venlafaxine in rats’, *Drug Metabolism and Disposition*, 47(12), pp. 1425–1432.

Zygmunt, T., Trzaska, S., Edelstein, L., Walls, J., Rajamani, S., Gale, N., Daroles, L., Ramírez, C., Ulrich, F. and Torres-Vázquez, J. (2012) ‘“In parallel” interconnectivity of the dorsal longitudinal anastomotic vessels requires both VEGF signaling and circulatory flow’, *Journal of Cell Science*, 125(Pt 21), pp. 5159–5167.